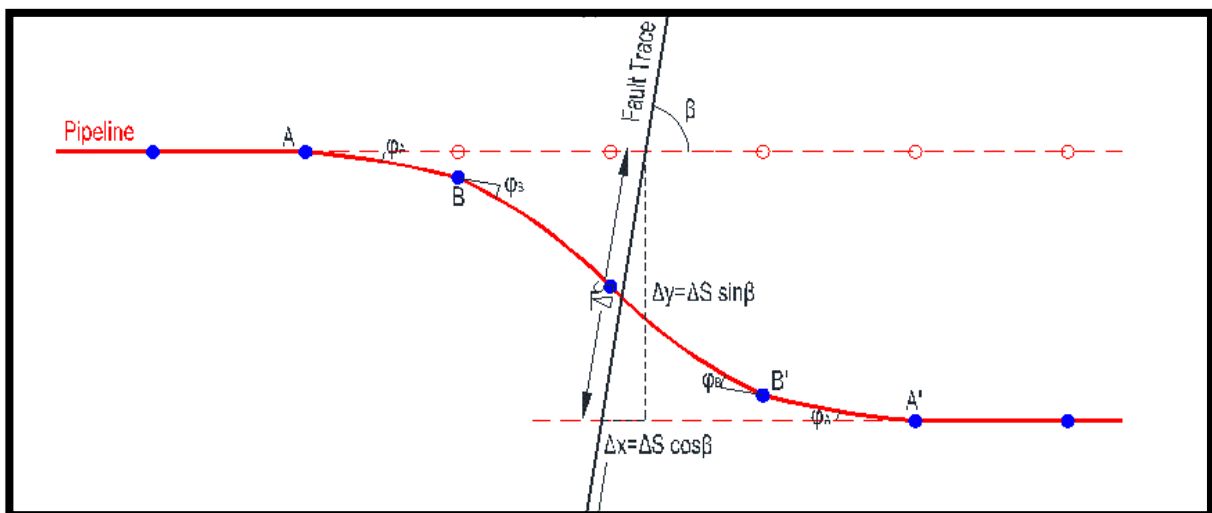




MASTER THESIS  
**PARAMETRIC EVALUATION OF PIPELINES  
WITH FLEXIBLE JOINTS IN AREAS OF LARGE  
GROUND DEFORMATION:  
CROSSING WITH STRIKE SLIP FAULTS**



**Mariana Ioannou**

*Supervisor: George D. Bouckovalas, Prof. N.T.U.A.*

Athens, June 2015



# Preface

---

Initially, I need to express my gratitude to Mr. George Bouchovalas, Professor at the Department of Civil Engineering of N.T.U.A., for the assignment of the thesis and his support throughout its conduction giving me in this way the opportunity to enrich my knowledge.

I would also like to thank Alexandro Valsamis *Ιδιαίτερα θα ήθελα να ευχαριστώ τον Αλέξανδρο Βαλσαμή*, Postdoctoral Researcher at the Department of Civil Engineering of N.T.U.A.. His excellent scientific specialization, combined with his endless willingness to help me in any way, were of significant importance for the completion of the present work.

I have to express my gratitude to Mr. Leonidas Zampas, Director of Projects in ΑΣΠΡΟΦΟΣ ΑΕ. company , for the useful -for the completion of the present work- techno-economical data that he gave me.

It would be a great omittance not to mention my colleague but also friend Maria Dagalaki for the understanding, the excellent cooperation we have had and her support during any difficulty I faced.

With this thesis, my presence in this program in reaching to its end. In addition to this I would like to thank Mr.Dimitrios Loukides and Mr. Dimos Charnpis, Proffessors at the Department of Civil and Environmental Engineering of the University of Cyprus for motivating me in attending the specific postgraduate studies.

During those two years, I made lots of friends and met worthy colleagues. I want to thank all my colleagues for the pleasant environment they created for me, their support and cooperation.

Also, I'd like to thank all my friend who in their own way each one, encouraged and supported me during my studies.

Last but not least, I ought to thank the people who are always by my side, in good and bad times, my parents Giannakis and Egli, my sister Katia and Charis.



# Table of Contents

---

<b>1 Introduction.....</b>	<b>7</b>
<b>2 Type and effectiveness of flexible joints.....</b>	<b>10</b>
2.1 General information .....	10
2.2 Historically.....	11
2.3 Types of commercially available flexible joints .....	14
2.3.1 Slip expansion joints .....	15
2.3.2 Expansion/ Ball joints .....	16
2.3.3 Flexible «Bellows» type Joints .....	17
2.3.4 Complex joints .....	19
<b>3 Proposes analytical methodology for strike slip-faults.....</b>	<b>20</b>
3.1 General information .....	20
3.2 Analysis assumptions.....	20
3.3 Similarities & differences with continuous pipelines .....	23
3.4 Methodology Description .....	26
<b>4 Presentation of numerical methodology for strike slip faults.....</b>	<b>34</b>
4.1 General Information.....	34
4.2 Simulation of pipeline using finite elements .....	34
4.3 Soil simulation .....	36
4.4 Simulation of flexible joints.....	43
4.5 Typical Results.....	45
4.5.1 Numerical continuous pipeline analysis .....	45
4.5.2 Numerical analysis of a pipeline consist of flexible joints .....	50
<b>5 Comparison between the proposed analytical methodology and numerical analysis results.....</b>	<b>56</b>
5.1 Numerical Analysis Presentation.....	56
5.2 Comparing the results of analytical and numerical analyses .....	58
5.3 Diagrams of relative error in the proposed method .....	71
5.4 Conclusions.....	78
<b>6 Comparison of the proposal methodology with usage of flexible joint against the conventional ones.....</b>	<b>79</b>
6.1 Introduction.....	79
6.2 Methodologies to face ground displacements due to rupture of a strike slip fault .....	79
6.3 Methodologies' evaluation concerning the effectiveness and the cost of each one.....	85
<b>7 Conclusions.....</b>	<b>90</b>

<b>8 References.....</b>	<b>94</b>
<b>Appendix A' Parametric Numerical Analyses for strike slip faults.....</b>	<b>98</b>

# 1

## Introduction

---

The seismic imposed permanent ground deformation, such as those caused by the rupture of active faults, the horizontal spread of liquefied soil or landslides, are some of the most serious risks for the underground oil or gas pipelines . This is mainly due to (a) the pipes are linear structures too long and therefore it is almost impossible for them not to be crossed with active faults or areas with potential soil failures (landslides, horizontal spread), and (b) such displacements are much larger than those caused by the earthquake and in addition to this they are permanent as well.

Between the various causes of permanent ground displacements, this thesis focuses on the design of underground pipelines against displacement due to rupture of active faults. The main feature of these large displacements is that they are unique they can not be avoided by preventing the causes of the fault (e.g. soil improvement or enhancement of soil, applying drainage network, constructing retaining walls, etc.) but only with the proper the design of the pipeline. The deformed body after rupturing of a strike fault slip crossing with a pipeline in a random intersection angle, is shown in Figure 1.1.

The usual "conventional" methodologies to cope with permanent ground displacement due to the rupture of active faults can be divided into three categories depending on the main mechanism by which they try to prevent the deformation imposed to the pipeline:

(A) reducing the lateral friction between the pipeline and the ground (e.g. use of geotextiles, backfilling with sand)

(B) Strengthening of the pipeline in order to take the appropriate deformations (e.g. increased the pipeline wall thickness or changing the type of steel that is used) and

(C) reduction of the ground reaction in the rupture area to the transverse displacements of the pipeline (e.g. extension of the trench, construction of an exterior underground box made of Reinforced Concrete).

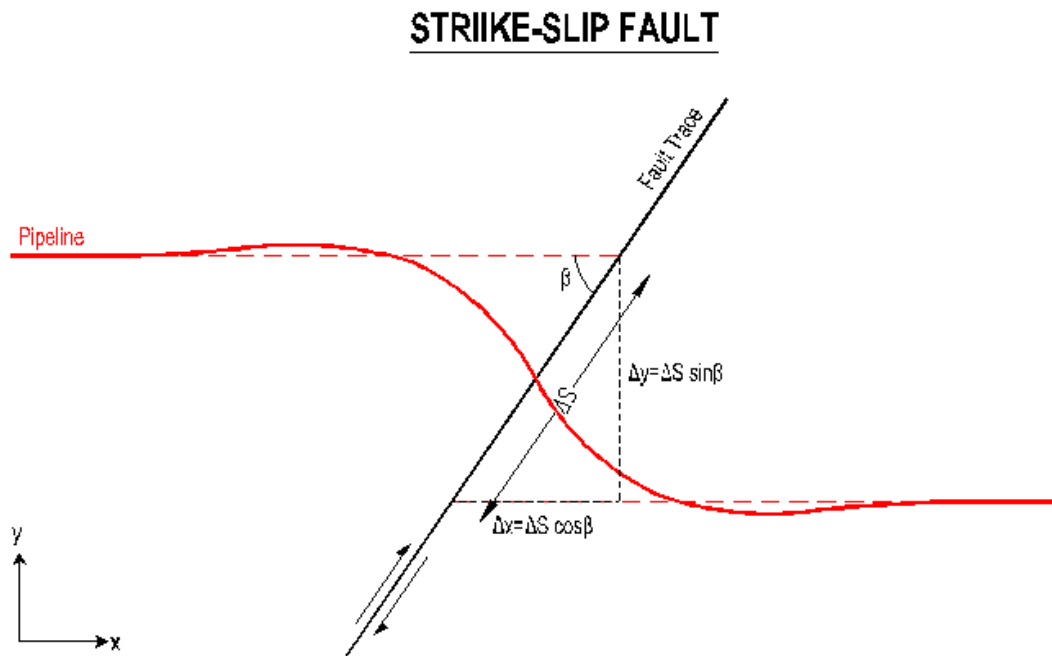


**Figure 1.1:** Deformed pipeline intersects the strike slip fault

However, all the above methods can be applied for small to medium displacements of the fault, to be more specific 2.5-3 diameters of the pipeline. The exception is the construction of the outer casing box made of concrete (culvert), but this is an expensive method, as a result the cost is getting higher as the ground deformation has been increased. Considering the above thoughts, in the Geotechnical Division of NTUA they have studied an alternative design of pipelines in areas of large ground displacement, using flexible joints, through numerical analysis and small-scale experiments. Due to a research program it has been developed a new analytical methodology for the analysis and design of segmented pipelines with flexible joints in at active fault crossing in order to see how these joints affect the basic design parameters.

Thus, the main subject of this thesis is the parametric evaluation of the proposed analytical methodology for pipes with flexible joints that crosses strike-slip faults. At

the same time it has been made a techno-economical evaluation of this design method against the conventional ones.

More specifically:

- The **Chapter 2** refers to a literature review on the availability and the use of flexible joints in areas of permanent large ground displacements.
- The **Chapter 3** refers to an extensive description of the proposed analytical methodology for strike slip faults.
- The **Chapter 4** presents the numerical methodology applied to the strike slip faults and indicatively the results of two typical analysis.
- The **Chapter 5** compares the results of the analytical methodology with results derived from the numerical analysis in the case of strike-slip faults.
- The **Chapter 7** encloses a techno-economical comparison between the new pipeline design method against large ground displacements due to the rupture of active faults using flexible nodes and the "conventional" design methods.
- Finally, **Chapter 8** summarizes the main conclusions of this thesis.

# 2

## Type and effectiveness of flexible joints

### 2.1 General information

Using flexible joints is an alternative technique for pipe design against permanent ground displacements that occur during the rupture of tectonic faults that aims to the reduction of the imposed deformations of the pipe and its possible failure. To specify, flexible joints are special structures that are placed along the pipe, in the region that contains the fault and regarding their type, are capable of gathering the imposed deformations reducing in this way the extra tension (axial or bending) in the rest connected pipe sections. Therefore, eventually the pipe develops deformations under the ultimate limits, eliminating the danger of its failure.

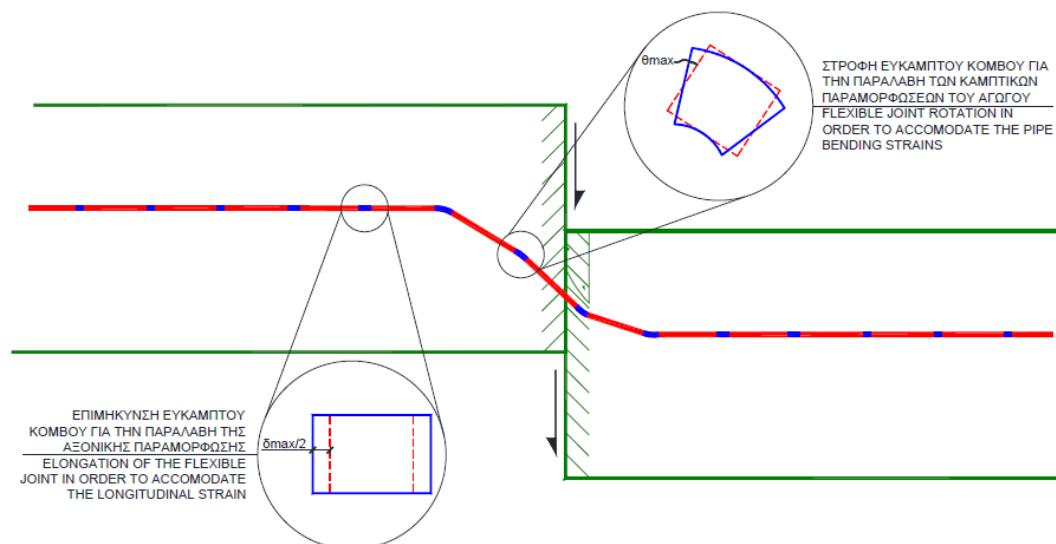
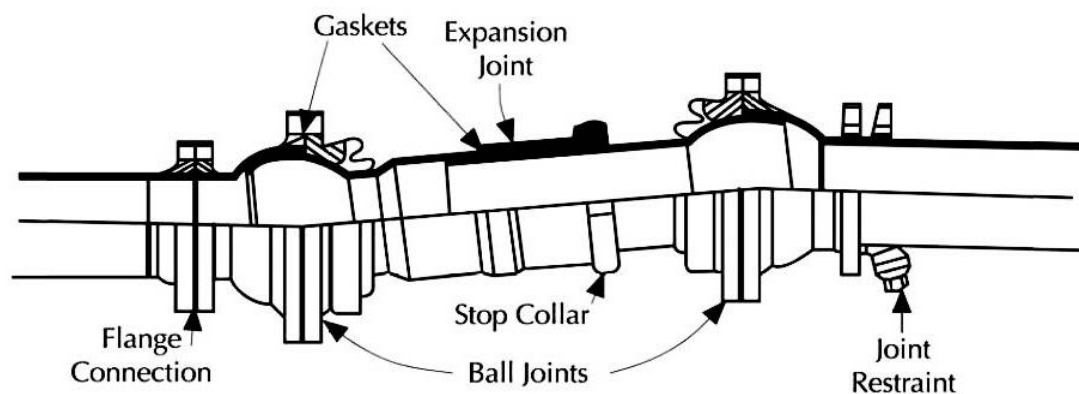


Figure 2.1: Representation of how the flexible joints work

## 2.2 Historically

Most publications found in international references, are about the usage of flexible joints in low pressure sewage or water supply pipelines. However, the publications regarding this technique on underground pipes that undergo large ground deformations are much fewer.

Dealing with local large ground displacements using flexible joints was first introduced by Ford (1983). The suggested representation (Figure 2.2) consisted of two successive “ball type” joints receiving the rotation that they are connected together by an expansion joint. According to Ford (1983) this device can be used in regions that large differential settlements are expected (e.g. pipelines under buildings etc).



**Figure 2.2:** Proposed representation of flexible Joints by Ford (1983).

Isenberg & Richardson (1989) investigated on the available flexible joints and their usage on sewage and watersupply pipeline studies. Their investigation lead to the conclusion, that the exact location of the joint as well as the range of the expected deformations are crucial for the accuracy of the study. Regarding that, devices that were available to the market had to be improved through the evolution of geotechnical engineering in order to make them more efficient.

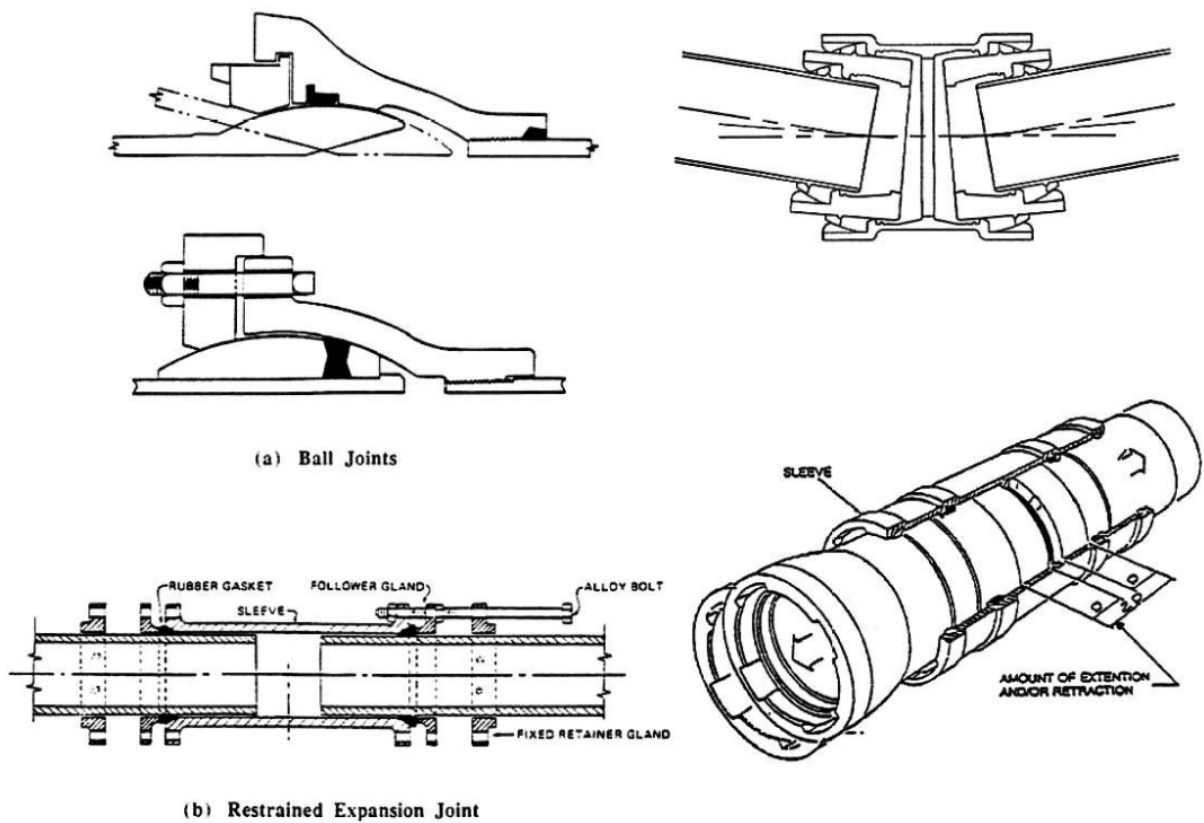


**Figure 2.3:** Flexible Joints investigated by Isenberg & Richardson (1989)

Ballantyne (1992) suggested that flexible joints should be used along with “conventional” methodologies for the pipelines design against permanent ground displacements that are ranged between 2.5cm and 100 cm. The joints allowed greater deflection; extension or compression compared to segmented pipes joints. Therefore they had to be specifically designed. Additionally, he established criteria that had to be met in order for the flexible joints to work properly, something that couldn’t be achieved by the available commercial joints of the time.

O’Rourke & Liu (1994, 2012) investigated the usage of Dresser expansion joints (simple sliding joints) in order to deal with ground displacements and they discovered that these joints could affect both positively and negatively the pipe’s behavior. To specify, positive influence is been shown in Figure 2.4.a where the values of tensile and compressive stress of the pipe are lowered to  $t_u L_1$  and  $t_u L_2$  respectively to the initial  $t_u L/2$ . On the other hand, using these joints had a negative effect (presented on Figure 2.4b), where the reduction of tensile stress to  $t_u L_1$  comes along with increase of compressing stress to  $t_u L_3$ .



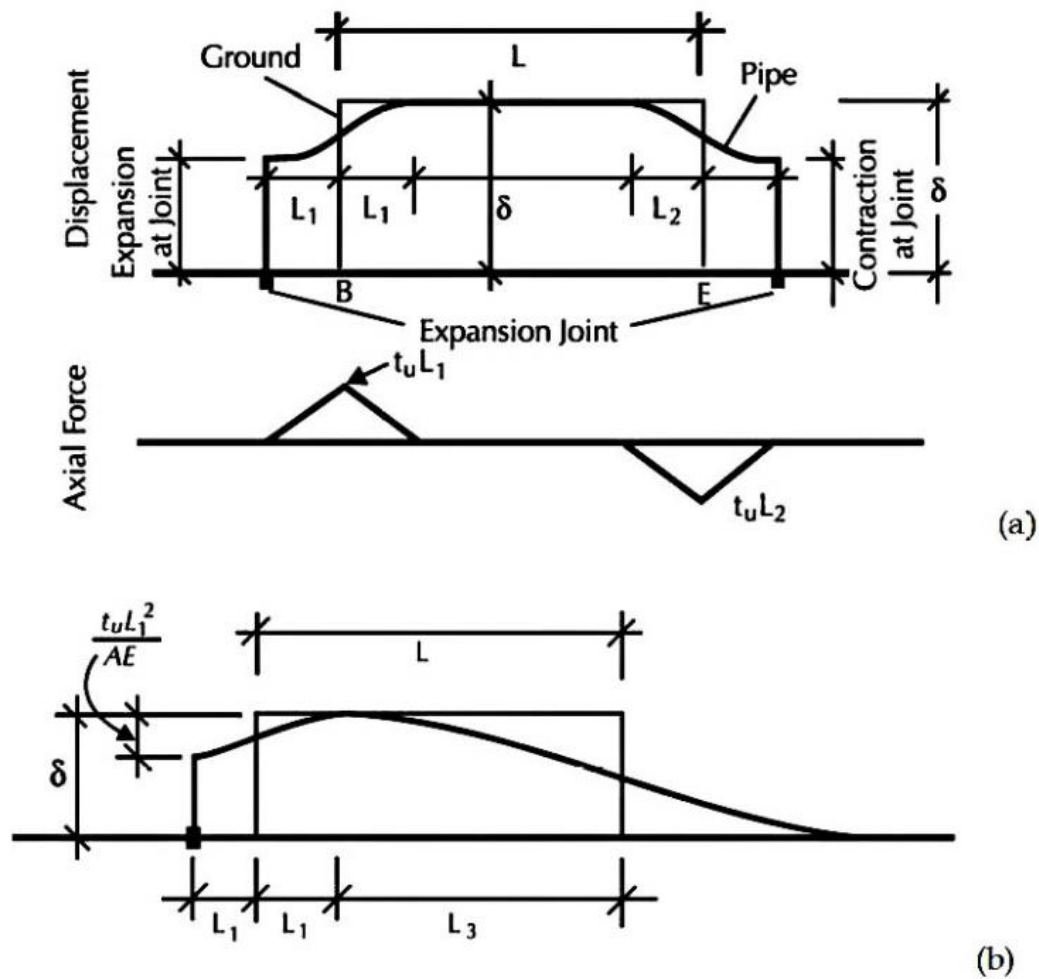
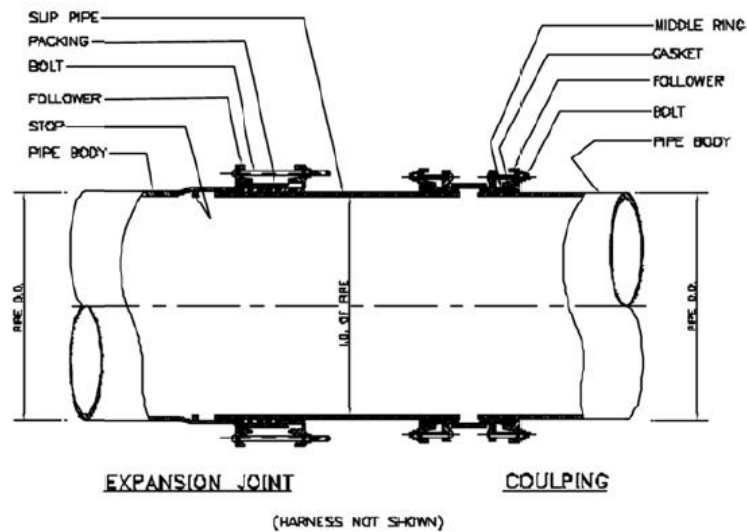


**Figure 2.4:** Possible (a) positive and (b) negative affection of an expansion joint (O' Rourke & Liu, 2012)

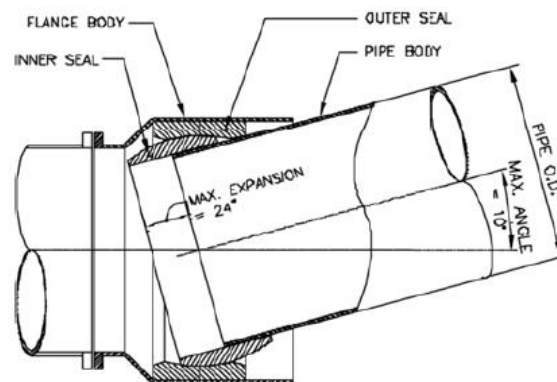
Wang (1996) dealt with the strengthening of existing pipelines and proposed replacing fixed-rigid joints between sections of pipelines with more flexible and /or restrained joints. However he didn't extend his study to the properties required of these nodes and whether it is commercially available. That's why his proposals were purely qualitative.

Cheng (2001) later explored alternative ways of receiving large displacements on water pipes due to fault rupture, both types of nodes are been shown in Figure 2.5. Although both types of nodes are able to receive both expansion and rotation, the second type can be rotated and as a result to accept abrupt displacements, such as those caused by rupture of the fault. Nevertheless, it was considered that the

conventional design is not enough and as a result no use was made of any of the above joints in the final design of the pipeline.



(a)



(b)

Figure 2.5: Joint types studied by Cheng (2001)

### 2.3 Types of commercially available flexible joints

Depending on the method of receipt of imposed displacements, commercially available flexible joints are divided into four categories: simple slip expansion joints, joints like "ball", joints like "bellows" and complex joints.

### 2.3.1 Slip expansion joints

The slip expansion joints consist of two pipe segments which are not welded together but they are inserted into one another. In this way, relative displacement along them is allowed, while the rotation capacity is zero or very low. The maximum allowable relative movement, the resistance to further elongation (beyond the allowable) and the method of sealing the joint are of great importance for the joints.

Such joints are commercially available from several companies, with some of them used in high pressure fuel transfer networks having maximum permissible internal pressure above 1000psi (~6.9MPa). Also there are no constructional limitations on the diameter of the pipeline.

For ordinary slip expansion joints are applied the restrictions theoretically are analyzed by O'Rourke & Liu (1994, 2012). To be more specific in order to have a positive affection to the imposed deflections it is necessary to have at least two flexible joints covering the range of the imposed deflection. The first joint must be at the head of the imposed deflection and the second at the end of that. In addition to this joints have to be deformed according to the estimated displacement that the rupture of the fault can cause.

However, the complexity of these provisions and the great uncertainty about the exact location and the extent of the trace of fault area make this solution extremely expensive, while not sufficiently effective, since they don't reduce at all the deflections due to bending, of the pipeline.

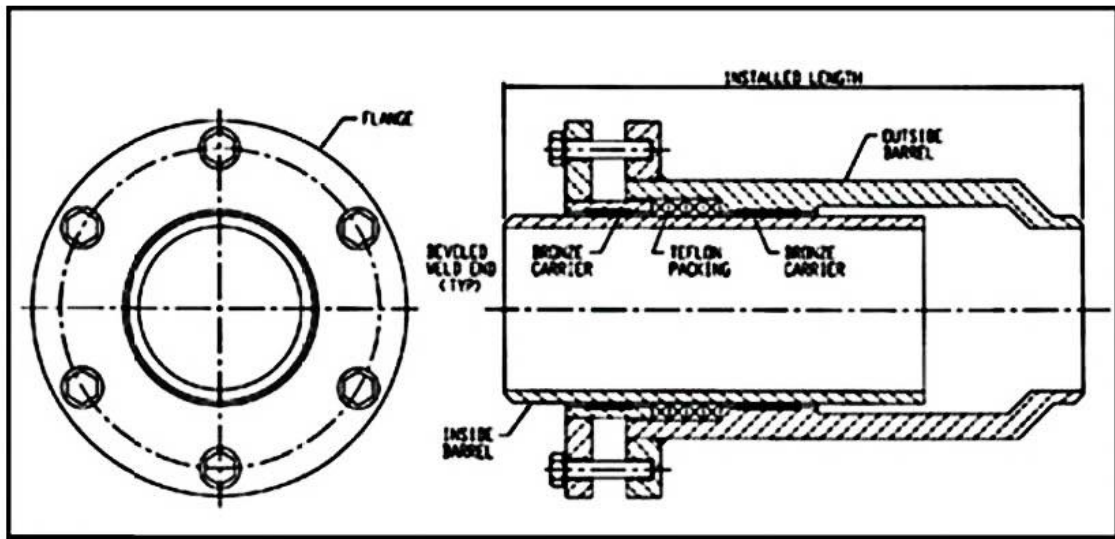
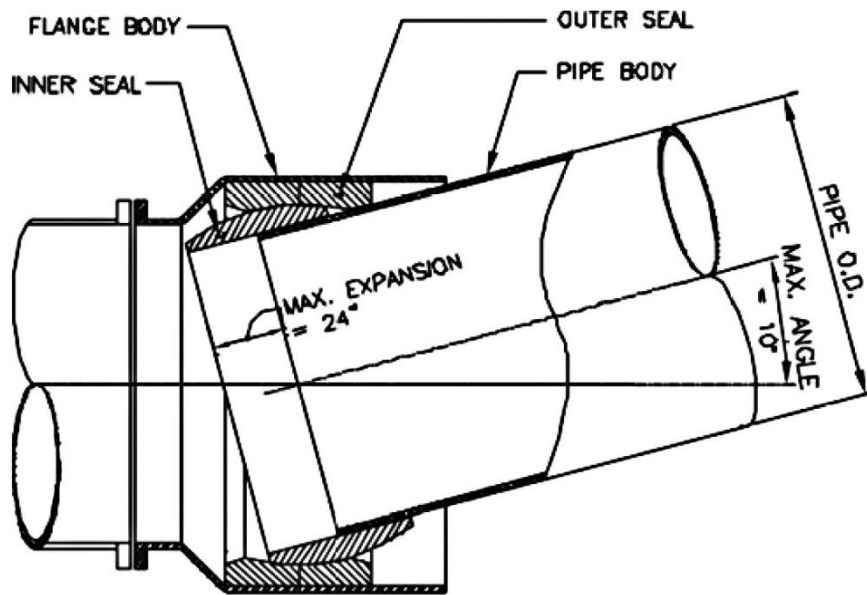


Figure 2.6: Typical presentation of an expand joint (by U.S. Bellows Inc.)

### 2.3.2 Expansion/ Ball joints

These joints consist of a segment with an end in a round shape, which enters another segment within appropriately shaped slot as illustrated in Figure 2.7. Deflections can be taken from that provision as the relative rotation of the two sections of the pipeline is allowed. Axial deformation can be obtained only insofar as allowing relative expansion between the straight portion and the spherical cap. The main construction difficulty of these joints is to develop resistant limit (stop) which prevents relative expansion to exceed the permitted slip value.

The currently commercially available "sphere" type joints are made of low strength or synthetic materials and the allowable internal pressure of the steel is greater than 350psi (~ 2,4MPa), making them inappropriate for oil or gas networks of medium and high pressure pipelines .



**Figure 2.7:** Typical presentation of a sphere type joint that is able to be expanded as well (by EBBA Iron Inc. according to Koike et al 2001)

### 2.3.3 Flexible «Bellows» type Joints

Flexible «Bellows» type joints consist of thin-walled corrugated steel and so are designed to have great flexibility when they are imposed to axial loads, internal pressure and bending moments. The Figure 2.8 shows the various types of movement which can be received by these kind of joints.

The thickness and type of the cross section of each fold determine the resistance to deformation as well as the capability of maximum deformation. In Figure 2.9 are presented ten different types of folding sections according to Wilson (1984), each of which presents different characteristics of flexibility and resistance to axial loads. The most common type of cross section is that of "Lyra" or "S shape" (figure f).

The desired combination of resistance to internal pressure, to axial loads and deformation capacity is achieved with the appropriate modifications in the design of sections, such as changes in the level of the folds, the radius of the curves, the number of successive metal layers and the total thickness of the wall.

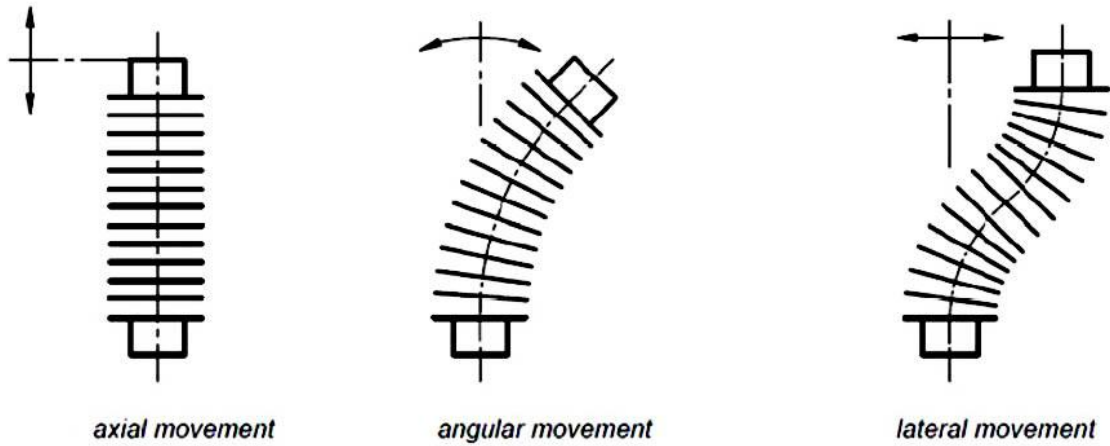
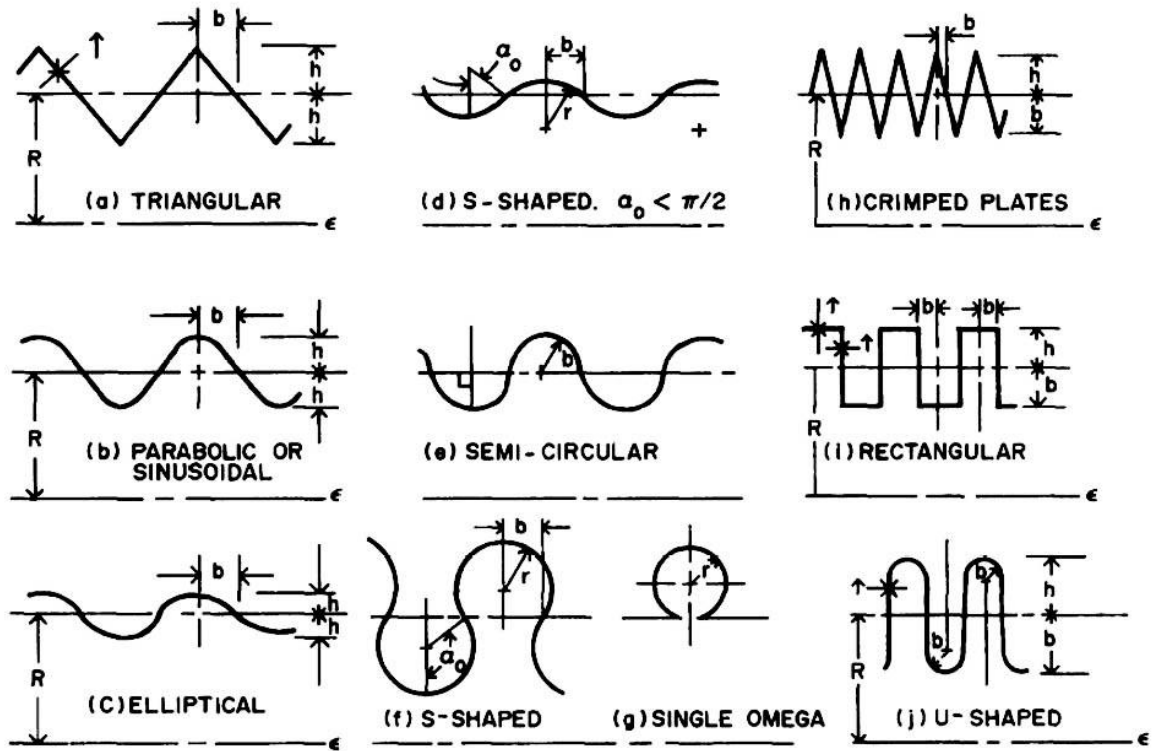


Figure 2.8: The types of movement which can be received by "Bellows" (by BOA



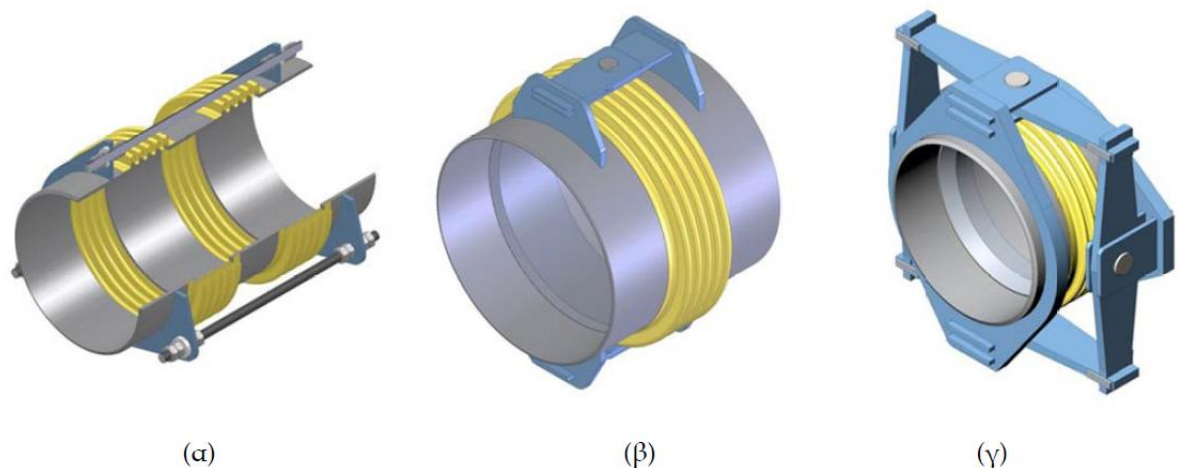
Group)

Figure 2.9: The ten different "Bellows" types of folding sections (according to Wilson 1984)

Nowadays, flexible "Bellows" type joints are mainly used for industrial purposes in order to receive pipe expansions caused by temperature changes. Such joints are produced by several companies, with diameters greater than 100mm and resistance to internal pressure up to 1500psi (~ 10.4MPa). Due to the flexible design of the folds, the relatively low cost and ease of installation in the field, these joints are a good

solution to the reduction of imposed deformations in pipelines due to tectonic faults rupture. Additionally in order to limit some of the available degrees of freedom, the joints can be equipped with rods or joints. Thus, for example in Figure 2.10 the presented joints only allow lateral movement or rotation around one or two axes.

Particular care is needed in covering these joints in geo-textile, so as to allow their free deformation without being obstructed by growing friction with the surrounding backfill due to the presence of folds in the joint. Also quite important is to limit or even eliminate permanent deformation of the joint due to internal pressure of the oil or gas that is going to be carried.



**Figure 2.10:** Complex joints of "Bellows" type with with permitting (a) the lateral movement, (b) the rotation in one axis and (c) the rotation in two axis (figures by Eagleburgmann group)

### 2.3.4 Complex joints

The foregoing joints categories can be combined properly creating in this way, complex joints formations (e.g. joint type combination of "sphere" and expand sliding node, or a combination of two" Bellows" type joints), which are both found in the literature (e.g. Ford 1983, Isenberg & Richardson 1989) and in catalogues of flexible joints made by production companies. These provisions do not need to be further analyzed, as essentially combine the above solutions.

# 3

## Proposes analytical methodology for strike slip-faults

---

### 3.1 General information

The literature review conducted in the previous section shows clearly that it has not been developed a detailed methodology of estimating deformation of flexible pipelines with joints. The most relevant existing methodologies to the studied pipeline category are related to segmented pipelines, although the segmented pipelines joints are considered weak, allowing freedom of some displacement and rotation and their design reduces the extent of displacement and rotation at a joint to meet the relevant acceptable limits. Flexible joints are designed to limit distortions of developing deformations in the pipeline and safely receive of the imposed axial and shear stresses, without being vulnerable part of the pipeline.

The proposed methodology is based on the methodologies presented by Karamitros et al. (2007,2011) and Trifonov & Cherniy (2010).

### 3.2 Analysis assumptions

Below are presented the assumptions that the methodology is based on, emphasizing on the steps of the method which make use of relations and iterative loops, so as to fully understand the theory and the logic part of the use of methodology. More specifically:

- The studied stainless steel pipeline is thin-walled and has an outer diameter  $D$  and a thickness  $t$  as shown in Figure 3.1. The area and the area moment of inertia of the cross section can be found from the following relationships.

$$A_s = \pi(D - t)t \quad (3.1)$$



$$I = \pi \left( \frac{D-t}{2} \right)^2 t \quad (3.2)$$

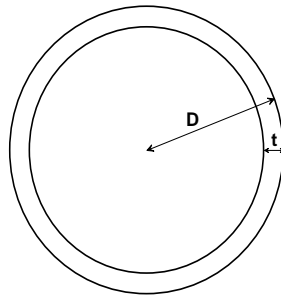


**Figure 3.1:** Pipeline cross section geometry

- The Relationship between the stress and strain of steel is described by the bilinear stress-strain diagram shown in Figure 3.2, with elastic modulus  $E_1$  and  $E_2$  in the elastic area and the plastic area, respectively. Also in Figure 3.2.,  $\sigma_1$  is the yield stress point and  $\epsilon_1$  is the yield deformation point. The maximum allowable stress is defined as  $\sigma_2$  and the maximum allowable deformation is defined as  $\epsilon_2$  and if those two value points are exceeded, theoretically the material led to failure.

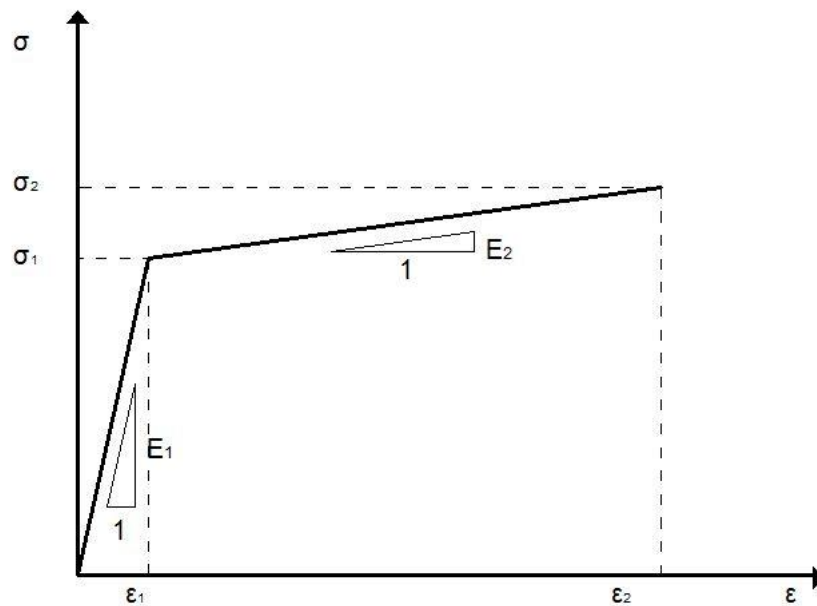


**Figure 3.2:** Bilinear stress-strain diagram of the stainless steel pipeline

- The strike-slip fault intersects in one point the pipeline and its fracture zone thickness is zero. Thus the displacements of the fracture can be resolved into components along the X and Y axis where X axis is the one parallel to the pipeline axis and the Y axis is perpendicular to X axis, as illustrated in Figure 3.3

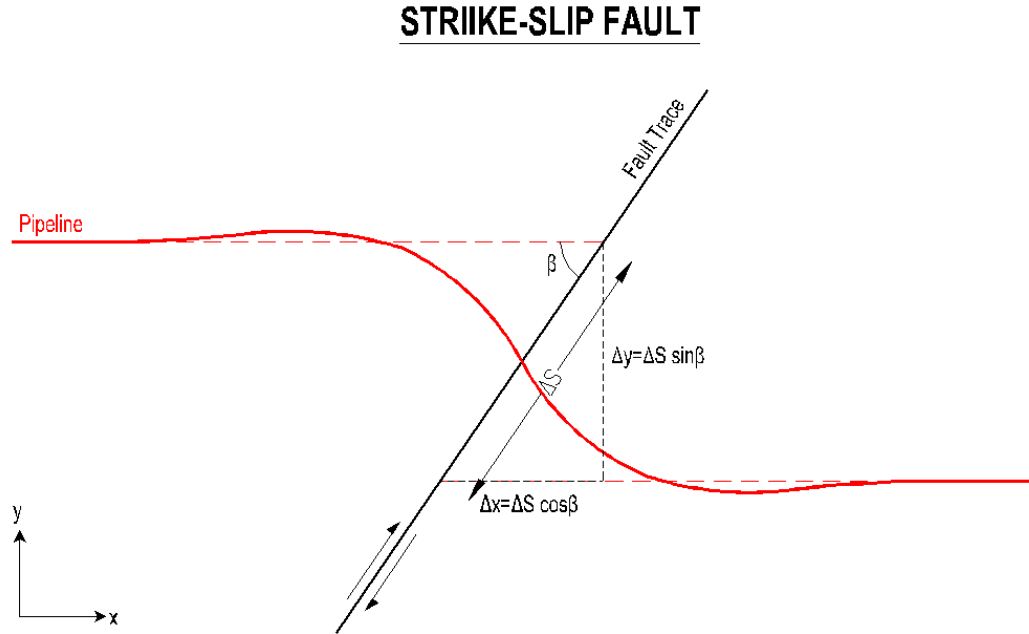


**Figure 3.3:** The displacement of the fracture strike slip fault is resolved into components  $\Delta x$  and  $\Delta y$ .

- The interaction between the pipeline and the surrounding soil backfill is ensured by elastoplastic winkler springs, for the frictional forces in the axial direction of the pipeline, and for cross-resistance of soil due to the displacement of the pipeline as well.
- The superposition theorem is applied on the imposed loadings (axial and lateral), despite the strong non-linear nature of the problem.
- Despite the significant deformations which are expected to be developed in the fault region, it is assumed that its cross section is flattened.
- The flexible joints can turn around vertical axis Z at a constant rotational stiffness  $C_r$ . The stiffness of the joints on the rest axes corresponds to the stiffness that the intermediate part of the pipeline have. Generally, the rotational stiffness  $C_r$  is too small and as a result the joints actually behave as hinges and small bending moments are developed on them.

- Considering that there is uncertainty about the exact position of the fault intersection with the pipeline, the design should cover the area around the fault's track with flexible joints with fixed distance between them. For this reason, there are two joints on either side of the fault trace in the analytical simulation. Besides, it was considered that the fault intersects with the pipeline in the middle, between the two nodes or adjacent to one of them.

### **3.3 Similarities & differences with continuous pipelines**

The presence of flexible joints in the pipe affects the behaviour of the pipe at the fault rupture compared to the behaviour of the continuous pipelines. The Figure 3.4 (a) and Figure 3.4 (b) show the deformed body when the fault intersecting the pipe in the middle between the two nodes or intersecting the pipeline adjacent to a joint. For comparison, Figure 3.4 (c) illustrates the deformed body intersecting the pipeline axis, in the case of pipeline without flexible joints.

From Figure 4.4 we extract some similarities between the two problems:

- The pipeline is held symmetrical at the intersection point with the fault-slip, where bending moment is zero due to body balance. Thus, it is sufficient to solve only the half body by simulate the other half body with a hinge.
- There is an anchoring length in which a relative sliding is developed between the pipe and the surrounded backfill, due to axial stresses imposed by the rupturing of the fault with the pipeline which are gradually reduced due to the presence of friction forces. Since the axial stress can exceed the steel yield stress, a flexible and a plastic anchor lengths are defined.
- When a part of the section is yielding due to presence of axial force and bending moment, a special methodology to calculate the bending strain is applied, as described in a following part of this chapter.

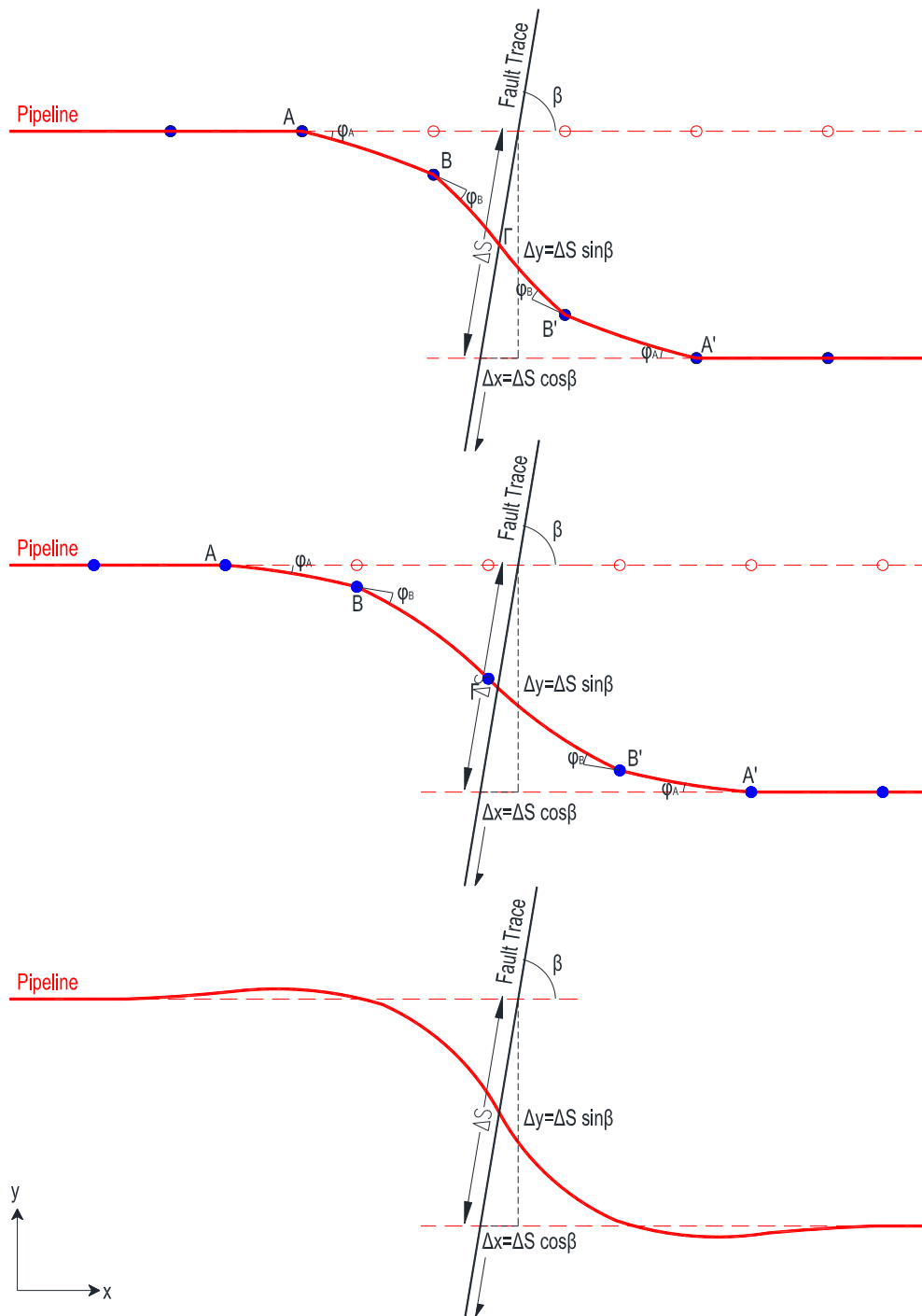


**Figure 3.4:** Deformed pipeline body intersecting with strike slip fault (a) between two flexible joints, (b) adjacent to one of them, and (c) at a place without flexible joints

The main differences between the two problems according with the static model of the entire body is shown in Figure 3.5 and listed below:

- Flexible joints have lower torsional stiffness than the continuous sections of the pipeline, and thus Z axis rotation is concentrated to them, while the intermediate parts of the pipeline remain relatively straight and small bending deformations are developed on them.
- The curved length, which is the part with large transverse displacements, is not dependent on the strength of the side springs, the rigidity of the pipeline and the magnitude of the imposed-displacement by the fault. The same happen in the case of the continuous pipeline. For the current studied problem the above assumptions are directly acceptable since the curved length is between  $AB\Gamma B'A'$  points. What is not assumed from the beginning are the angles  $\varphi_A$  and  $\varphi_B$ , otherwise the percentage of the overall transverse displacement which will be received due to joints rotation in the segments AB και  $B\Gamma$  respectively.
- Since the part of the pipeline prior to point A has negligible transverse displacements, there is no need to be solved as semi-infinite beam on elastic supports, thus that part of the pipeline is simulated as a hinge. An axial force is applied because of the balance of the segment AB and it is practically equal to the axial force that is developed in the part of the pipeline prior to point A, and it is received by the friction along this section.
- The lateral displacements between joints A and B may be small and not sufficient to exhaust the limit value of lateral soil resistance, so it is assumed that at this segment of pipeline the loading of the soil has a maximum value  $p_u^*$ , which for very small lateral displacement values of joint B does not necessarily match with the soil ultimate strength,  $p_u$ . To simplify the equations, the imposed load is obtained as stable distributed rather than triangular distributed, with a maximum value equal to half the maximum applied value. Regarding the part of the pipeline following the joint B, the soil lateral resistance can be obtain as stable and equal to the maximum value, since it reaches that stable value very quickly, even for zero displacements of joint B.

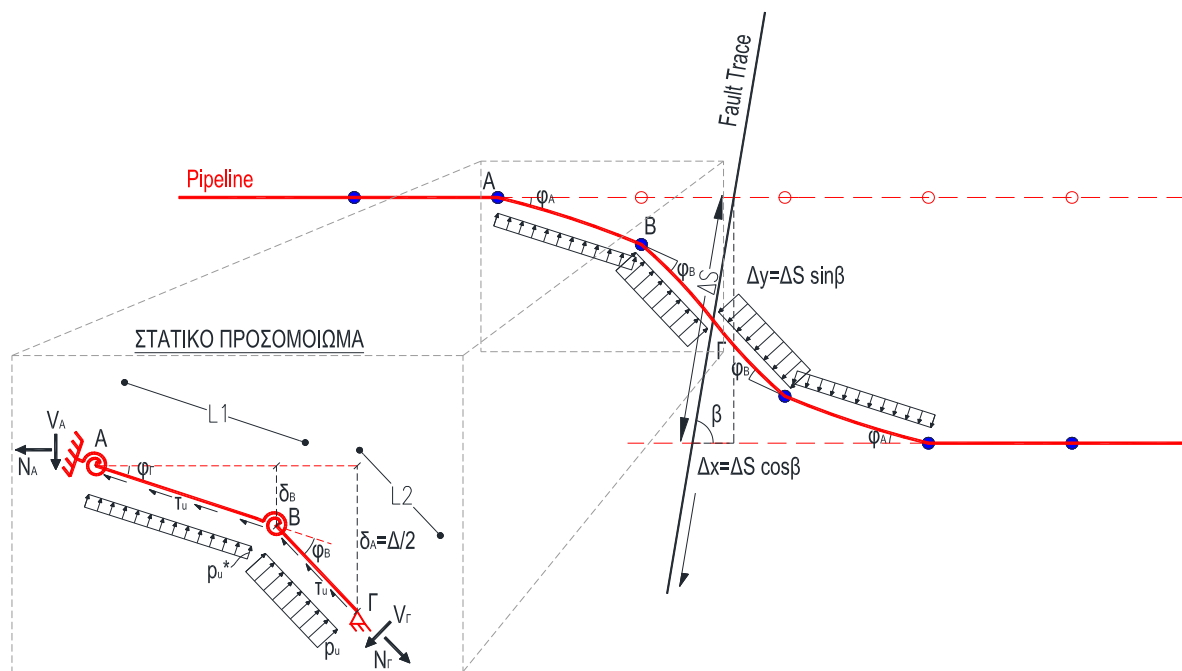


**Figure 3.5:** Static simulation of the entire body studied for the development and evaluation of the analytical methodology

#### 4.4 Methodology Description

Regarding the assumptions already mentioned, the methodology is based on an repeated algorithm presented below. The process is scheduled in a simple code excel in which key parameters of analysis imported and using macros, the problem solution is completed and diagrams about the fundamental elements of the analysis are produced.

##### Step 1: Initial "elastic" solution of the studied body

The body is solved as static one using the initial pipe stiffness values for all the rods. Due to the complex form of equations, an iterative solution process is required.

As mentioned above, the simulation model is symmetrical to the intersection with the pipeline and the trace of the fault. This applies to both studied cases, when the fault passes exactly in the middle between the two joints or adjacent to one of the two joints. As a consequently only the half body can be solved by simulating it with a hinge where the intersection of the fault with the pipeline is. The half body is divided into two segments, AB and BΓ, as shown in Figure 3.5. Both parts are considered as

elastic beams, which are under simultaneous loading of axial forces and bending moments. It should be noted that large axial forces caused due to longitudinal deformation of the fault affect significantly the developed shear forces and moments due to second order effects.

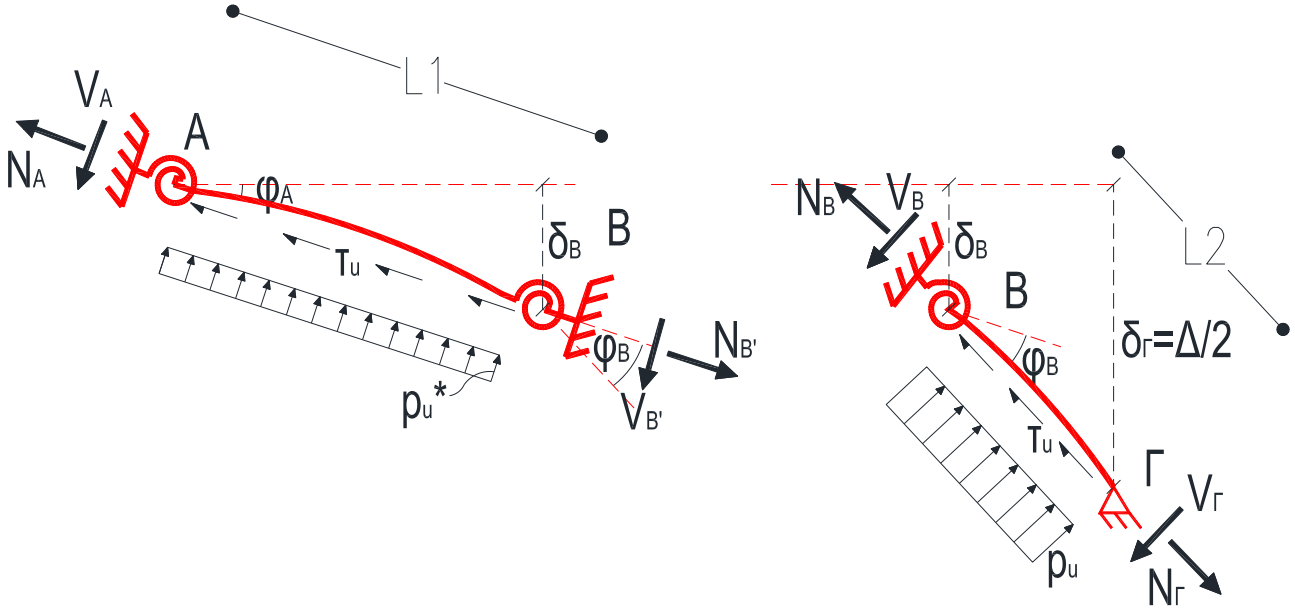


**Figure 3.6:** Split analysis of the pipeline in its deformed state

The fundamental relationship that describes the deformation of an elastic beam, on which are simultaneously applied axial and transverse forces, is:

$$EI \frac{d^4 w}{dx^4} - N \frac{d^2 w}{dx^2} = q \quad (3.3)$$

- where
- $w$  the transverse displacement of the pipeline
  - $E$  the elastic modulus of the pipe material
  - $I$  the moment of inertia of the cross section
  - $N$  the axial force to the pipeline
  - $q$  the transverse load applied to the pipeline.

This relationship can be used to estimate the transverse displacement of the beam at each position. Its integration relatively to the deformed body, produce the following relationship:

$$w(x) = w(0) + \varphi(0) \frac{\sinh ax}{a} + \frac{M(0)}{EIa^2} [\cosh ax - 1] \quad (3.4)$$

where  $\alpha^2 = N/EI$

- $w(0)$  the transverse displacement of the beam in the first part of the studied body ( $x=0$ ),  
 $\varphi(0)$  the rotation because of the pipeline bending at the same point,  
 $M(0)$  the bending moment and  
 $V(0)$  the shear force exerted at the same point.

The equation 3.4 can be used for both segments AB and BΓ (index 1 and 2 respectively) of the pipeline, whereas the accurate initial boundary conditions due to pipeline's bending, the rotation at the joints and the balanced forces exerted at the joints. The parameters of equation 3.4 regarding the studied problems have the values shown below:

$$\begin{array}{ll} w_1(0)=0 & w_2(0)=\delta_1(L_1) \\ \varphi_1(0)=0 & \varphi_2(0)=0 \\ M_1(0)=-M_A=C_r*\varphi_A & M_2(0)=-M_B=C_r*\varphi_B \\ V_1(0)=V_A & V_2(0)=N_1(L_1)*\sin\varphi_B-V_1(L_1)*\cos\varphi_B \end{array}$$

where  $C_r$  is the rotational stiffness of flexible joints.

As a result, the solution of equation 3.4 may give the rotation, the shear force and the bending moment at each position:

$$\varphi(x) = w'(x) \quad (3.5)$$

$$V(x) = E_i I_i w'''(x) - N(x) \cdot w'(x) + V_A/2 \quad (3.6)$$

$$M(x) = \int_0^x V(x)dx \quad (3.7)$$

The first four derivatives of the transverse displacement of the beam,  $w$ , are presented below:

$$w'(x) = \varphi(0) \cosh ax + \frac{M(0)}{EIa} \sinh ax + \frac{V(0)}{EIa^2} [\cosh ax - 1] + \frac{q}{N} \left[ \frac{\sinh ax}{a} - x \right] \quad (3.8)$$

$$w''(x) = a \varphi(0) \sinh ax + \frac{M(0)}{EI} \cosh ax + \frac{V(0)}{EIa} \sinh ax + \frac{q}{N} [\cosh ax - 1] \quad (3.9)$$

$$w'''(x) = a^2 \varphi(0) \cosh ax + a \frac{M(0)}{EI} \sinh ax + \frac{V(0)}{EI} \cosh ax + a \frac{q}{N} \sinh ax \quad (3.10)$$

$$w''''(x) = a^3 \varphi(0) \sinh ax + a^2 \frac{M(0)}{EI} \cosh ax + a \frac{V(0)}{EI} \sinh ax + a^2 \frac{q}{N} \cosh ax \quad (3.11)$$



The total displacements ( $w$ ) caused by the internal forces and bends of the flexible joints are given by Equations 3.12 and 3.13 for beams AB (1) and BΓ (2), respectively:

$$\begin{aligned} \delta_1(x) &= w_1(x) + x \cdot \sin \varphi_A = \\ &= \frac{M(0)}{E_1 I_1 a^2} [\cosh ax - 1] + \frac{V(0)}{E_1 I_1 a^2} [\cosh ax - 1] + \frac{q_u^*}{N(x)} \left[ \frac{\cosh ax - 1}{a^2} - \frac{x^2}{2} \right] + x \cdot \sin \varphi_A \end{aligned} \quad (3.12)$$

where  $0 \leq x \leq L_1$ .

$$\begin{aligned} \delta_2(x) &= w_2(x) + x \cdot \sin(\varphi_A + \varphi_B + w'_1(L_1)) = \\ &= \delta_1(L_1) + \frac{M(0)}{E_1 I_1 a^2} [\cosh ax - 1] + \frac{V(0)}{E_1 I_1 a^2} [\cosh ax - 1] + \frac{q_u}{N(x)} \left[ \frac{\cosh ax - 1}{a^2} - \frac{x^2}{2} \right] + \\ &+ x \cdot \sin(\varphi_A + \varphi_B + w'_1(L_1)) \end{aligned} \quad (3.13)$$

where  $0 \leq x \leq L_2$ .

The Equations 3.12 and 3.13 include three major unknowns: The angles  $\varphi_A$  and  $\varphi_B$  of the two flexible joints and shear force  $V_1(0) = V_A$ , that belong to the part of the pipeline prior the hinge at point A, which is not analysed. Furthermore, at each position of the pipeline is required the knowledge of the axial force  $N(x)$ . Thus, to solve the problem, the following four balanced and continuity equations are used:

- (1) The momenta at flexible joint B should be equal to the inner moment of the joint:

$$M_1(L_1) = -M_B = C_r \cdot \varphi_B \approx 0 \quad (3.14)$$

- (2) Because of symmetry, the moment at the intersection position with the fault must be equal to zero:

$$M_2(L_2) = 0 \quad (3.15)$$

- (3) The sum of the transverse displacements must be equal to the total transverse displacement imposed by the fracture, and more specifically, because of symmetry:

$$\delta_2(L_2) = \delta_1(L_1) + w_2(L_2) = dy/2 \quad (3.16)$$

- (4) The axial force can result from the compatibility of deformations of the entire pipeline, in other words the equality of the elongation imposed on the pipeline due to fault's displacement (required elongation  $\Delta L_{req}$ ) and the elongation

resulting from the developed stress in the pipeline (obtainable elongation  $\Delta L_{av}$ ):

$$\Delta L_{req} = \Delta L_{av} \quad (3.17)$$

From the usage of equation 3.17 can analytically calculate the horizontal force  $N_{\Gamma}$  at the area where the pipeline and the fracture meet as a function of angles  $\varphi_A$  and  $\varphi_B$ , and then the loading distribution with distance from the fault according to the following relationship:

$$N(x) = \begin{cases} N_{\Gamma} - (L_2 - x)t_u & \text{for bar } B\Gamma \\ N_B - (L_1 - x)t_u & \text{for bar } AB \end{cases} \quad (3.18)$$

More specifically, the required elongation is taken equal to

$$\Delta L_{req} = \Delta x + 2 \left( \frac{L_1}{\cos \varphi_A} - L_1 \right) + 2 \left( \frac{L_2}{\cos(\varphi_A + \varphi_B)} - L_2 \right) \quad (3.19)$$

which is equal to the one resulting by the fault's horizontal displacement  $\Delta x$  and the required elongation due to the rotation of the pipeline's segments AB and B $\Gamma$ .

The available elongation  $\Delta L_{av}$  is resulting from the integration of the axial deformations along the part of the pipeline where relative sliding with the surrounding soil exists. In other words the anchored length is given by the formula:

$$\Delta L_{av} = 2 \int_0^{L_{anch}} \varepsilon(L) dL \quad (3.20)$$

where L is the distance from the fault and factor '2' express the fact that elongation occurs in both sides of the fault.

Since the surrounding soil exerts a frictional force  $\tau_u$  along the pipeline, the anchored length is equal to:

$$L_{anch} = \frac{F_a}{\tau_u} = \frac{\sigma_a A_s}{\tau_u} \quad (3.21)$$

where  $F_a$  and  $\sigma_a$  are the axial force and stress respectively, which are developed at intersection position of the fault and the pipeline, as well as the axial stress of the pipeline at a distance L from the fault is:

$$\sigma(L) = \sigma_a - \frac{\tau_u}{A_s} L \quad (3.22)$$

The axial stress developed in the pipeline is found in two ways, depending on whether its value is less or greater than  $\sigma_1$  (yield point). Regarding the bilinear model of Figure 3.2 for the material of the stainless steel pipeline, in the case that the stress  $\sigma_\alpha$  is lower than  $\sigma_1$ , so only elastic deformations are produced in the pipeline due to the axial force, then:

$$\Delta L_{av} = 2 \int_0^{L_{anch}} \frac{\sigma(L)}{E_1} dL = \frac{\sigma_\alpha^2 A_s}{E_1 \tau_u} \quad (3.23)$$

and in order to have the compatibility of deformations  $L_{av} = L_{req}$ , the axial stress at the intersection position with the fault in the case only elastic stresses are developed, it derives that:

$$\sigma_\alpha = \sqrt{\frac{E_1 \tau_u \Delta L_{req}}{A_s}} \quad (3.24)$$

Correspondingly, if the required elongation is greater than the  $\sigma_1$ , and as a result  $\Delta L_{req} > \frac{\sigma_1^2 A_s}{E_1 \tau_u}$ , also plastic deformations are developed due to the axial stress and the equation 3.20 becomes:

$$\Delta L_{av} = 2 \left[ \int_0^{L_1} \left( \varepsilon_1 + \frac{\sigma(L) - \sigma_1}{E_2} \right) dL + \int_{L_1}^{L_{anch}} \frac{\sigma(L)}{E_1} dL \right] \quad (3.25)$$

where  $L_1$  is the length at which plastic deformations are developed and is equal to:

$$L_1 = \frac{(\sigma_\alpha - \sigma_1) A_s}{\tau_u} \quad (3.26)$$

Applying equations 3.20, 3.21, 3.25 and 3.26, the result is that the axial stress at the position of the intersection with the fault, in the case only plastic deformations are developed, is equal to:

$$\sigma_\alpha = \frac{\sigma_1 (E_1 - E_2) \pm \sqrt{\sigma_1^2 (E_2^2 - E_1 E_2) + E_1^2 E_2 \Delta L_{req} \frac{\tau_u}{A_s}}}{E_1} \quad (3.27)$$

Regardless of whether  $\sigma_\alpha$  is found by Relationships 4.24 or 4.27, the axial force  $F_\alpha$  at the intersection position of the pipeline and the fault is:

$$F_\alpha = \sigma_\alpha A_s \quad (3.28)$$

As mentioned above, due to the complex form of the other analytical relationships, for the final solution was applied a simple numerical methodology, in which at each step there is a small corrections of the three magnitudes. Specifically, regarding  $\phi_A$ ,  $\phi_B$  and

$V_A$ , the following initial values in the first step were taken:  $\varphi_A = 0.1^\circ$ ,  $\varphi_B = 2.0^\circ$  and  $V_A = 100\text{kN}$ . On the following steps  $\varphi_A$ ,  $\varphi_B$  and  $V_A$  are increased or reduced by a small percentage of error in the computation of  $d_y-\delta_2(L_2)$ ,  $M_2(L_2)$  and  $M_1(L_1)$  respectively.

**Step 2: Calculation of maximum stresses, deformations and Current Modulus of Elasticity**

When the pipeline is in the plastic section under the simultaneous action of axial and bending forces, the deformations differentiate and are not only direct function of stress values, but also function of their distribution in the cross section. The Figure 4.7 shows an indicative distribution of stress and strain, in case only one part of the section has yielded (theory of flat section).

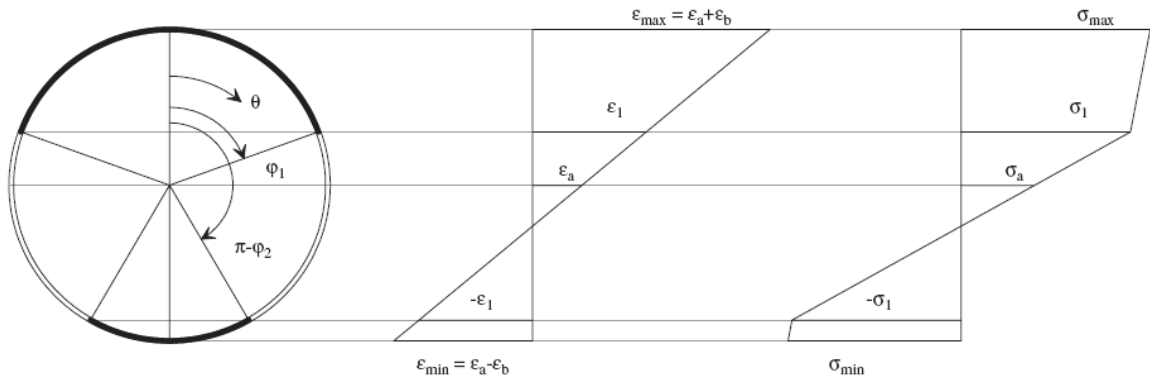


**Figure 3.7:** Distribution of stress and strain along the height of cross-section (by Karamitros et al., 2007)

In order to find the maximum stress & strain, is selected the most adverse section of each bar, which are the sections in which the maximum moment is developed, and the stress distribution that must exist in order to develop the particular combination of moment and axial force, regarding the theory of section flatness. Then the system is solved:

$$N = \int_{-R}^{+R} \sigma(z) dz \tag{3.29}$$

$$M = \int_{-R}^{+R} z \cdot \sigma(z) dz \tag{3.30}$$

where the stress can be compute through deformations using the Equation 4.31, which follows the bilinear law that was presented in Figure 3.2. Moreover, it was considered

that the deformation has an average value of  $\varepsilon_\alpha$ , and varies linearly with distance from the center of the cross section  $z$  according to Equation 3.32. Hence:

$$\sigma(z) = \frac{(E_1 - E_2)\varepsilon(z)}{\left[1 + \left(\frac{(E_1 - E_2)\varepsilon(z)}{\sigma_1}\right)^r\right]^{1/r}} + E_2\varepsilon(z) \quad (3.31)$$

$$\varepsilon(z) = \varepsilon_\alpha + kz \quad (3.32)$$

The solution in this case is done iteratively correcting at each step the values of  $\varepsilon_\alpha$  and  $k$  until to verify the Relationships 4.29 and 4.30.

**Step 3: Correction of the current modulus of elasticity and repetition of the process.**

Due to the fact that all the calculations so far have been assuming that the pipeline behaves elastically, on that step the current modulus of elasticity  $E_{cur}$  is found for each bar by using the Equation 3.33 and the computations are repeated for steps 1 and 2 until the system balance.

$$E_{cur}^{i+1} = \frac{E_{cur}^i + \frac{\sigma_\alpha}{\varepsilon_\alpha}}{2} \quad (3.33)$$

So, at the end of the iterative solution process that was described above, all the parameters and its values needed for the design of joints and pipeline are available. Specifically on **Step 1** the following are calculated:

- values of angles  $\varphi_A$  and  $\varphi_\Gamma$ ,
- the shear forces  $V_A$ ,  $V_B$  and  $V_\Gamma$ ,
- the axial forces  $N_A$ ,  $N_B$  and  $N_\Gamma$ .

and flexible joints must be chosen so as to have:

- ability to rotate:  $\varphi_K = SF * \max(\varphi_A, \varphi_B)$
- shear resistance of joint:  $V_K = SF * \max(V_A, V_B, V_\Gamma)$
- resistance to axial force:  $N_K = SF * \max(N_A, N_B, N_\Gamma)$

where SF are the factors of safety regarding with existing regulations.

όπου SF οι συντελεστές ασφαλείας σύμφωνα με τους ισχύοντες κανονισμούς.

The **Step 2** is about the design of the pipeline, since it gives the unknown moments, stresses and strains of the intermediate sections of the pipeline.

# 4

## Presentation of numerical methodology for strike slip faults

---

### 4.1 General Information

Due to lack of sufficiently substantiated experimental results or historical facts about using flexible joints to eliminate the deformations in the pipeline, the accuracy of the proposed analytical methodology will be checked by conducting numerical analyses. Those numerical analyses should be able to simulate the imposed of large displacements at the intersection between the pipeline and the active fault simulating the elastoplastic behavior of a stainless steel pipeline. Therefore it has been selected to implement the Nonlinear Finite Element Methods using the program ANSYS.

### 4.2 Simulation of pipeline using finite elements

The pipeline was divided into 2-nodal, isoparametric, three-dimensional, elastoplastic, linear pipe elements which have the mechanical characteristics of a cylindrical pipeline, with the required outer diameter  $D$  and wall thickness  $t$ .

On the perimeter of each section are defined eight (8) integration points where the stress and deformations of the pipeline are computed taking into account the contribution of axial forces and bending moments. It has to be mentioned that the internal pressure of the pipeline is not included in the simulation model.

The stress-strain curve that is connected with the **simulation model of a stainless steel pipeline** was inserted in program as a multi-linear curve based on the mathematical relationship Ramberg-Osgood for steel L450 (API X65). So they have

been used 48 line segments for the outputted curve of the material and the Poisson's ratio has been taken equal to 0.20.

Because of the fault rupture **the permanent soil displacement** imposed on the basis of the soil springs, along the section of the pipeline located in the moving segment of the fault. Also it is assumed to ignore the possible favourable effects of soft soil between the pipeline and the bedrock in both numerical and analytical model, because it leads to the distribution of displacement in a form of curve S in the majority of the pipeline length and not pointy. Similarly to the analytical methodology, the total displacement of the strike slip fault is resolved and analysed into two orthogonal components ( $\Delta x$  and  $\Delta Y$ ).

#### Algorithm for Solution of Nonlinear Equations.

Το σύστημα εξισώσεων με το οποίο γίνεται η επίλυση προβλημάτων με τη μέθοδο των Πεπερασμένων Στοιχείων έχει την εξής μητρική μορφή:

$$[K] \cdot \{u\} = \{F^a\} \quad (4.1)$$

where

- $[K]$  stiffness matrix
- $\{u\}$  vector of unknown values of degrees of freedom
- $\{F^a\}$  vector of imposed loads

The stiffness matrix  $[K]$  is a function of the unknown degrees of freedom or their derivatives, as a result the Relationship (4.1) is not linear and so in order to solve it we use the iterative method Newton-Raphson (Figure 4.1), which is described by the following equations:

$$[K_i^T] \cdot \{\Delta u_i\} = \{F^a\} - \{F^{nr}\} \quad (4.2)$$

$$\{u_{i+1}\} = \{u_i\} - \{\Delta u_i\} \quad (4.3)$$

where

- $[K_i^T]$  The tangential stiffness matrix
- $i$  The indicator of the current iteration
- $\{F^{nr}\}$  The vector of nodal actions needed to balance the internal tensions of the elements.

In each iteration the  $[K_i^T]$  and  $\{F^{nr}\}$  are found as a function of the values of  $\{u_i\}$ . Thus, the right part of the Relationship (4.2) shows the deviation of the final solution since it is essentially the residual vector (off-balanced) loads.

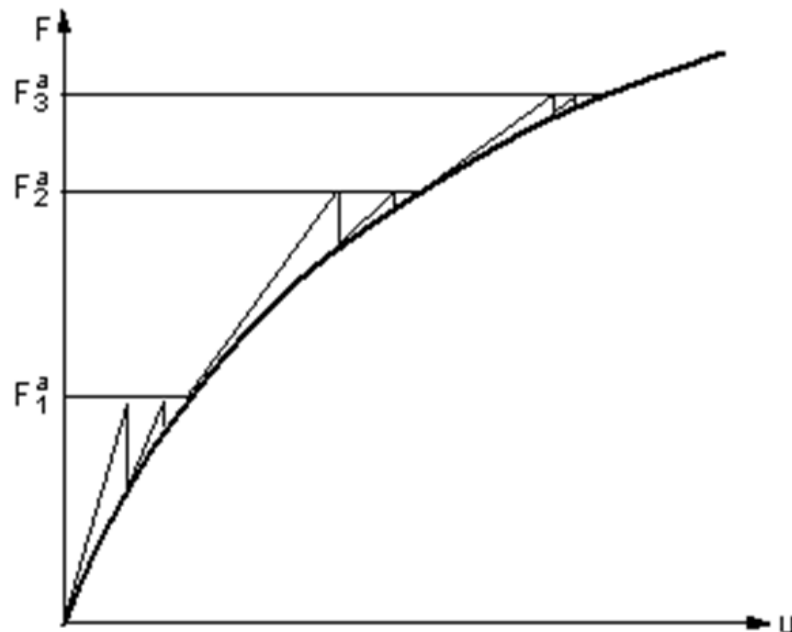
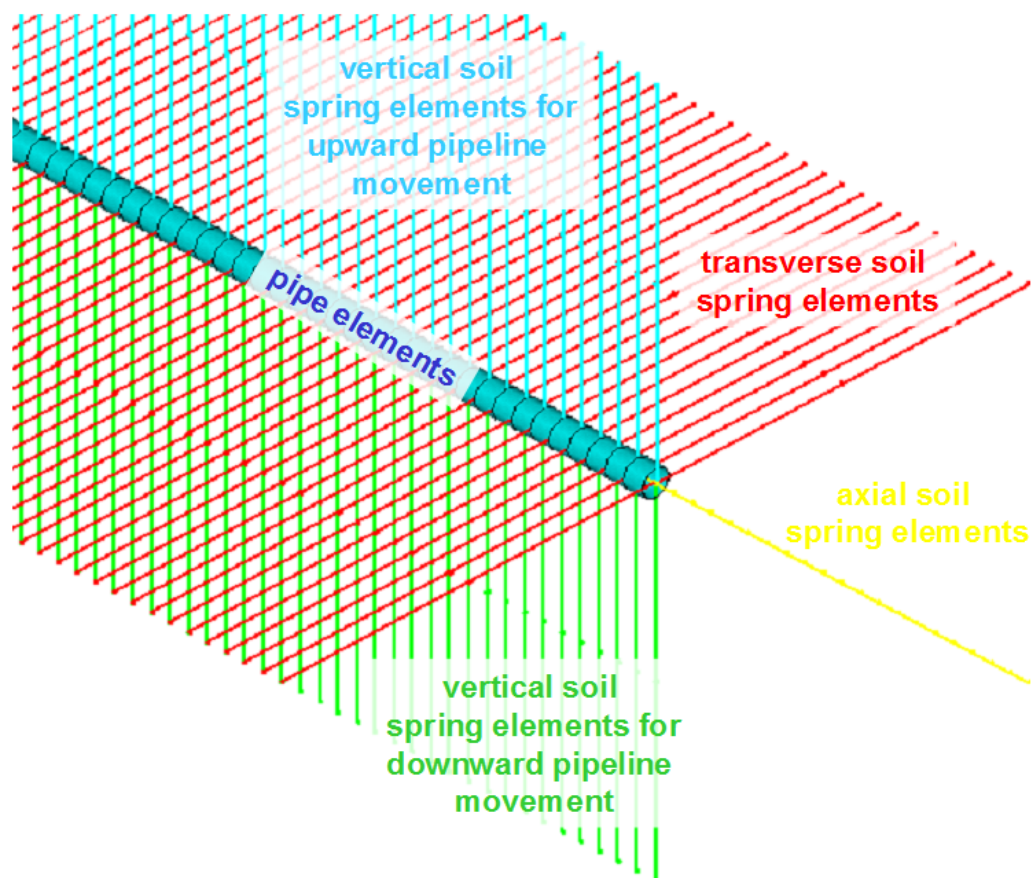


Figure 4.1: Newton-Raphson incremental method

### 4.3 Soil simulation

The interaction of the soil with the pipeline is simulated with five elastoplastic springs per section, the four of which are located in both transverse directions, y and z, and one in the axial direction x of the pipeline, (Figure 4.2), with the free edge of each spring having fixed end support. In addition, the same parameters are used for soil springs on the analytical solution and numerical as well, in order to be compatible to each other.





**Σχήμα 5.2:** Simulation of the interaction of soil pipeline with elastoplastic springs

It is also assumed that the pipeline is disposed within the trench filled with the proper type of backfill in order to make it possible to fully develop the failure of soil into this trench. Thus the springs do not match to the properties of natural soil, but to the backfill material (loose to medium dense sand).

The numerical analyses that carried out was considered that the pipeline is placed at a depth of 1.20m in fine quartz sand with the following properties:

Bulk density:	$\gamma = 18\text{kN/m}^3$
Internal friction angle:	$\varphi = 36^\circ$
Angle of friction between pipeline and soil:	$\delta = 24^\circ$
Coefficient of neutral earth pressure:	$K_0 = 0,50$

### ❖ Axial Springs

The limit axial spring forces correspond to friction exerted on the outer cylindrical surface along the pipeline and are calculated based on theories similar to those implemented on simulating the load transfer in axially loaded pileline-soil interfaces. Regarding with sands and other non-cohesive soils (e.g. gravel), such forces shall be taken after the integration of shear stress along the interface pipeline - soil. So for an entirely buried pipeline the maximum axial resistance  $t_u$  per unit length is given by:

$$t_u = \frac{\pi \cdot D}{2} \cdot \gamma \cdot H \cdot (1 + K_0) \cdot \tan \delta \quad (4.4)$$

where

$K_0$	coefficient of neutral earth pressure
$H$	distance from the soil surface until the center of the pipeline cross-section
$D$	external pipeline diameter
$\gamma$	backfill specific weight
$\delta$	angle of friction between pipeline and backfill

The friction angle  $\delta$  is equal to 50÷100% of the friction angle of the fill, depending on the surface roughness of the pipeline. In numerical solution it has been chosen for the horizontal springs a mean angle  $\delta=2/3\phi$ .

The maximum axial resistance is initially achieved at a relative displacement  $x_u$  approximately at 2.5 to 5.0 mm (0.1 to 0.2 in), for dense to loose sands respectively (Singhal, 1980), while for the springs that have been used was obtained relative displacement equal with 3.0mm (0.12in).

### ❖ Transverse Horizontal Springs

The transverse horizontal springs are a simulation of the surrounding soil's resistance in any horizontal displacement of the pipeline. So the mechanisms of interaction of soil and pipeline are similar to those of the vertical anchor plates or foundations that move horizontally on the surrounding soil, thus triggering a mechanism of passive earth pressures.

For non-cohesive soils, the relationship between the force  $p$  per unit length of the pipeline and the horizontal displacement  $y$ , is expressed by the form (Trautmann & O'Rourke,1983):

$$p = \frac{y}{A + B \cdot y} \quad (4.5)$$

where

$$A = 0,15 \cdot y_u / p_u$$

$$B = 0,85 / p_u$$

$$p_u = \gamma \cdot H \cdot N_{qn} \cdot D$$

$N_{qn}$  = Horizontal bearing capacity factor computed by Figure 4.4 (Trautmann & O'Rourke,1983).

$$y_u = (0,07 \div 0,10) \cdot (H + D/2) \quad \text{for loose sand or}$$

$$y_u = (0,02 \div 0,03) \cdot (H + D/2) \quad \text{for dense sand}$$

To simulate the bilinear elastoplastic relationship in equation (4.5) for  $p=0.5p_u$ , the previous values of  $y_u$  should be multiplied by 0.26.

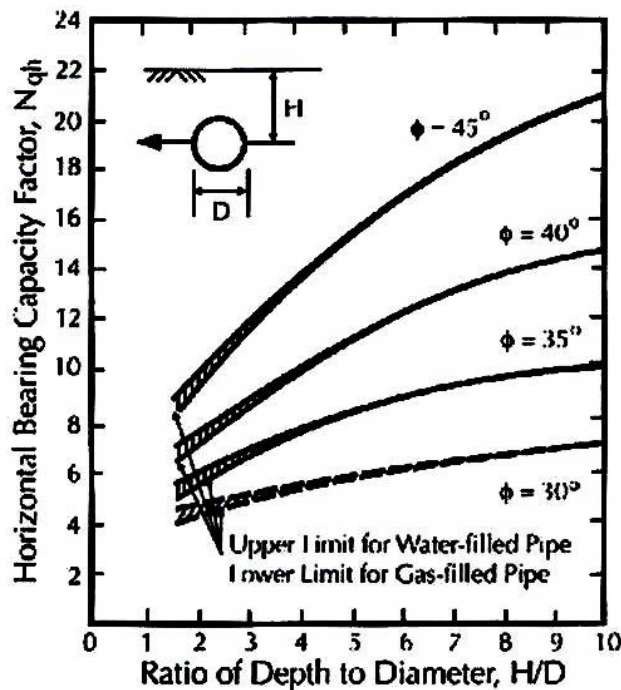


Figure 4.3: Horizontal bearing capacity factor according to Trautmann & O'Rourke (1983)

❖ Vertical Transverse Springs

Concerning with the transverse vertical springs, soil resistance forces are unbalanced, since the result for the "downward" and the "upward" ground movement is different due to the significantly lower resistance of the relatively thin layer of backfill located over the pipeline.

Regarding with the downward movement of the pipeline is considered to act as a cylindrical foundation – strip foundation and the maximum soil resistance  $q_u$  per unit length is given by the conventional bearing capacity theory. As a consequence for non-cohesive soils force the maximum soil resistance is computed by the following equation:

$$q_u = \gamma \cdot H \cdot N_q \cdot D + 0,5 \cdot \gamma \cdot D^2 \cdot N_\gamma \quad (4.6)$$

όπου

$N_q, N_\gamma$  bearing capacity factors for strip foundations that are loaded vertically downwards. They are computed from Figure 4.4 as a function of the friction angle  $\phi$  (Meyerhof, 1955)

$\gamma$  backfill specific weight

$H$  depth from the ground surface to the pipe axis

$D$  outer diameter of the pipeline

Assuming a bilinear elastoplastic load-displacement relationship for fully buried pipelines, the displacement when the pipe enter in the yield area is in the range of 10% to 15% of the pipeline diameter ( $z_{u,dn} = 0.10D \div 0.15D$ ), for dense to loose sands, respectively .

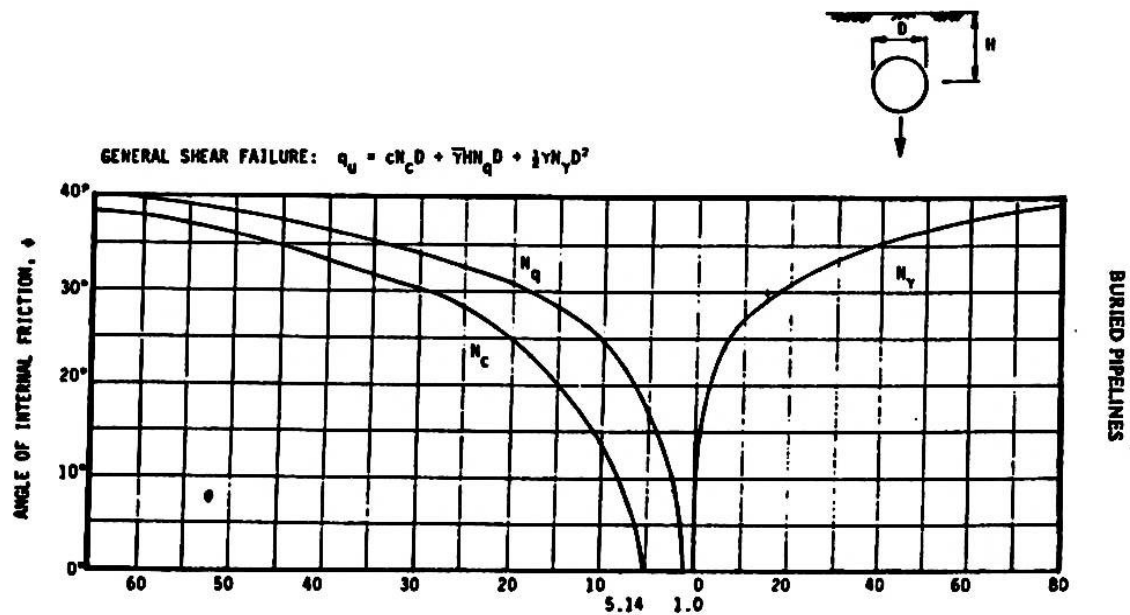


Figure 4.4: Coefficients of vertical (downward) load bearing capacity, according to Meyerhof (1955)

Regarding upward movement direction based on tests performed on pipelines buried in dry uniform sand, it has been exposed that the following relation that connect the  $q$  force and the vertical upward displacement  $z$  (Trautmann & O'Rourke 1983):

$$q = \frac{z}{A + B \cdot z} \quad (4.7)$$

where

$$A = 0,07 \cdot z_u / q_u$$

$$B = 0,93 / q_u$$

For non-cohesive soils the maximum resistance to vertical upward displacement is expressed as (Trautmann & O'Rourke, 1983):

$$q_u = \gamma \cdot H \cdot N_{qv} \cdot D \quad (4.8)$$

where the coefficient  $N_{qv}$  is given in Figure (4.5) as a function of the ratio of the depth  $H$  of the axis pipeline to the diameter  $D$  and friction angle of the backfill  $\phi$ .

For the calculation of the springs based on the two groups of curves of figure (4.5), we use the dashed lines, in order to increase the resistance imposed on the lateral displacement of the pipeline and thus to the developed stresses and deformations.

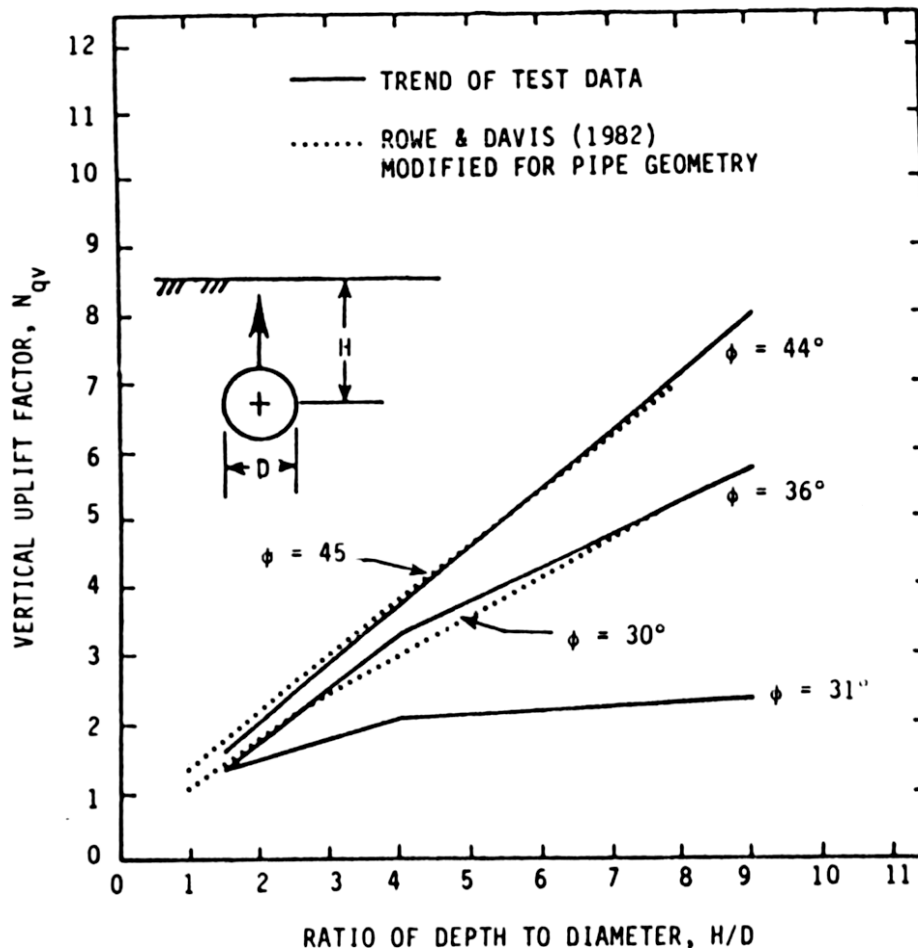


**Figure 5.5:** Coefficients of vertical (upward) load carrying capacity according to Trautmann & O'Rourke (1983)

Based on field tests (Esquivel-Diaz, 1967, Trautman and O'Rourke 1983) the value of upward displacement required in order to enter in yield area is  $z_{u,up}=(0.010\div 0.015)$  for dense to loose sands, respectively. If is adapted to the relationship 4.5 a bilinear elastoplastic expression for  $q=0.50q_u$ , the  $z_{u,u}$  factor should be multiplied by 0.13 approximately.

The limit values of load and yield displacements of the springs used in the numerical simulation of the problem are summarized in Table 4.1.

**Table 4.1:** Characteristics of soil springs used in numerical analyses

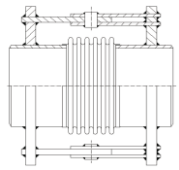
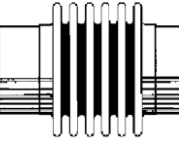
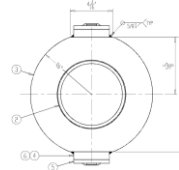
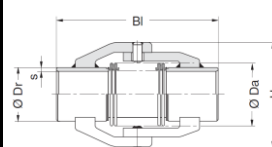
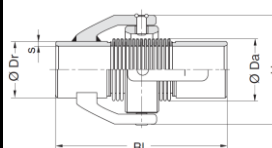
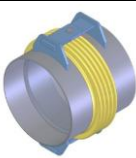
	<b>External pipe diameter, D (mm)</b>	762.0
<b>AXIAL SPRINGS</b>	Ultimate load $t_u$ (kN/m)	22.75
	Yield displacement $x_u$ (mm)	3.0
<b>TRANSVERSE SPRINGS</b>	Ultimate load $p_u$ (kN/m)	134.45 ( $N_{qh}=6.2$ )
	Yield displacement $y_u$ (mm)	35.7
<b>VERTICAL SPRINGS (-UPWARD DIRECTION)</b>	Ultimate load $q_u$ (kN/m)	41.20 ( $N_{qv}=1.9$ )
	Yield displacement $z_{u,up}$ (mm)	2.57
<b>VERTICAL SPRINGS (-DOWNWARD DIRECTION)</b>	Ultimate load $q_u$ (kN/m)	1021.83 ( $N_q=37, N_r=42$ )
	Yield displacement $z_{u,dn}$ (mm)	95.3

#### 4.4 Simulation of flexible joints

Commercially available flexible joints that can be used in cases such as the studied one are type «Bellows», whose mechanical properties are presented in Table 4.2. According to these figures, in the Finite Element Analysis program the flexible joints are simulated as specific data type of a Revolute Joints (combination 7). These elements have not got any length and they are able to rotate around an axis with torsional stiffness which can be defined. At the same time it is possible to define a value for the maximum rotation, value that refers either to the “failure” of the joint and as a result it hasn’t got any more the ability to transfer moments, or either to the "locked" of the joint, as a result in this case its rotation value is computed as the maximum one. Regarding the other characteristics of the joint, due to the lack of more accurate data from the manufacturers, the values that have been chosen were corresponding with the straight continuous segments of the pipeline, which are the following:

Axial stiffness of the axis x, y and z:	674310 kN/m
Rotational stiffness to the axis z:	2 kNm/deg
Rotational stiffness relative to the axes x and y:	78000 kNm/deg

Πίνακας 4.2: Characteristics of commercially available flexible joints

A/A	ΠΡΟΣΦΟΡΑ	ΣΧΕΔΙΟ ΚΟΜΒΟΥ	ΚΑΤΑΣΚΕΥΑΣΤΙΚΕΣ ΛΕΠΤΟΜΕΡΙΕΣ								
			P <sub>INT</sub> Σχεδιασμού	Εσωτερική διάμετρος	Δυνατότητα στροφής	Στροφικό ελατήριο	Δυνατότητα αξον. μετακ.	Αξονικό ελατήριο	Δυνατότητα εγκ.μετακ.	Εγκάρσιο ελατήριο	Περιορισμός Μετακινήσεων
1	HKS-angular-expansion joint		1102.3 psi 76.0 bar 7.60 MPa	4.50 in (114.3 mm)	5°	146Nm/° 1292.2 lbin/°	N/A	N/A	N/A	N/A	Περιορισμός αξονικής και εγκάρσιας μετακίνησης
2	US-BELLOWS Single Expansion joint		150 psi 10.3 bar 1.03 MPa	4.50 in (114.3 mm)	10°	4.7 Nm/° 42 lb in/°	1.05 in	92 kN/m 816 lb/in	0.30 in	161 kN/m 1429 lb/in	Κανένας
3	US-BELLOWS Hinged Expansion joint		150 psi 10.3bar 1.03MP a	4.50 in (114.3 mm)	20°	8.8 Nm/° 79 lb in/°	N/A	104 kN/m 920 lb/in	N/A	303 kN/m 2685 lb/in	Περιορισμός αξονικής και εγκάρσιας μετακίνησης
4	BOA Group BKT-7510 joints		232 psi 16.0bar 1.60MP a	4.50 in (114.3 mm)	13.5°	8.0 Nm/° 71 lb in/°	N/A	N/A	N/A	N/A	Περιορισμός αξονικής και εγκάρσιας μετακίνησης
5	BOA Group BKT-7610 joints		232 psi 16.0bar 1.60MP a	4.50 in (114.3 mm)	13.5°	8.0 Nm/° 71 lb in/°	N/A	N/A	N/A	N/A	Περιορισμός αξονικής και εγκάρσιας μετακίνησης
6	EAGLE-BURGMANN Hinged Expansion joint		145 psi 10.0 bar 1.00 Mpa	4.50 in (114.3 mm)	20°	4.0 Nm/° 35 lb in/°	N/A	118 kN/m 673.8 lb/in	N/A	584 kN/m 3335 lb/in	Περιορισμός αξονικής και εγκάρσιας μετακίνησης



## 4.5 Typical Results

Bellow is presented in detail the results of two typical indicative analyses:

- The first analysis concerns a fault, which crosses a continuous pipeline without flexible joints in the middle. The angle of the plane of the fault with the horizontal is  $\beta=90^\circ$  and the ratio of the fault displacement to the diameter of the pipeline is  $D_f/D=4$ . To be more specific the overall displacement of the fault is equal to 3m.
- The second analysis concerns a pipeline with 6 flexible joints that are located per 6m in the area around the fault. The fault crosses the pipeline in the middle of the 3<sup>rd</sup> and 4<sup>th</sup> joints and the angle of the plane with the horizontal is  $\beta=90^\circ$ . Also in this case the t ratio of the fault displacement to the diameter of the pipeline is  $D_f/D=4$ . To be more specific the overall displacement of the fault is equal to 3m.

### 4.5.1 Numerical continuous pipeline analysis

The Figures 4.6 and 4.7 present the deformed pipeline. Specifically Figure 4.6 shows the change in rotation of the continuous pipeline, while Figure 4.7 shows the pipeline in the transverse vertical direction. Also in all the figures with dashed vertical black line is presenting the position of the fault.

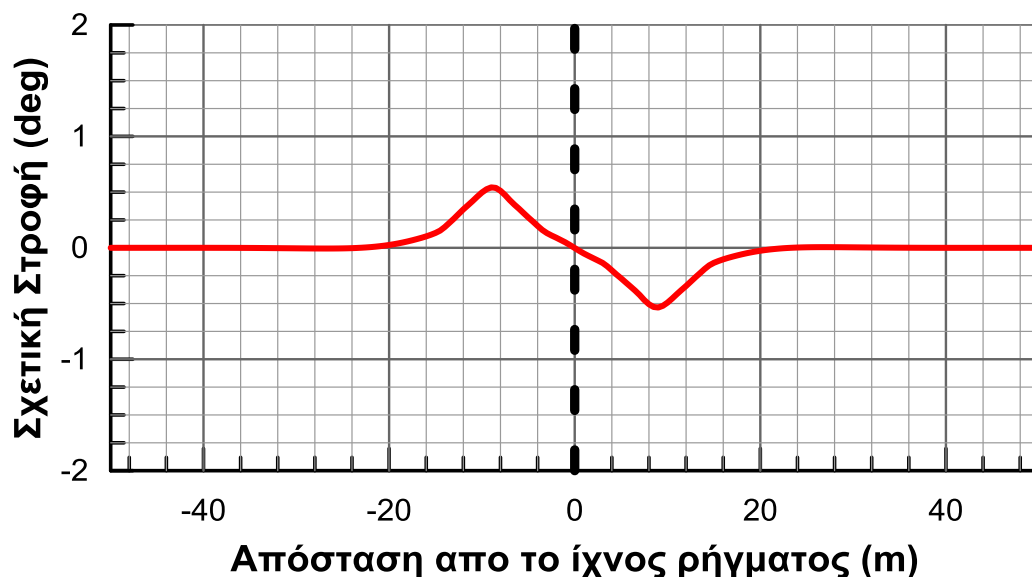


Figure 4.6: Relative rotation along the pipeline

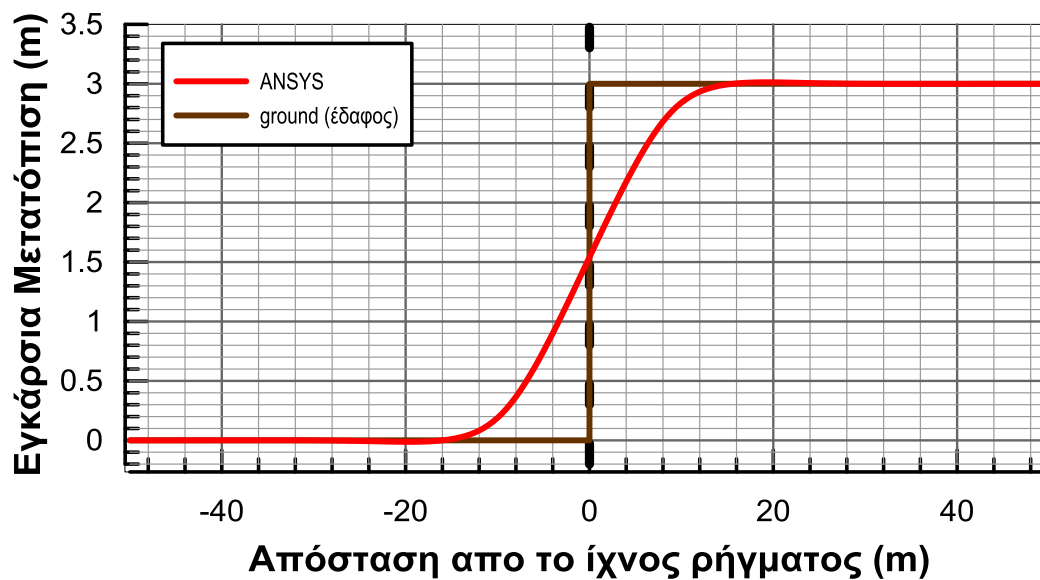


Figure 4.7: Displacements of the pipeline in the transverse vertical direction

The Figures 5.8 and 5.9 show the distribution of the axial forces of the transverse springs (transverse horizontal and transverse vertical) and the distribution of the forces of the axial springs, along the pipeline respectively.

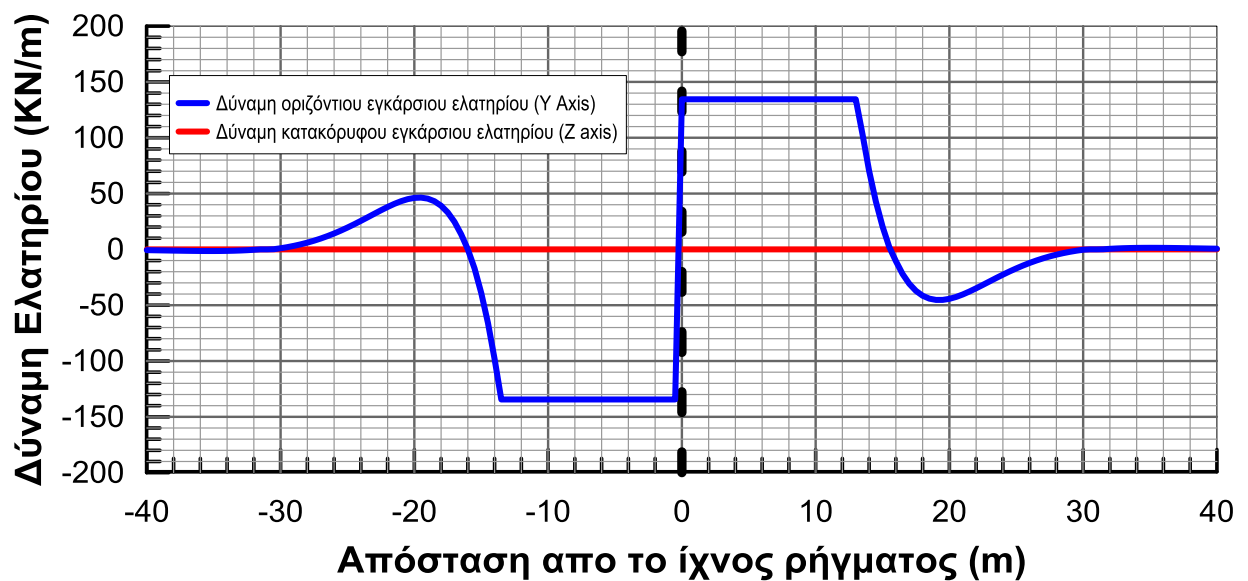
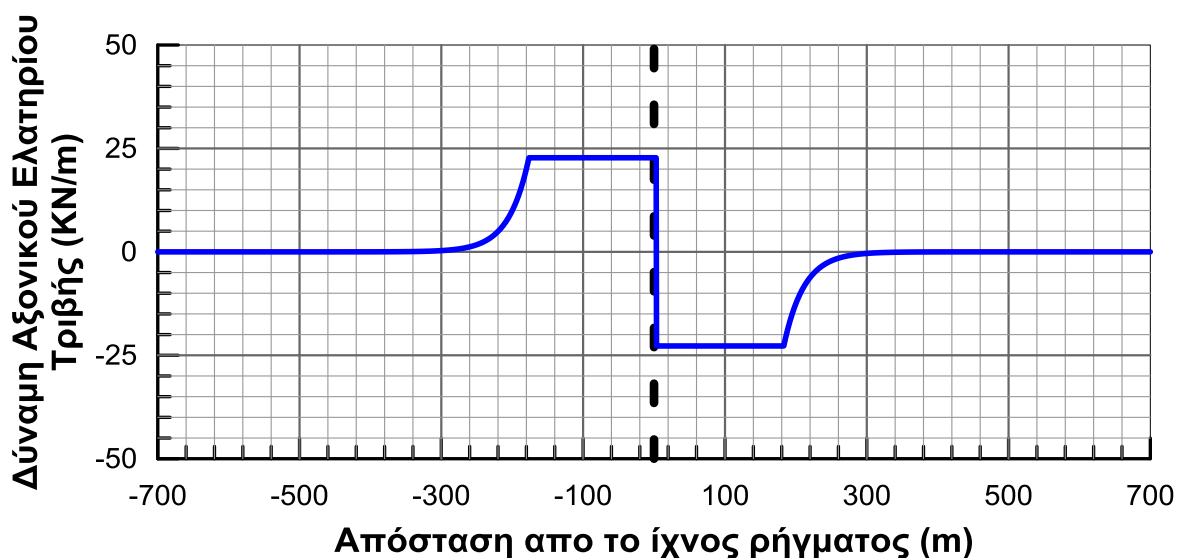


Figure 4.8: Distribution of forces in transverse springs along the pipeline



**Figure 4.9:** Distribution of forces of axial springs along the pipeline

From Figure 4.8 is observed that the curved length of the pipeline, more specifically the length where the pipe is curved and large transverse displacements developed therein, is 30m on both sides of the fault.

From Figure 4.9 is extracted that the anchored length, more specifically the distance to the fault where the relative sliding between the pipe and ground is equal to zero and therefore the imposed deformation are equal to zero as well is 340m.

The Figures 4.10, 4.11 and 4.12 presents the diagrams of distributions of internal forces developed in the pipeline. Specifically Figure 4.10 shows the axial forces along the pipeline, Figure 4.11 presents the shear forces, and Figure 4.12 presents the bending moments. It is observed that the variation of the moments in the area of the fault trace is between -3050kNm up 3090kNm.

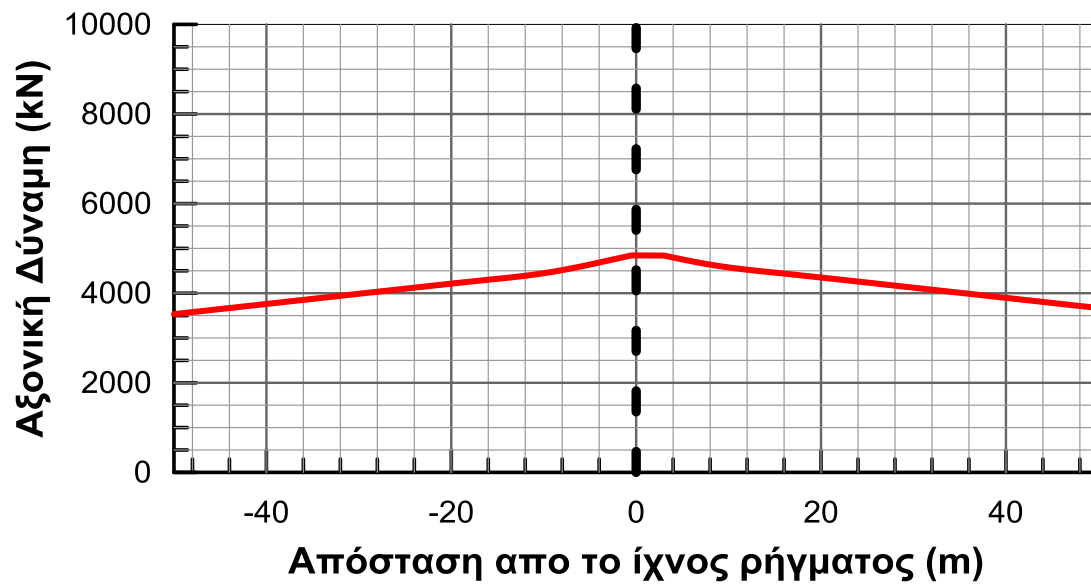


Figure 4.10: Distribution of axial forces developed along the pipeline

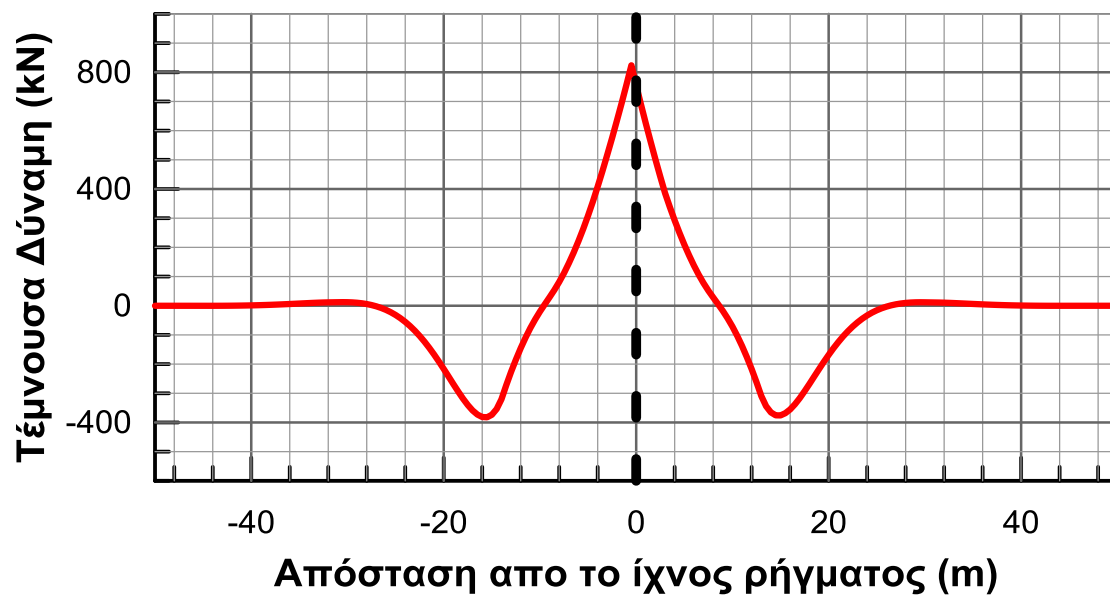


Figure 4.11: Distribution of shear forces developed along the pipeline

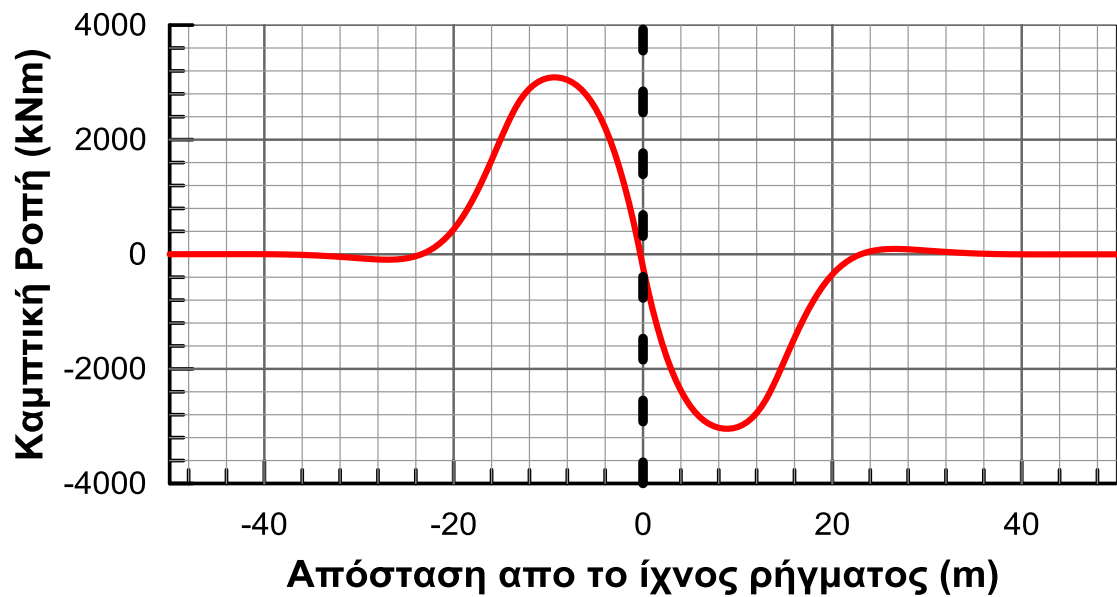


Figure 4.12: Distribution of bending moments developed along pipeline

Figure 5.13: Distribution of bending moments developed along pipeline

Finally in Figures 4.13 and 4.14 is illustrated the distribution of the maximum and minimum stresses and axial deformation, respectively, that are developed along the pipeline.

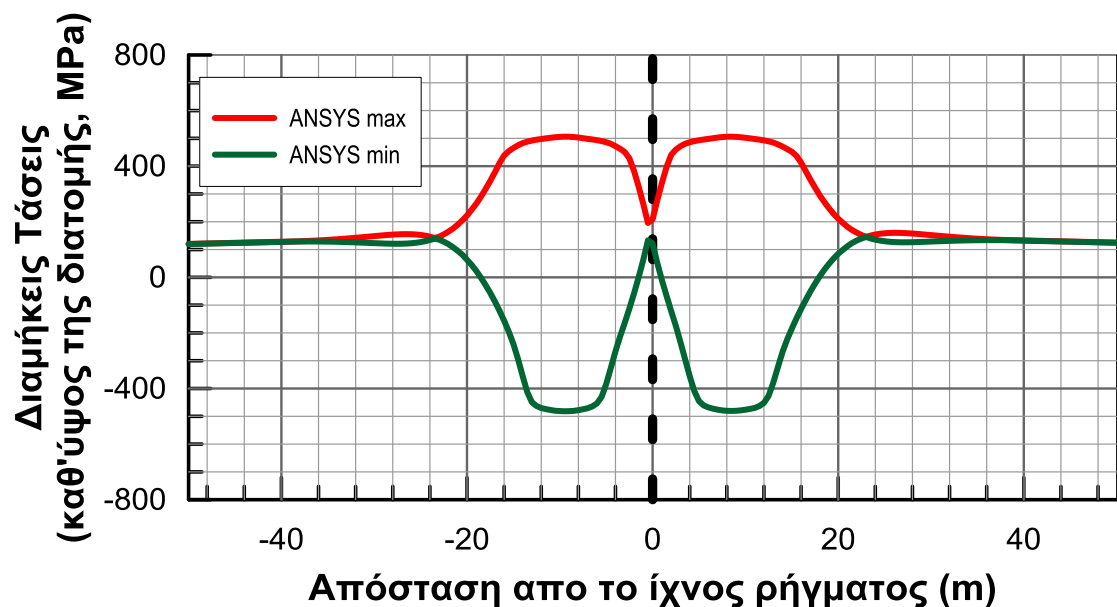
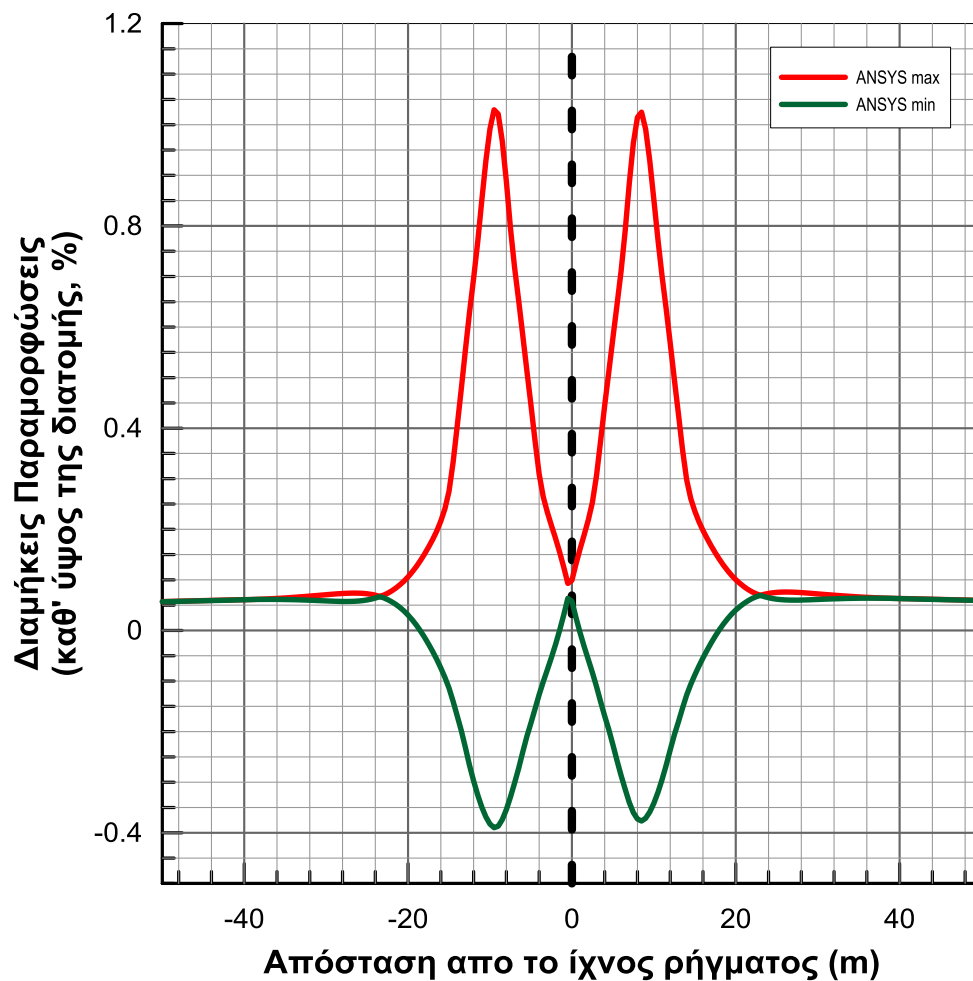


Figure 4.13: Distribution of maximum and minimum axial stress developed along the pipeline



**Figure 4.14:** Distribution of maximum and minimum axial strain developed along the pipeline

It is observed that the axial deformation that is the most common pipeline control criterion is ranged between -0.4% (compressive) to 1.03% (stretching).

#### 4.5.2 Numerical analysis of a pipeline consist of flexible joints

As mentioned above, the analysis is about a pipeline with 6 flexible joints located per 6m in the area around the trace of fault, which intersects the pipeline between of the 3<sup>rd</sup> and 4<sup>th</sup> joints. The angle of the plane of the fracture with the horizontal is  $\beta=90^\circ$  and the overall movement of the fault is equal to 3m.

On Figures 5.15 and 5.16 is illustrated the change in rotation of the pipeline rotations and displacements in the transverse vertical direction, respectively. In all figures the black dotted line marks the site at which the fault intersects with the pipeline, while the positions of the flexible joints are indicated by the gray dashed lines.

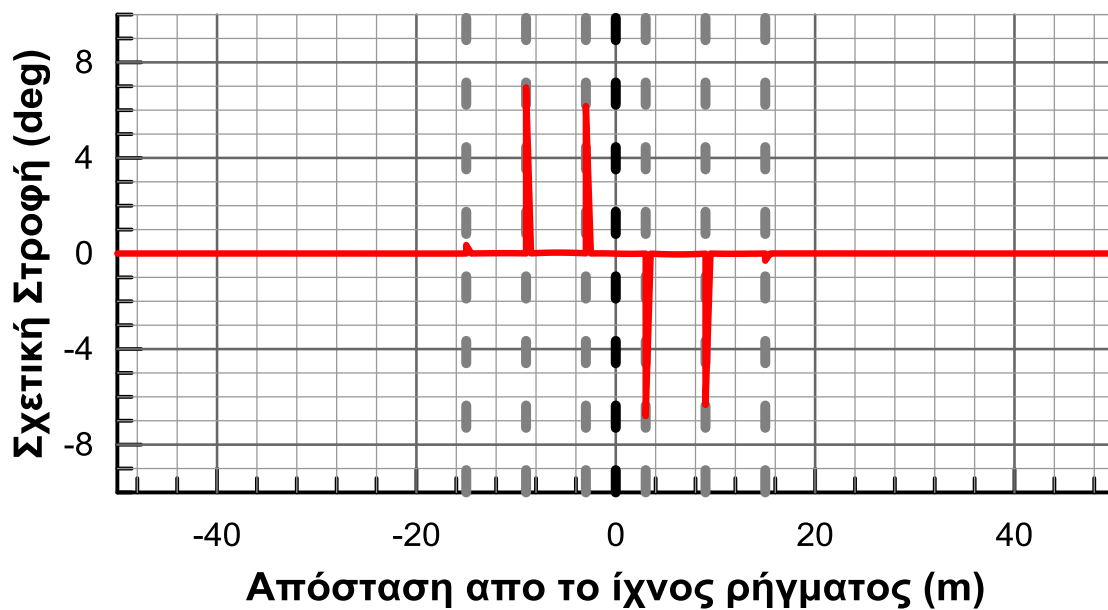


Figure 4.15: Relative rotation along the pipeline

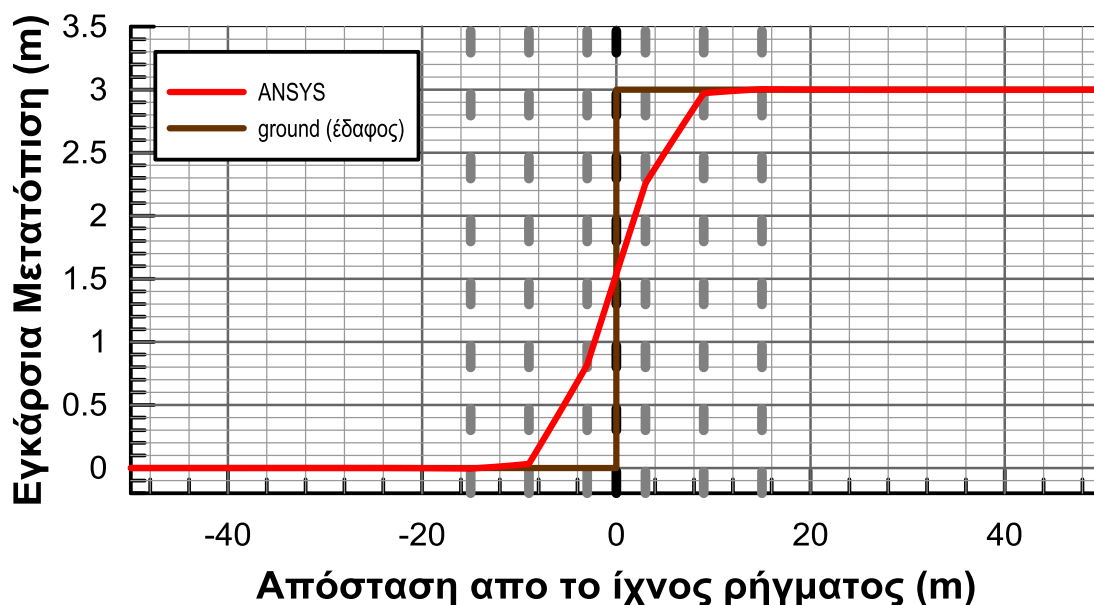


Figure 4.16: Displacements of the pipeline in the transverse direction

In Figures 5.17 and 5.18 is shown the distribution of axial forces of the transverse spring below (transversal horizontal and transverse vertical) as well as the axial springs along the pipeline respectively.

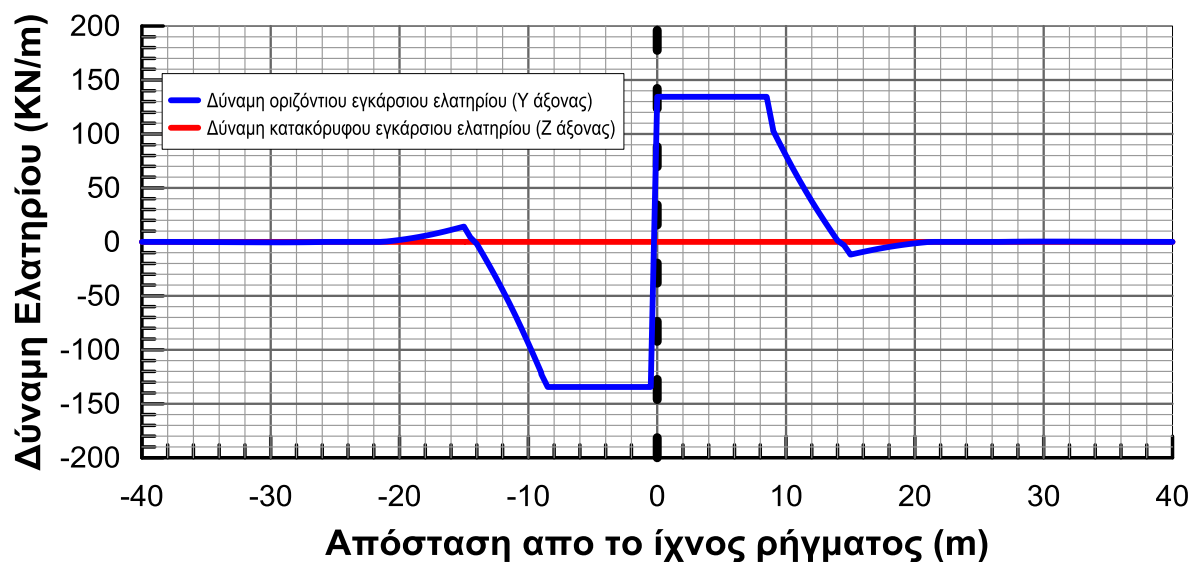


Figure 4.17: Distribution of forces in transverse springs along conduit

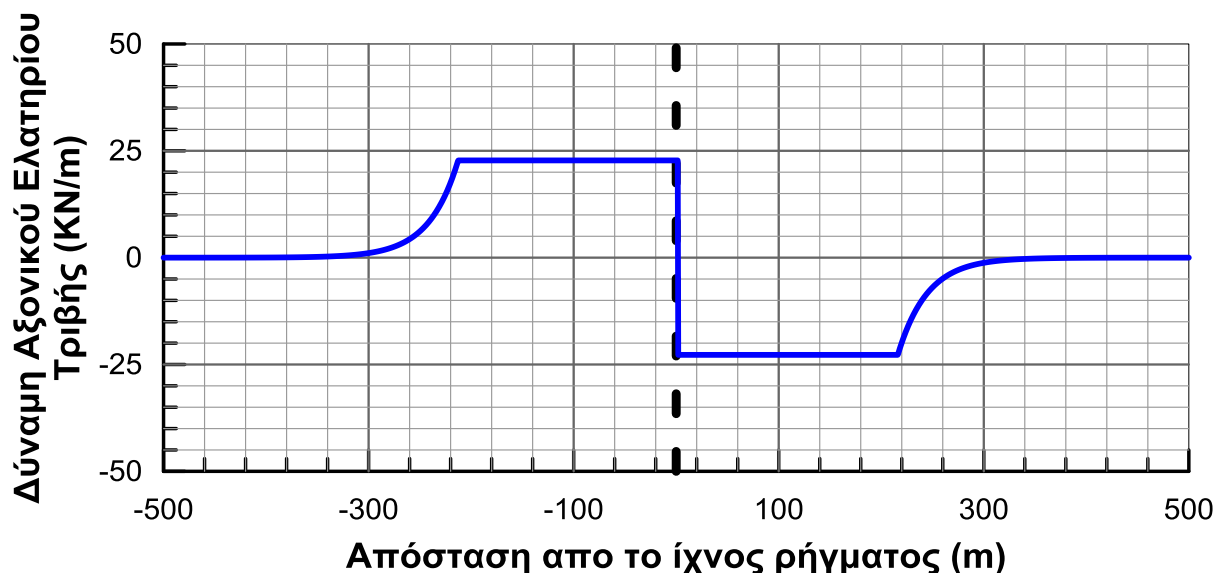


Figure 4.18: Distribution of forces of axial springs along the pipeline

From Figure 4.17 is observed that the curved length of the pipeline that is the length in which the pipeline is curved and large transverse displacements are developed at 23m, on both sides of the fault.

From Figure 4.18 is illustrated that the anchored length, that refers to the distance to the fault where the relative sliding between the pipeline and the soil is equal to zero and therefore the imposed deformation are equal to zero as well, is 340m.



The Figures 4.19, 4.20 and 4.21 illustrate the diagrams of the distributions of axial forces, shear forces and bending moments that are developed in the pipeline, respectively.

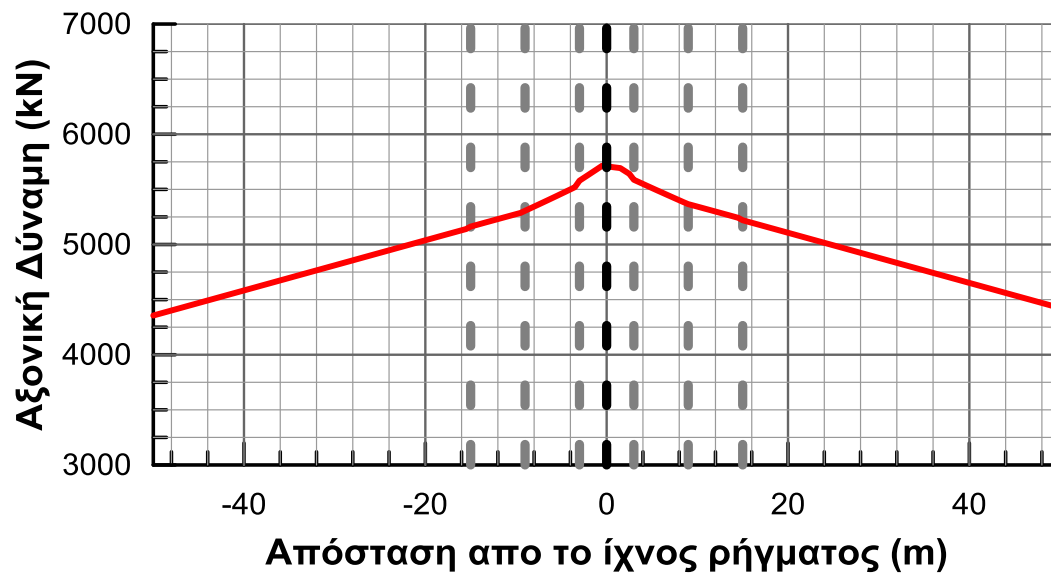


Figure 4.14: Distribution of axial forces developed along the pipeline

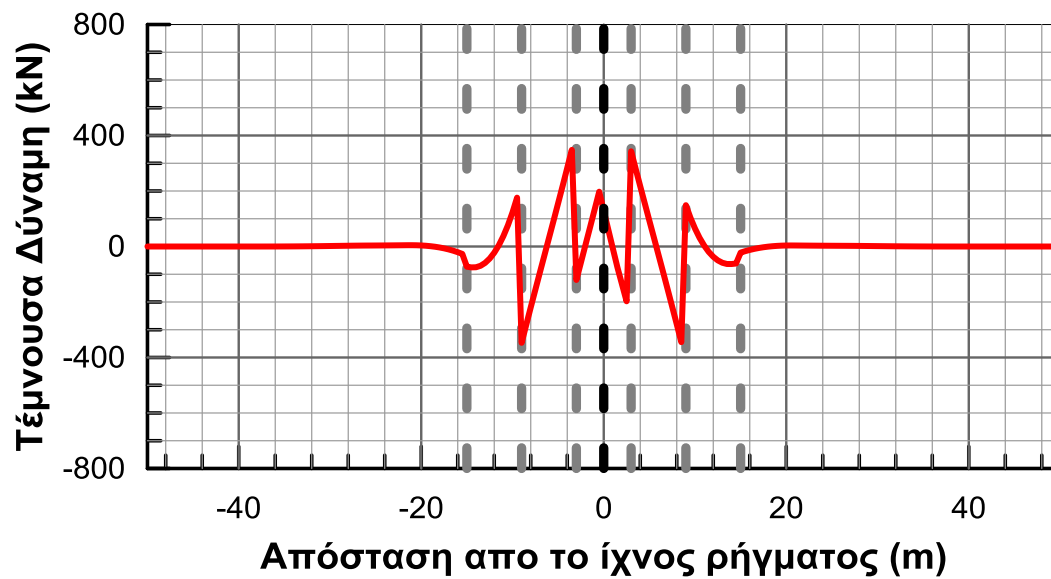
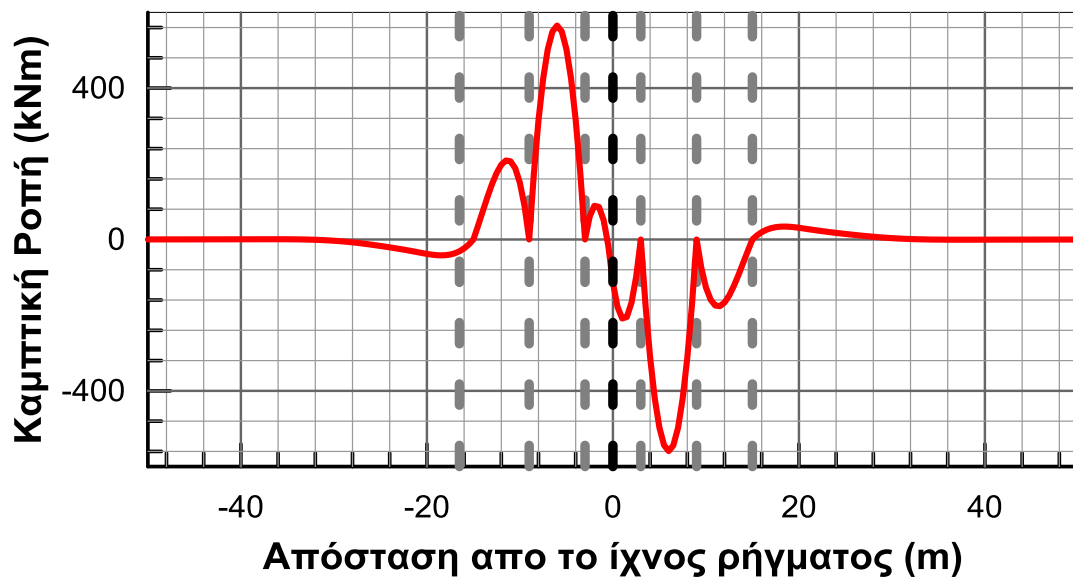
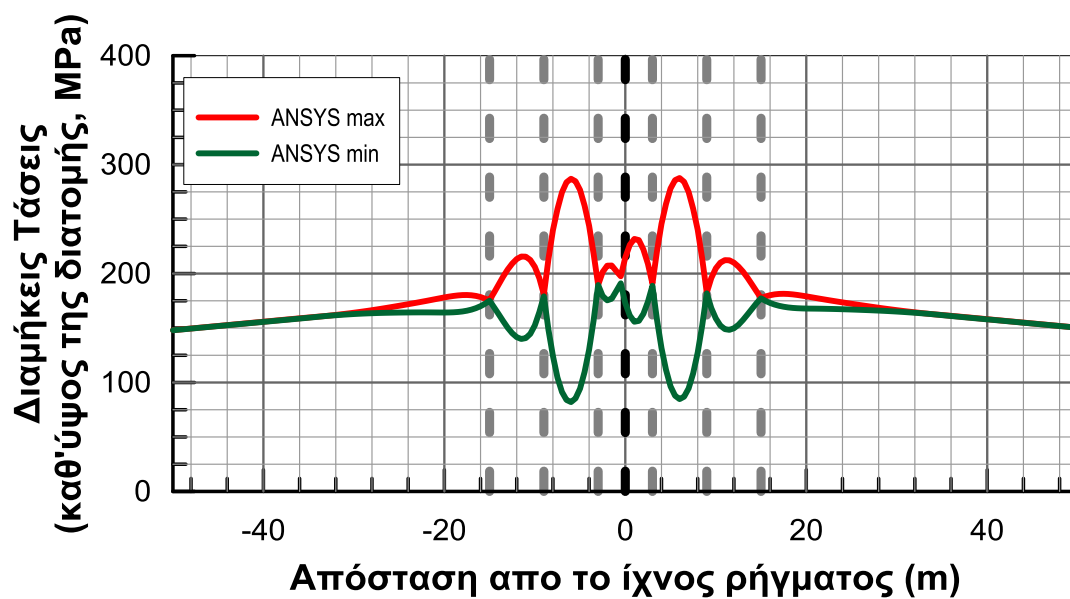


Figure 4.20: Distribution of shear forces developed along the pipeline



**Σχήμα 5.21:** Κατανομή των καμπτικών ροπών που αναπτύσσονται κατά μήκος του αγωγού

It is observed that the range of bending moment is now significantly reduced to -555kNm to 560kNm from -3050kNm up 3090kNm that was before. Additionally in Figures 4.22 and 4.23 is illustrated the distribution of the maximum and minimum stresses and axial deformations, respectively, developed along the pipeline.



**Figure 4.22:** Distribution of maximum and minimum axial stress developed along the pipeline

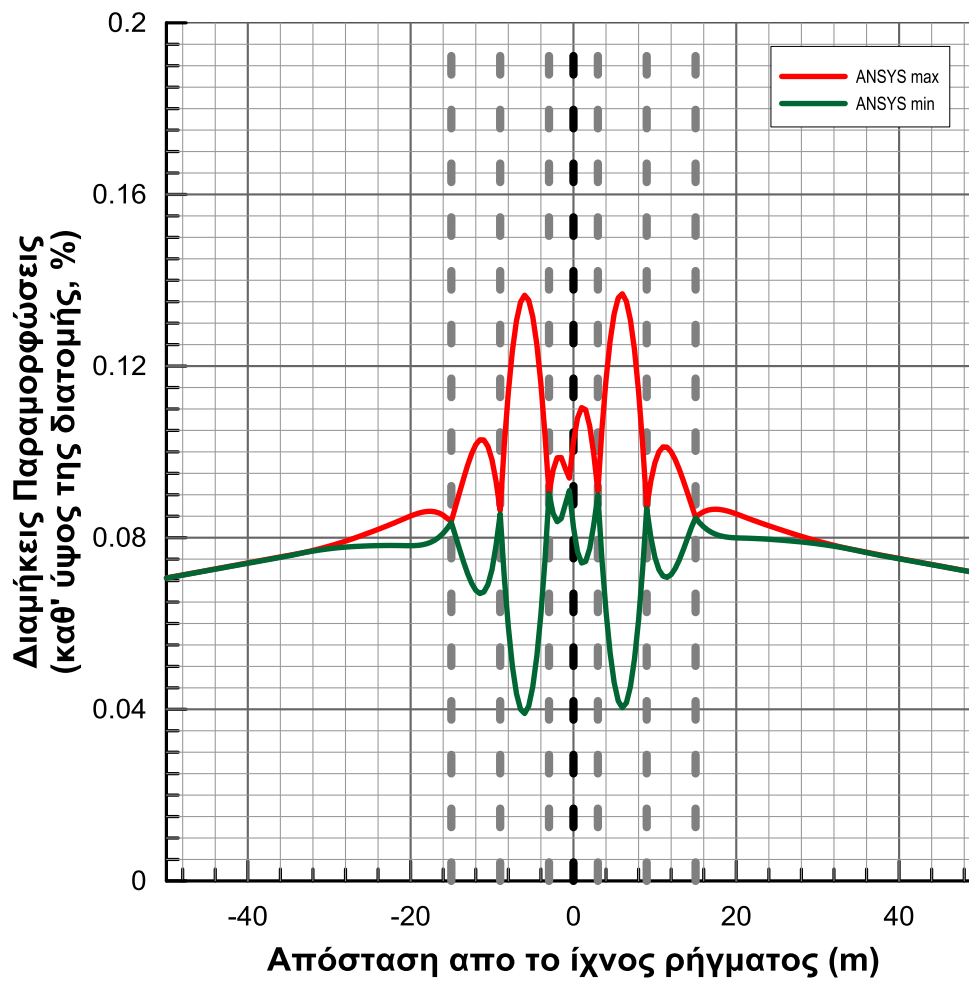


**Figure 4.23:** Distribution of maximum and minimum axial strain developed along the pipeline

It is observed that the axial strain have drastically reduced from -0.04% (compression) to 0.14% (tension), from -0.4% to 1.03% that was ranging before for continuous pipeline.

# 5

## Comparison between the proposed analytical methodology and numerical analysis results

---

### 5.1 Numerical Analysis Presentation

In order to verify the accuracy of the proposed analytical methodology for strike slip faults, presented in detail in Chapter 4, a total of 40 numerical analyses were performed. The pipeline used for the above mentioned analyses had six flexible joints, with 0.762m diameter and wall thickness equal to 12.5mm. The analyses results were compared with the estimated values of the analytical methodology.

The analyses were divided into three groups according to the distance between the flexible joints (6m, 8m, and 12m), and for each group 15, 17 and 8 analyses were performed respectively. The analyses are comprised of the combination of the angle values  $\beta=90^\circ$ ,  $60^\circ$  και  $30^\circ$  and the ratio values  $D_f/D = 1, 2$  and  $4$ , i.e. of a total fault displacement equal to 0.75m, 1.5m and 3m. Taking into consideration that flexible joints are considered to be used in cases of large fault displacements, where conventional design methods are inadequate, the main findings on the methodology will be drawn from the results for the greater fault displacements (1.5m and 3m), while the analyses for fault displacement equal to 0.75m were complementary. The analyses relate to the cases that the fault is crossed: (a) exactly in the middle of the pipeline, between the third and fourth flexible joint or (b) at the edge of the pipeline, just after the third joint.

The specifications and values of the parameters used for each analysis are summarized in the following table. (Table 5.1)

**Table 5.1:**Main characteristics of the performed parametric numerical analyses

A/A	Distance between joints (m)	Cross section place	Angle $\beta$ ( $^{\circ}$ )	Fault displacement (m)	Dx (m)	Dy (m)
<b>FLEXIBLE JOINTS PER 6m</b>						
1	6	In the middle	90	3	0.000	3.000
2	6	In the middle	60	3	1.500	2.598
3	6	In the middle	30	3	2.598	1.500
4	6	At the edge	90	3	0.000	3.000
5	6	At the edge	60	3	1.500	2.598
6	6	At the edge	30	3	2.598	1.500
7	6	In the middle	90	1.5	0.000	1.500
8	6	In the middle	60	1.5	0.750	1.299
9	6	In the middle	30	1.5	1.299	0.750
10	6	At the edge	90	1.5	0.000	1.500
11	6	At the edge	60	1.5	0.750	1.299
12	6	At the edge	30	1.5	1.299	0.750
13	6	In the middle	90	0.75	0.000	0.750
14	6	In the middle	60	0.75	0.375	0.649
15	6	In the middle	30	0.75	0.649	0.375
<b>FLEXIBLE JOINTS PER 8m</b>						
16	8	In the middle	90	3	0.000	3.000
17	8	In the middle	60	3	1.500	2.598
18	8	In the middle	30	3	2.598	1.500
19	8	At the edge	90	3	0.000	3.000
20	8	At the edge	60	3	1.500	2.598
21	8	At the edge	30	3	2.598	1.500
22	8	In the middle	90	1.5	0.000	1.500
23	8	In the middle	60	1.5	0.750	1.299
24	8	In the middle	30	1.5	1.299	0.750
25	8	At the edge	90	1.5	0.000	1.500
26	8	At the edge	60	1.5	0.750	1.299
27	8	At the edge	30	1.5	1.299	0.750
28	8	In the middle	90	0.75	0.000	0.750
29	8	In the middle	60	0.75	0.375	0.649
30	8	In the middle	30	0.75	0.649	0.375
31	8	At the edge	90	0.75	0.000	0.750
32	8	At the edge	60	0.75	0.375	0.649
<b>FLEXIBLE JOINTS PER 12m</b>						
33	12	In the middle	90	3	0.000	3.000
34	12	In the middle	30	3	2.598	1.500
35	12	At the edge	90	3	0.000	3.000
36	12	In the middle	90	1.5	0.000	1.500
37	12	In the middle	60	1.5	0.750	1.299
38	12	In the middle	30	1.5	1.299	0.750
39	12	In the middle	60	0.75	0.375	0.649
40	12	In the middle	30	0.75	0.649	0.375

## **5.2 Comparing the results of analytical and numerical analyses**

Detailed comparisons, for the entire length of the pipeline, are presented in Appendix A diagrams. For each analysis, the fluctuation of the following physical quantities is presented and compared:

- Axial Force
- Shear Force
- Bending moment
- Relative rotation
- Strain
- Stress

In the following pages, the results of the proposed analytical methodology are compared to those of the parametric numerical analyses. The main purpose of this comparison is to validate the accuracy of the proposed analytical methodology, so that the beneficial contribution of joints can be estimated roughly in the future, without the need of complex numerical analyses. The following charts are “1 to 1” diagrams of the main quantities related to the design of a pipeline, i.e. internal forces, stress, strain and the rotation of joints. Additionally, one can derive from the charts the ratio of maximum values of those quantities. Finally, the number accompanying each point on the diagrams, corresponds to the number of each analysis as shown on Table 5.1.

Figure 5.1, includes the “1 to 1” comparison diagrams of the maximum values of Axial Force, considering that the pipeline crosses the fault at an angle of: (a) 90°, (b) 60°, and (c) 30°. The illustrated values of Axial Force resulted from the numerical and analytical calculations.

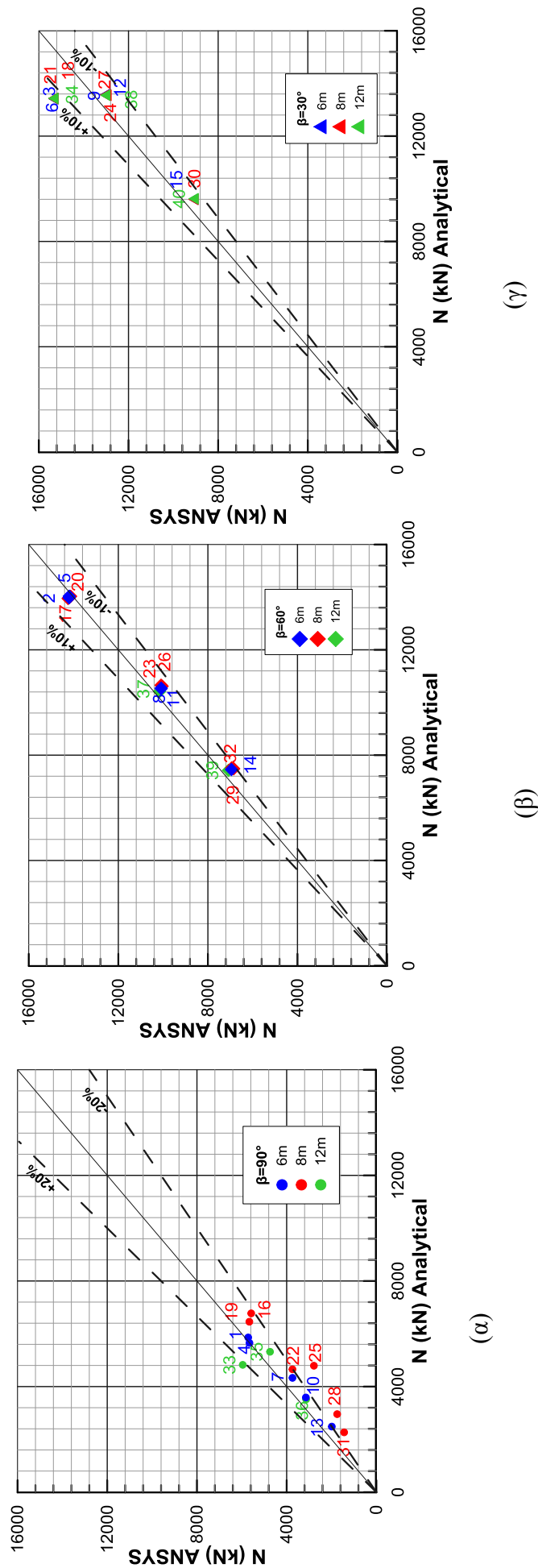


Figure 5.1: Comparison diagrams “1 to 1” of the maximum values of Axial Force, considering that the pipeline crosses the fault at an angle of: (a)  $90^\circ$ , (b)  $60^\circ$ , and (c)  $30^\circ$ .

In general, the values of Axial Force are sufficiently accurate. The standard deviation of the Axial Force, for intersection angles equal to  $60^\circ$  and  $30^\circ$ , reaches up to  $\pm 10\%$  while for intersection angles equal to  $90^\circ$  climbs at  $\pm 20\%$ , with a trend of overestimating the values of the Axial Force. The reason for this increase of the relative error, could be the way Axial Force is calculated. More explicitly, the Axial Force is calculated cumulatively from the applied elongation due to the displacement component  $D_x$  and the elongation due to the curvature of the pipeline, which can only be approximately estimated. As expected, the greater the angle of the pipeline crossing the fault, the lower the value of the Axial Force, since the  $D_x$  component of the fault displacement is decreasing. The smallest values of the Axial Force are expected for an intersection angle equal to  $90^\circ$ , since at this angle they are affected solely by the elongation due to the curvature of the pipeline. Consequently, the same absolute error of the Axial Force due to the curvature of the pipeline for intersection angles  $30^\circ$ - $60^\circ$ - $90^\circ$ , can be easily translated into a greater relative error of the lower – in general- values of the Axial Force, which are encountered when the intersection angle is equal to  $90^\circ$ . Moreover, the charts in Figure 5.1, clearly show that for the same fault displacement, the Axial Force is not affected by the distance between the flexible joints.

Being able to estimate the values of the Axial Force is of great importance to the credibility of the proposed methodology. The smallest under- or over- estimation of its value could lead to reduced or increased stresses respectively. However, in case the stress value exceeds the yield limit  $\sigma_1$  and the pipe enters the plastic zone, the smallest changes in stresses lead to great fluctuation of strain values which affect  $E_{cur}$  and consequently the estimated values of the Bending Moment and Shear Force. Therefore, if the pipe enters the plastic zone due to a small increase of the estimated stress, the overvaluation of strain will be disproportional while the bending moment and shear force will be underestimated.

Figure 5.2, includes the “1 to 1” comparison diagrams of Shear Force, considering that the pipeline crosses the fault at an angle of: (a)  $90^\circ$ , (b)  $60^\circ$ , and (c)  $30^\circ$ . The illustrated values of Shear Force, resulted from the numerical and analytical calculations.



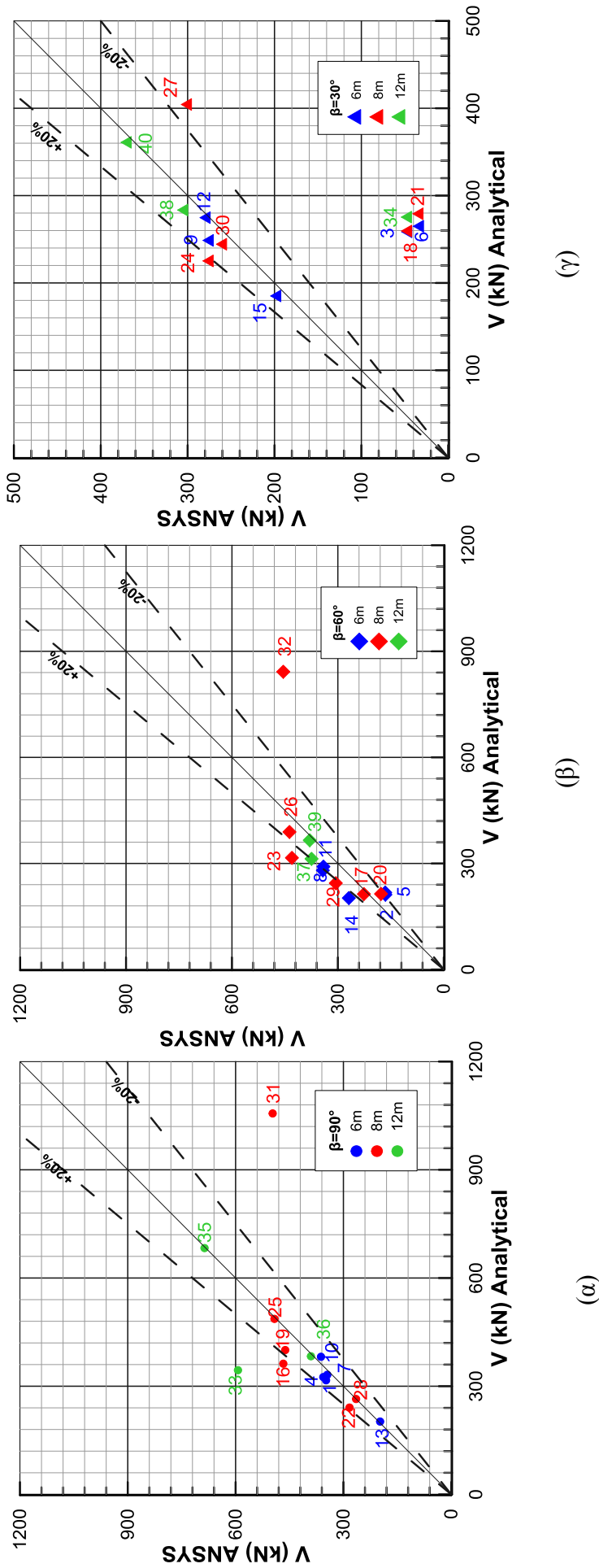


Figure 5.2: Comparison diagrams “1-1” diagrams, comparing the maximum values of Shear Force, while crossing the fault at an angle of: (a)  $90^\circ$ , (b)  $60^\circ$ , (c)  $30^\circ$

It is readily observed that the majority of Shear Force values present a deviation of  $\pm 20\%$ , regardless to the intersection angle. However, analyses 3, 6, 18, 21 and 34 do not comply with the aforementioned deviation, because the analytical values are greater than those estimated through numerical analysis. These analyses correspond to  $30^\circ$  intersection angle and 3m fault displacement. At these particular cases, as shown in Figure 5.1c, a very large Axial Force is developed, which is slightly underestimated by the analytical methodology ( $\sim 14\%$ ). As mentioned above, this insignificant underestimation of the Axial Forces due to the pipeline entering the plastic zone, produces a disproportionately large underestimation of the developed displacements, which in turn results in the overestimation of the elastic modulus  $E_{cur}$ , the bending moments and the shear forces in the pipeline.

It is also observed that analyses 31 and 32 presented in Figures 5.2a and 5.2b respectively, differ from the rest with regard to deviation of values. This occurs because the shift imposed by the fault to the pipeline is so small that the entire displacement takes place between its two adjacent joints. The described deformed pipe disagrees with the one assumed in the analytical methodology, which required the activation of at least to joints at each side. This limit in the implementation of the method is considered not important, since the use of flexible joints is meaningful only when large displacements are imposed by the fault, which the conventional design cannot address successfully.

Figure 5.3 includes the “1 to 1” comparison diagrams of Bending Moment, considering that the pipeline crosses the fault at an angle of: (a)  $90^\circ$ , (b)  $60^\circ$ , and (c)  $30^\circ$ , as obtained by numerical and analytical analyses. By examination of the diagrams in Figure 5.3 it becomes obvious that the conclusions obtained by Figure 5.2 with regard to the shear forces are also valid for the bending moments.

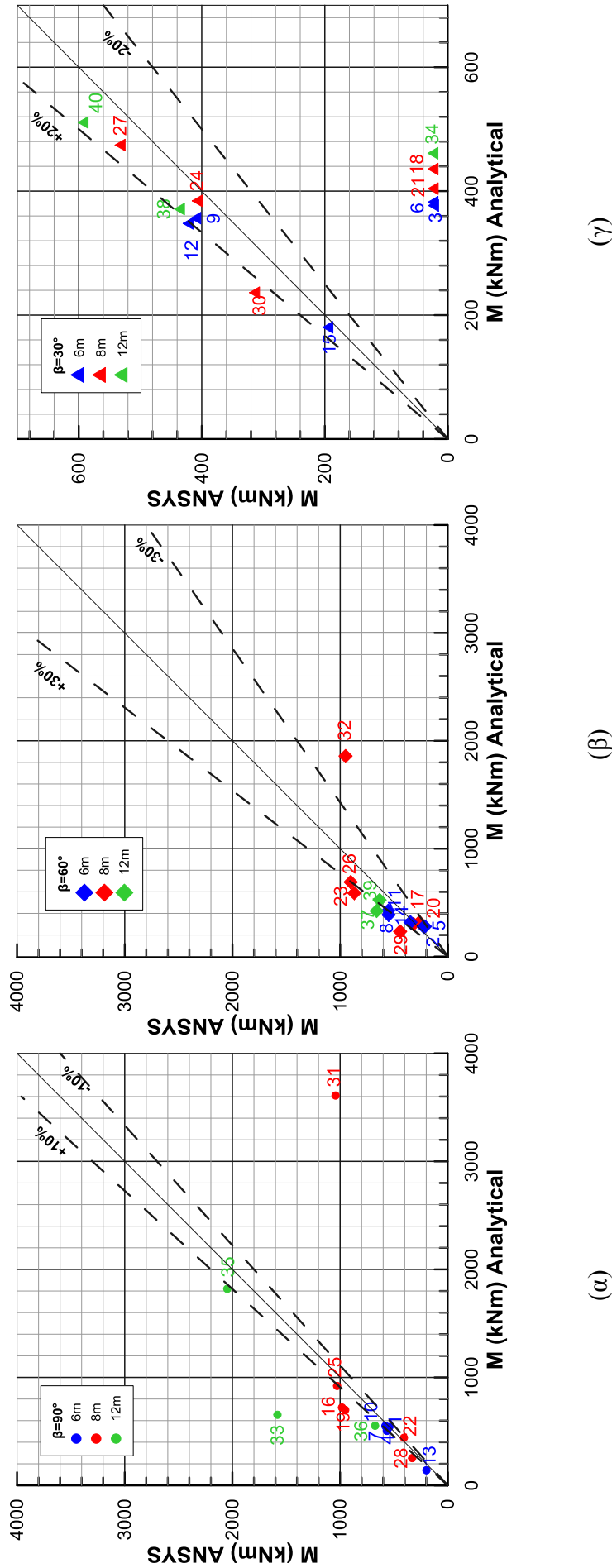


Figure 5.3: Comparison diagrams “1 to 1” of Bending Moment, considering that the pipeline crosses the fault at an angle of: (a)  $90^\circ$ , (b)  $60^\circ$ , and (c)  $30^\circ$

Figure 5.4 includes the “1 to 1” comparison diagrams of Relative Rotation, considering that the pipeline crosses the fault at an angle of: (a) 90°, (b) 60°, and (c) 30°, as obtained by numerical and analytical analyses.

In the case of maximum relative rotation the analytical method leads to satisfactory results with values deviating up to  $\pm 20\%$ , except for some analyses (analyses 2, 5, 6, 11, 17, 18 and 34) regarding an angle  $\beta$  equal to 30° and 60°. The latter present a slightly greater deviation, with the values resulting from the analytical method being the conservative ones.

Furthermore, in some analyses (analyses 2 and 5) in which the flexible joints are close together (6m), more joints than those estimated from the analytical method get activated. This causes an underestimation in rotations (3 instead of 2 joints are activated at each side of the fault). As already mentioned, analyses 6, 18 and 34 shown in Figure 6.4c, refer to a pipeline intersecting the fault at 30° with a 3m displacement.

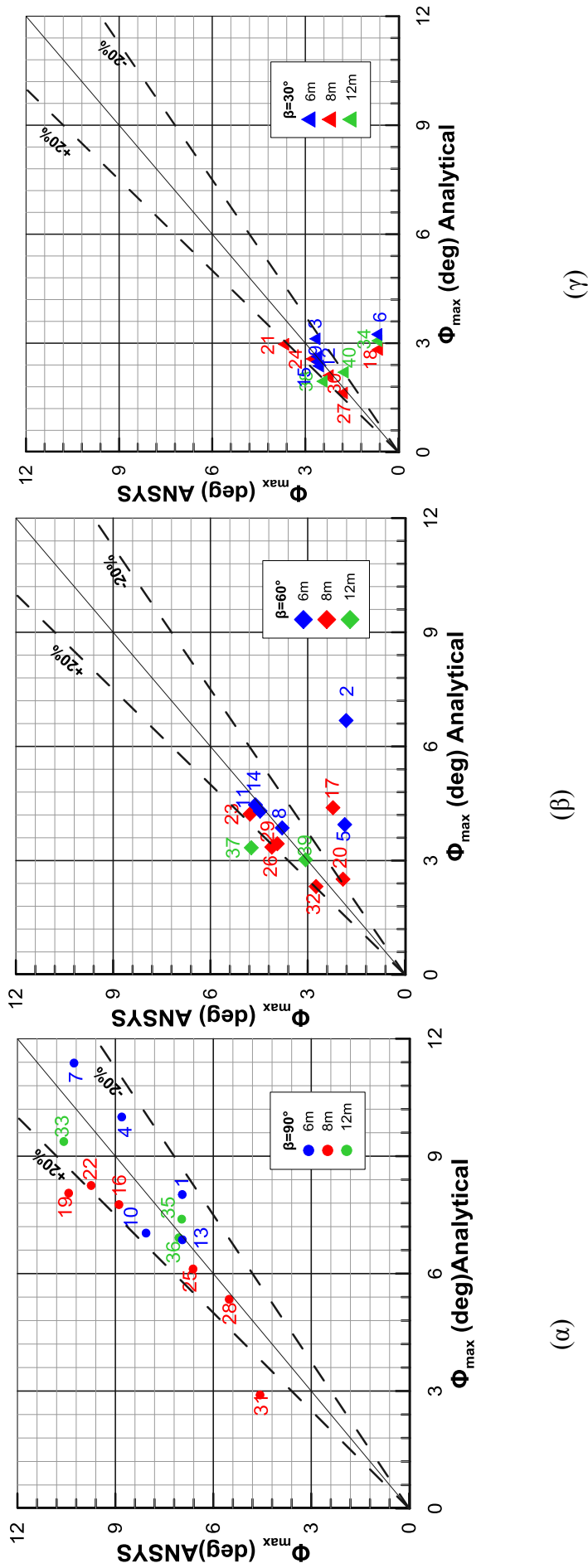


Figure 5.4: Comparison diagrams “1 to 1” of Relative Rotation, considering that the pipeline crosses the fault at an angle of: (a) 90°, (b) 60°, and (c) 30°

Figures 5.5 and 5.6 include the “1 to 1” comparison diagrams of Maximum and Minimum Stress, respectively, considering that the pipeline crosses the fault at an angle of: (a) 90°, (b) 60°, and (c) 30°, as obtained by numerical and analytical analyses.

The majority of the analyses presented in the following diagrams include results which approximate those produced from the numerical model, namely a deviation in maximum stresses reaching up to  $\pm 10\%$  in the case of 30° and 60° and up to  $\pm 20\%$  in the case of 90°. Especially analysis 33 concluded in the development of maximum stresses between the second and the third joint, a case which the methodology could not predict, since it estimates that maximum stresses develop between the third joint and the point of the intersection with the fault.

In the case of minimum stresses, on the other hand, it is observed through examples 3, 6, 18, 21 and 34, which refer to 3m. shift of the fault and 30° angle of intersection, that the analytical estimations deviate even more (up to 60% comparing to those estimated numerically) than those in the previously discussed diagrams (30° angle).

Figures 5.7 and 5.8 include the “1 to 1” comparison diagrams of Maximum and Minimum Strain considering that the pipeline crosses the fault at an angle of: (a) 90°, (b) 60°, and (c) 30°, respectively.

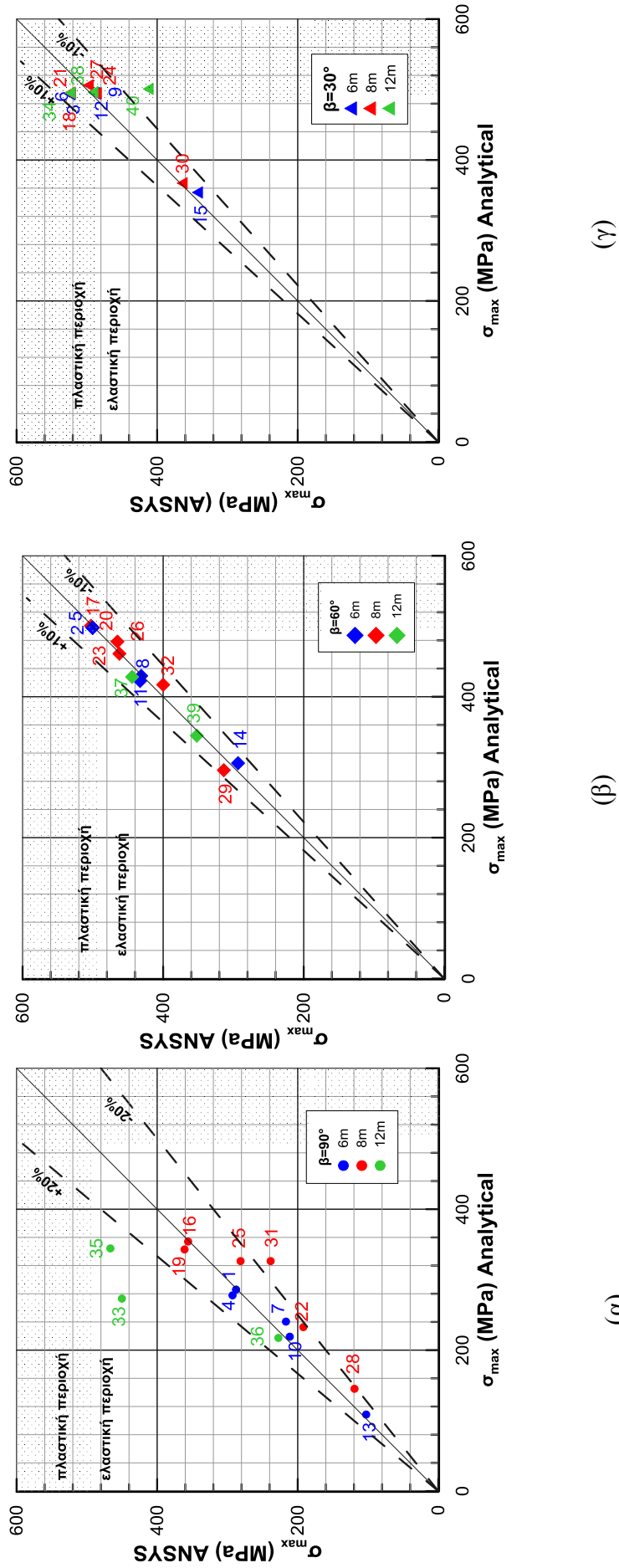


Figure 5.5: Comparison diagrams “1 to 1” of Maximum Stress, respectively, considering that the pipeline crosses the fault at an angle of: (a) 90°, (b) 60°, and (c) 30°

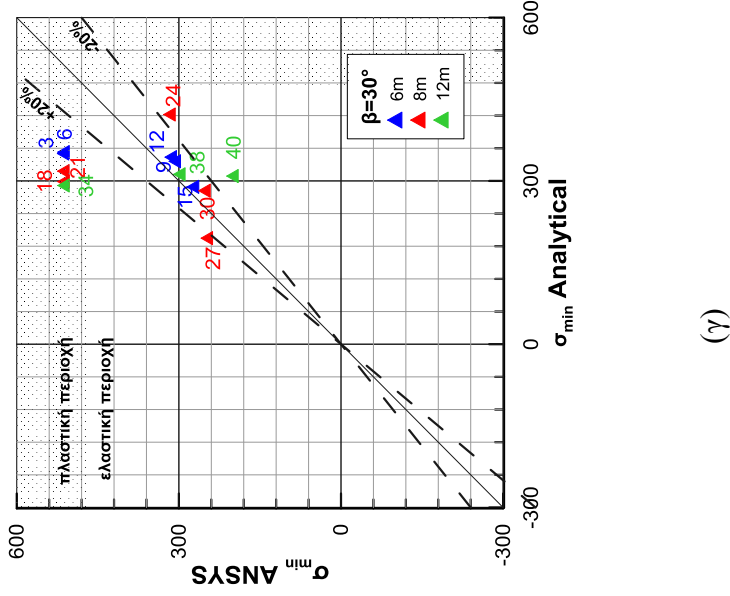
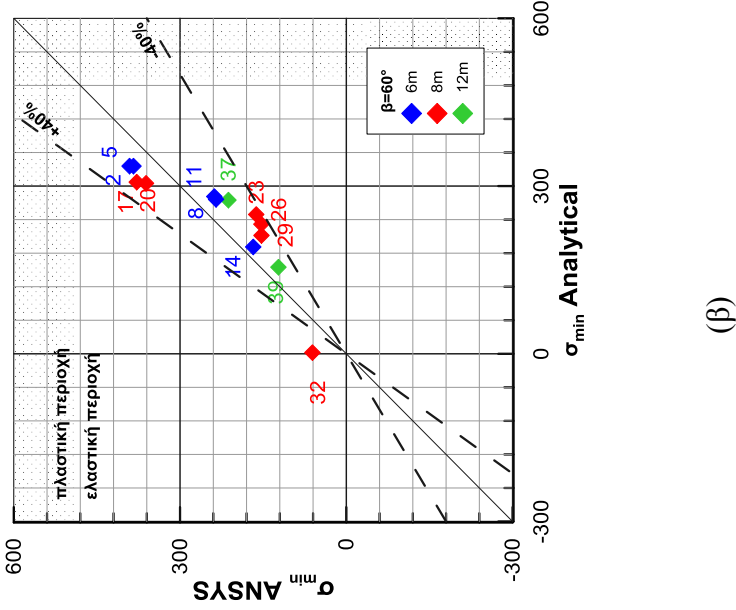
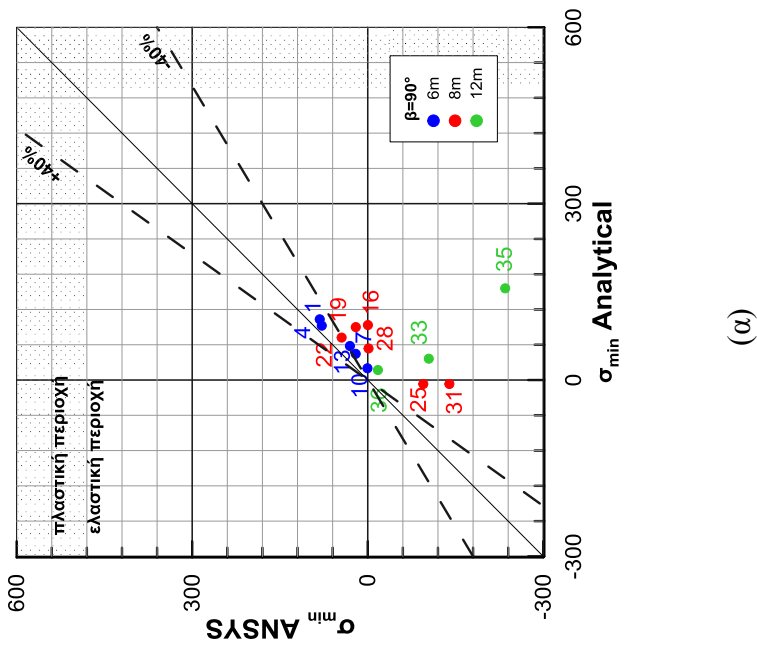


Figure 5.6: Comparison diagrams “1 to 1” of Minimum Stress, respectively, considering that the pipeline crosses the fault at an angle of: (a) 90°, (b) 60°, and (c) 30°



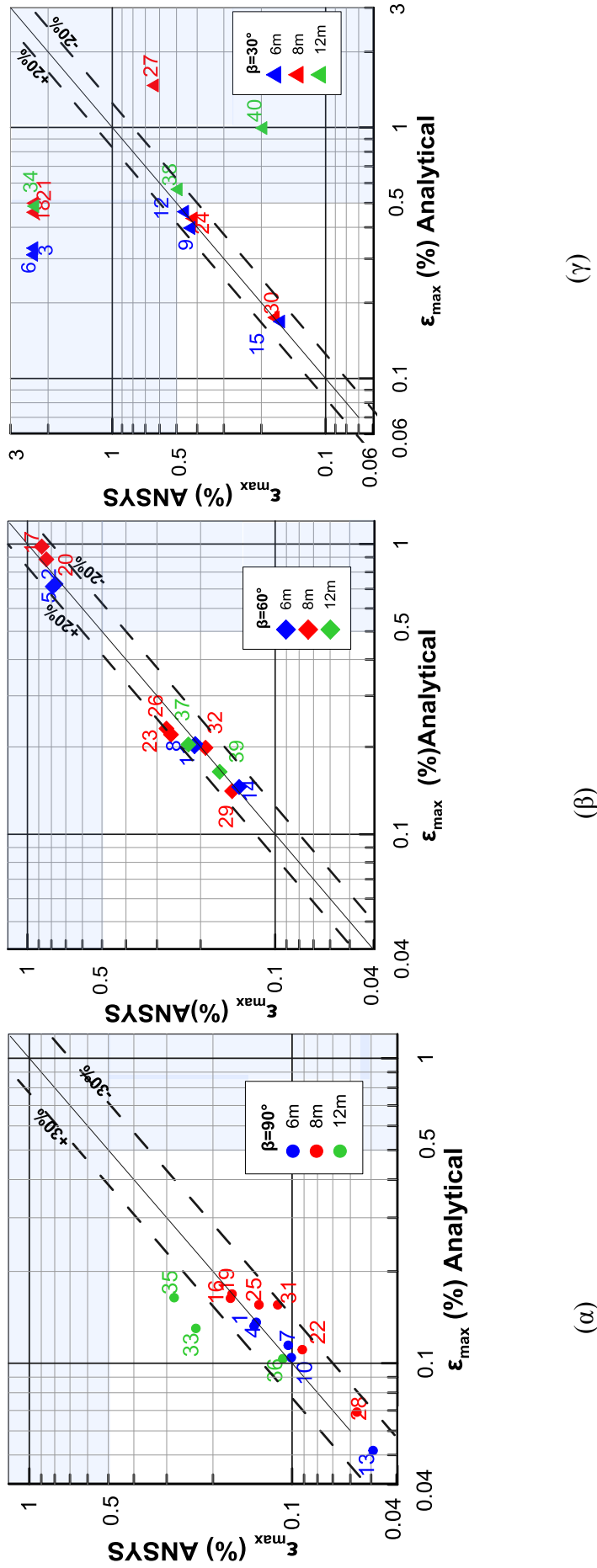


Figure 5.7: Comparison diagrams “1 to 1” of Maximum Strain considering that the pipeline crosses the fault at an angle of: (a) 90°, (b) 60°, and (c) 30°.

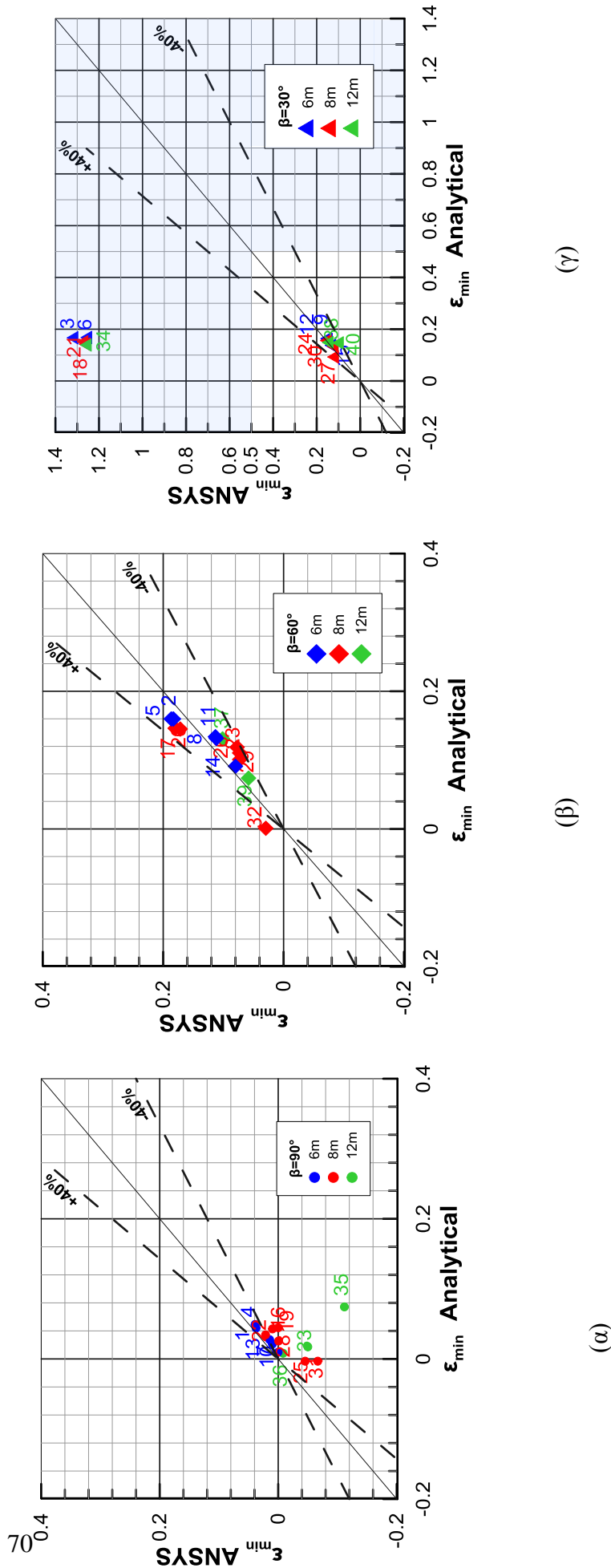


Figure 5.8: Comparison diagrams “1 to 1” of Minimum Strain considering that the pipeline crosses the fault at an angle of: (a) 90°, (b) 60°, and (c) 30°.

The majority of the analyses presented in these diagrams include results which approximate those produced from the numerical model. Maximum strains reach a deviation of  $\pm 20\%$  and minimum strains one of  $\pm 40\%$  in the case of  $30^\circ$  and  $60^\circ$ , while the corresponding values are  $\pm 30\%$  and  $\pm 40\%$  in the case of  $90^\circ$ . Figures 5.7c and 5.8c also display analyses referring to a pipe which intersects with the fault at an angle of  $30^\circ$ . However, these analyses reach a deviation greater than 100% caused by a slight underestimation of the stress, while the pipe has entered the plastic zone. This insignificant underestimation results in a disproportionately great underestimation of the deformation.

The region in which the pipe is considered to have failed is shaded with a light blue colour, in Figures 5.7 and 5.8. The yield limit for pipe parts welded together is generally considered equal to 0.5%, thus the same was chosen for the case of flexible joints.

### **5.3 Diagrams of relative error in the proposed method**

The preceding “1 to 1” comparisons create the necessity of constructing diagrams which depict the relative error as a function of the angle  $\beta$ , the distance between the flexible joints, as well as the fault displacement. These diagrams are constructed in order for the limits of implementation of the analytical method to be clarified.

In Figures 5.9 and 5.10 the diagrams of relative error over the fault displacement and the angle of the pipeline crossing the fault are presented. The first refers to a crossing in the middle of the pipe, while the second to a crossing at the edge. Each Figure depicts the relative error of: (a) axial force  $N$ , (b) shear force  $V$ , (c) bending moment  $M$ , (d) relative rotation  $\varphi_{max}$ , (e) maximum stress  $\sigma_{max}$ , (f) minimum stress  $\sigma_{min}$ , (g) maximum axial strain  $\varepsilon_{max}$ , (h) minimum axial strain  $\varepsilon_{min}$ .

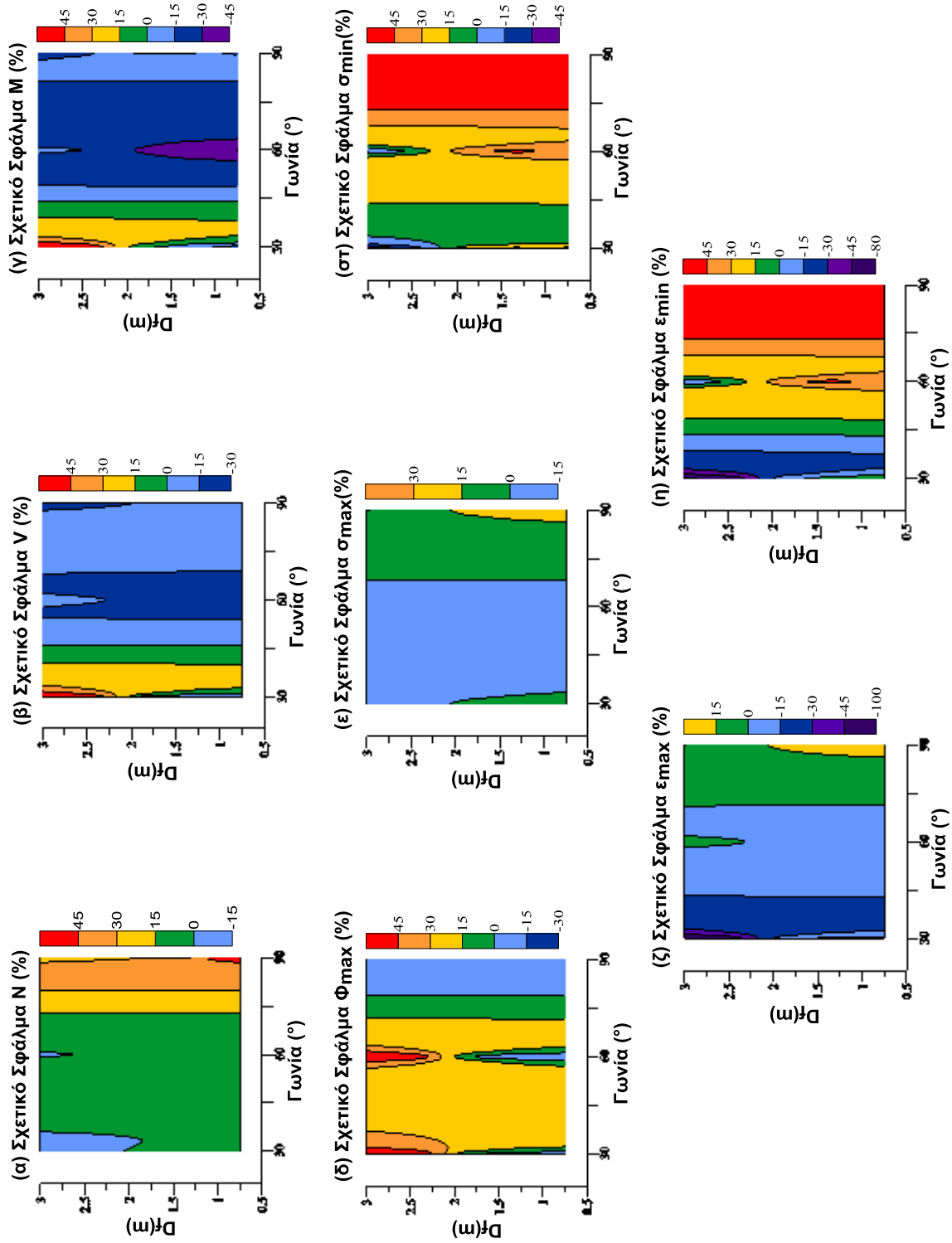


Figure 5.9: Diagrams of relative error over the fault displacement and the angle of the pipeline crossing the fault in the middle of the pipe with flexible joints placed per 8 meters

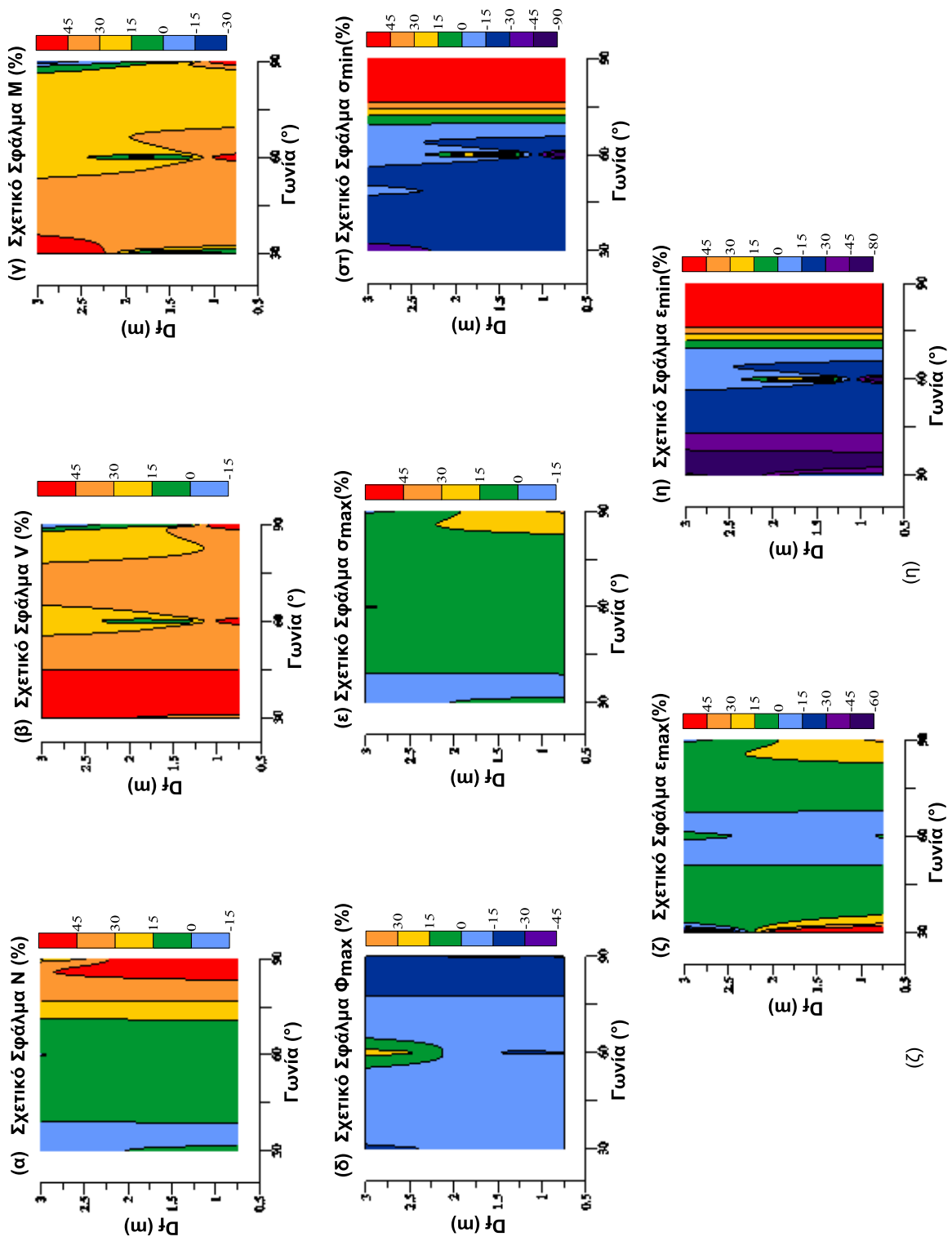


Figure 5.10: Diagrams of relative error over the fault displacement and the angle of the pipeline crossing at the edge of a joint with flexible joints placed per 8 meters

Figures 5.9 and 5.10 clearly demonstrate that axial forces exhibit a greater error at the angle of  $90^\circ$  than at any other angle. As previously noted, this is because no elongation parallel to axis x can be developed due to fault rupture while the angle remains acute. Therefore, in this case axial force depends solely on the curvature of the pipeline. However, the axial force caused by rotation can be estimated only approximately since it is indirectly calculated through the curvature of the pipe and, thus, the great error is expected.

In Figure 5.9 one may observe that errors (smaller than  $\pm 15\%$ ) are present in the analyses referring to an angle of  $30^\circ$  and to large fault displacement, whilst in Figure 5.10 and for  $30^\circ$  errors appear increased, whatever the displacement.

Both Figure 5.9 and 5.10 lead to the conclusion that the analyses concerning  $90^\circ$  display an increased error in minimum stresses and strains. All relative error values, with the exception of large errors in axial forces and minimum stresses and strains, remain within the range  $\pm 30\%$  for angles greater than  $60^\circ$ .

Figures 5.11 and 5.12 include the diagrams of relative error as a function of the distance between flexible joints and the angle of the pipeline crossing the fault in the middle and at the edge of the pipe, respectively. The crossing occurs immediately after the third joint. Each Figure depicts the relative error of: (a) axial force N, (b) shear force V, (c) bending moment M, (d) relative rotation  $\varphi_{max}$ , (e) maximum stress  $\sigma_{max}$ , (f) minimum stress  $\sigma_{min}$ , (g) maximum axial strain  $\epsilon_{max}$ , (h) minimum axial strain  $\epsilon_{min}$ .

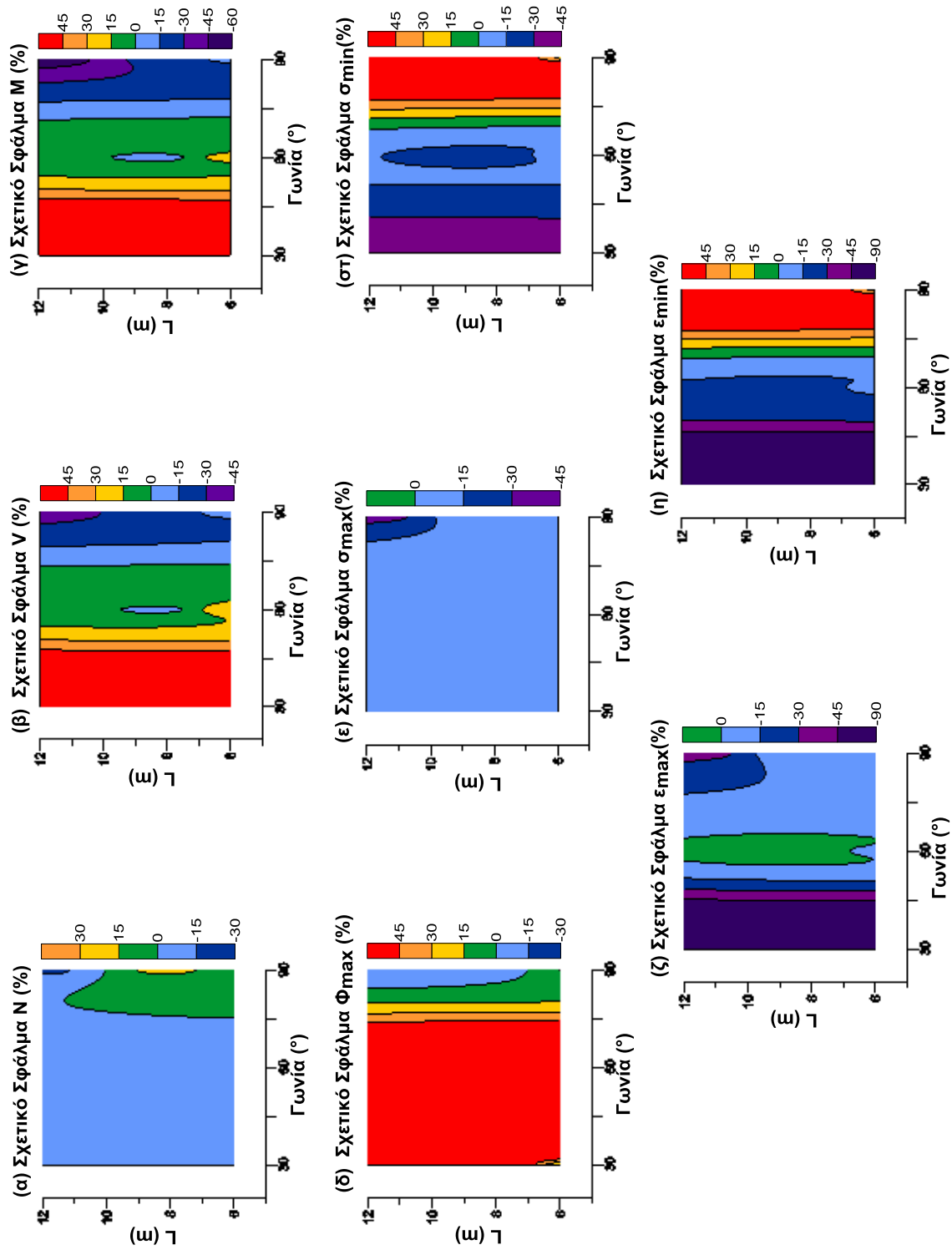


**Figure 5.11:** Diagrams of relative error as a function of the distance between flexible joints and the angle of the pipeline crossing the fault in the middle of the pipe and for fault displacement equals to 3 meters

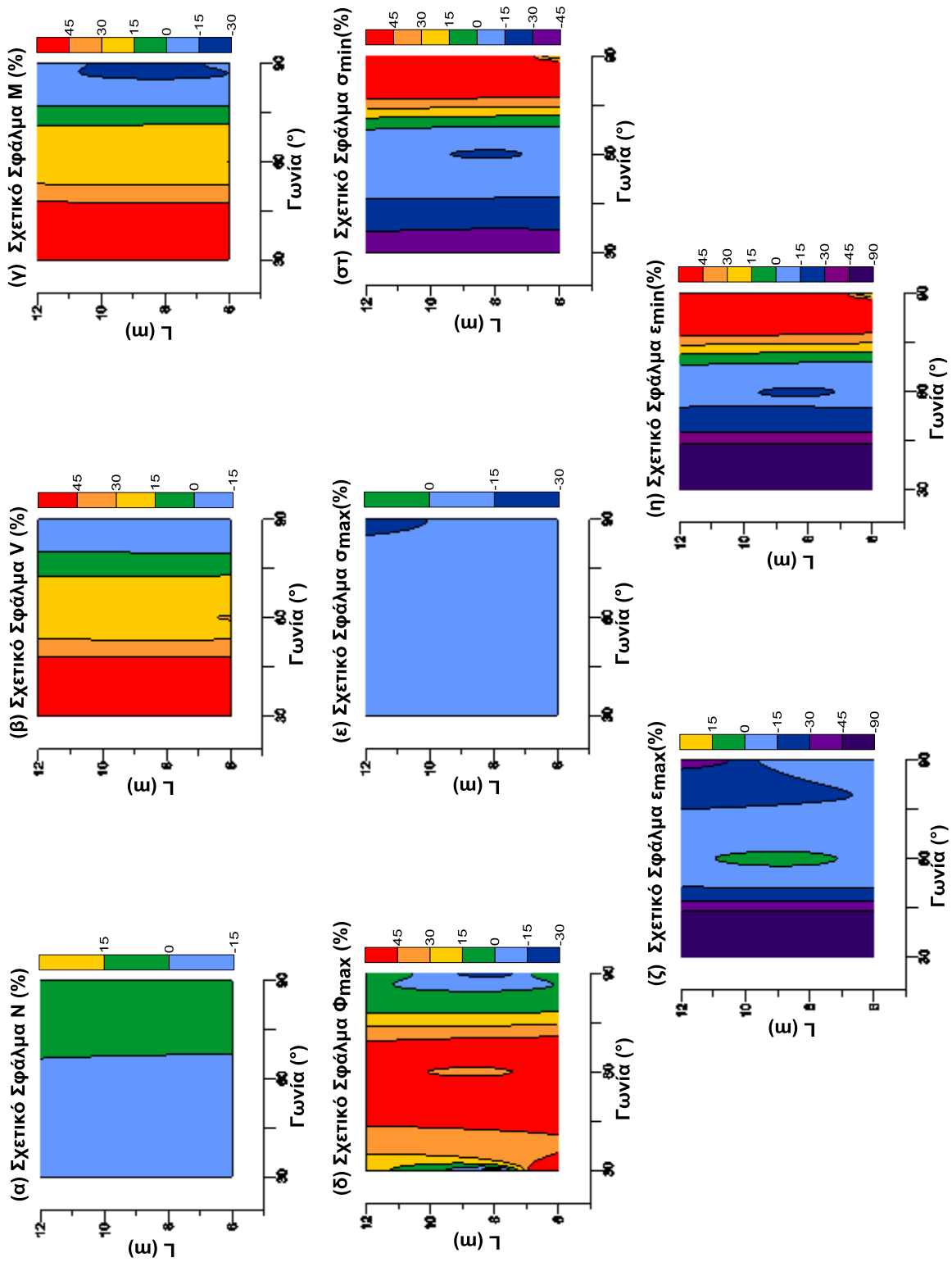


**Figure 5.12:** Diagrams of relative error as a function of the distance between flexible joints and the angle of the pipeline crossing the fault is at the edge of a joint for fault displacement equals to 3 meters



Figures 5.11 and 5.12 confirm the observations made about Figures 5.9 and 5.10. More specifically, there is an increased axial force at  $90^\circ$  compared with that at  $30^\circ$  and  $60^\circ$ . A large error (greater than +30%) also occurs at  $90^\circ$  with regard to minimum stresses and strains.

In Figure 6.11, which refers to the fault crossing in the middle of the pipe, an error in the maximum relative rotation greater than  $\pm 30\%$  is shown, when the angle is  $30^\circ$  and  $60^\circ$  and for all three cases of distances between joints. On the other hand, in Figure 5.12, which refers to the fault crossing the pipe at the flexible joint, the shear force, the bending moment and the minimum stress and strain present an error greater than  $\pm 30\%$  at  $30^\circ$ , regardless of the distance between flexible joints. The same error also applies for the maximum relative rotation, when joints are placed with a 6m distance between them.

Large relative errors are delusive in all cases of minimum strain and stress (Figures 5.11 and 5.12 f, h). They emerge from the very small, almost zero, values being compared. This can be verified if the analysis which includes 16-joints per 8m,  $\beta=90^\circ$ , fault in the middle,  $D_f=3m$ - (see the relevant diagrams of case A.16, Appendix A) and which seems to have an error in minimum strain equal to 30789% is examined. The value of the minimum strain of the section which is obtained via the analytical method is  $\epsilon_{min}=0.0445\%$ , while via the numerical method is  $\epsilon_{min}=-0.0014\%$ . However, if the minimum strain is examined as a physical quantity, using a theoretical and qualitative approach, the discrepancy observed in these previous values cannot be justified. The concept above can also explain the fact that the relative errors concerning the minimum stresses (Figure 5.12 and 5.11f) are actually smaller than those obtained by the analyses.

Therefore, the implementation of the analytical method will be considered safe and acceptable only if the fault intersects with the pipe at an angle greater than or equal to  $60^\circ$  and the shift of the fault is greater than  $1.5D$  ( $\sim 1.00m$ ). The analytical method is not recommended for small values of shift of the fault (equal to  $D$ ), in spite of the fact that usually it proves capable of producing satisfactory results for this case also.

## **5.4 Conclusions**

From the set of comparisons presented above, one can safely conclude that the proposed analytical methodology approaches sufficiently the mechanism of the phenomenon, since the analysis results of the majority of the examined cases are considered to be satisfactory.

However, throughout the aforementioned comparison of the analytical and numerical results, there have been set limits to the analytical methodology. More specifically, it has been noticed that, when the angle between the fault and the pipeline is considered equal to  $30^\circ$ , the joints may act beneficially but not enough to significantly affect the results, since the developing strains are caused by the longitudinal component of the ground displacement  $D_x$ . Therefore, despite the fairly satisfactory approach of the values of the developing axial forces and stresses, the pipeline is within the plastic zone due to the axial stresses. Thus, the slightest variations of the estimated stress values, can cause disproportionately large variations of the estimated strains, moments and shear forces. Nevertheless, setting a specific application limit of the methodology is of limited importance. Using flexible joints in cases where the small intersection angle between the pipeline and the fault causes so great axial forces is considered inappropriate, since developing strains would not be significantly impaired and therefore, a different case or an alteration to the pipeline alignment should be considered.

In addition, in some cases of really small fault displacements, the results of the proposed analytical methodology were not satisfactory enough. This is because the movement of the pipeline is limited to the first joint, while, according to the methodology, at least two joints from each side are considered to be activated. Nonetheless, this “weakness” cannot compromise the credibility of the methodology, since the use of flexible joints is considered appropriate only in cases of great displacements (equal to 2-4 times the pipeline diameter in the case of slip-faults).

# 6

## **Comparison of the proposal methodology with usage of flexible joint against the conventional ones**

---

### **6.1 Introduction**

The aim of this chapter is to perform a technical and financial comparison between the new methodology of designing pipelines against large ground displacements caused by the movements of tectonic plates with the use of flexible joints versus the conventional design methods. The purpose of this comparison is to conclude the limits of this method taking under consideration the performance of each one, the variety of its applications and its cost.

### **6.2 Methodologies to face ground displacements due to rupture of a strike slip fault**

In the conventional design method of underground pipelines, the reduction of imposed deformations in a pipelines that crosses a strike slip fault are being made through: (a) increase of the pipelines' s strength (b) reduction of the friction between the soil and the pipeline and therefore the further reduction of axial stress to the pipeline ( $\gamma$ ) increase of the possibility of free movement of the pipeline in the fault rupture area. This chapter will present and compare the method of using flexible joints against the following conventional methods:

- Increase of the pipelines walls' thickness
- Improvement of the stainless steel's strength
- Use of pumice to fill the trench
- Construction of an underground pre-manufactured box (culvert) made of reinforced concrete of suitable dimensions within which the pipeline can

move freely.

The examined cases concerned two different intersection angles of a strike slip fault with a pipeline  $90^\circ$  and  $60^\circ$ , since the effect of the flexible joints is affected greatly by the angle at which the pipeline crosses the fault. The reader should note here that based on the observations of chapter 5, flexible joints are not suitable for angles smaller than  $60^\circ$ .

For the study of the conventional design methods a continuous pipeline was used whose quality was API 5L Grade X65 and thickness  $t = 12.5\text{mm}$ . Initially it was examined the increase in the thickness of the pipeline wall, which has the effect of increasing the strength of the pipeline and reducing the developing deformations. In the present study we examined continuous pipes with an outside diameter  $D = 0.762\text{m}$  and thickness  $t = 12.5\text{mm}$ ,  $t = 16\text{mm}$  and  $t = 20\text{mm}$ . The realization of this analysis was done using the analytical methodology given by Karamitros et al. (2011) and through gradual increase of the impose displacement it has been derived the point at which the continuous pipeline with an initial thickness  $t = 12.5\text{mm}$  develops deformations equal to the fail limit of 0.5%. Then it has been considered the case in which the pipeline's thickness should be enhanced by increasing the wall thickness ( $t = 16\text{mm}$ ) and through the same analytical methodology it was determined the further positive displacement needed to be applied to the continuous pipeline in order to develop deformations equal to the limit 0.5%. The thickness of the pipe was then increased again ( $t = 20\text{mm}$ ) and this way the maximum impose displacement that this pipeline could undergo by the strike slip fault was determined.

To assess the influence of the type of steel in developing deformations, it was considered more appropriate-again using the analytical methodology Karamitros et al. (2011) -that the above analysis should be also made using quality steel API 5L Grade X65 as well as for an improved type of Steel Grade X70.

Regarding the procurement costs of the pipeline, according to data from a production factory this is according to the wall thickness of the pipe and the quality of the stainless steel according to the values presented in Table 6.1. To be able to compare the results through the methods given below, which methods in fact improve the area

around the trace of the fault, the cost was calculated on a “per meter of the pipeline” basis.

**Table 6.1:** Cost of supplying the pipelines based on the pipelines’ wall thickness and the stainless steels’ quality

	<b>API 5L Grade X65</b> <b>Unit price (€/tn)</b>	<b>API 5L Grade X70</b> <b>Unit price (€/tn)</b>
<b>Pipeline D=30”, t=12.5mm</b>	1120	1130
<b>Pipeline D=30”, t=16mm</b>	1200	1300
<b>Pipeline D=30”, t=20mm</b>	1308	1530

Analysis were also performed for the case where the pipeline is located inside a trench with pumice, which methodology aims at the reduction of applied forces to the pipeline. The reduced weight of these materials reduces the geostatic stresses imposed in the stream and therefore the friction forces generated in the soil and the pipeline interface, increasing in this way the pipeline’s anchored length and reducing the imposed deformation. To achieve the necessary elimination to the transverse resistance of the pipeline, the excavation is widened in the same way as in the other cases. The resulting analysis for this method of treatment involved continuous pipes of outside diameter  $D = 0.762\text{m}$ , thickness  $t = 12.5\text{mm}$  and steel API 5L Grade X65 and once again the study was based on the analytical methodology of Karamitros et al. (2011) after the soil simulation springs were modified according to the specific weight of pumice ( $\gamma = 8\text{kN} / \text{m}^3$ ), as shown in Table 6.2.

**Table 6.2:** Characteristics of the spring soils for filling the pumice trench ( $\gamma=8 \text{ kN/m}^3$ )

Type of Soil Spring	Force	Displacement
	(KN/m)	(mm)
Axial (friction)	10.11	3.0
Transverse horizontally	59.75	35.7
Transverse vertically (upwards)	18.31	2.57
Transverse vertically (downwards)	454.15	95.3

The pumice's cost was assume to be  $40\text{€}/\text{m}^3$ , which includes both the supply of the pumice as well as the backfilling of trench. This way in order to calculate the final cost of this method, the latter was multiplied with the area of the trench's section (see Figure 6.1) and then added the cost of supplying the pipeline (which was considered as per meter).

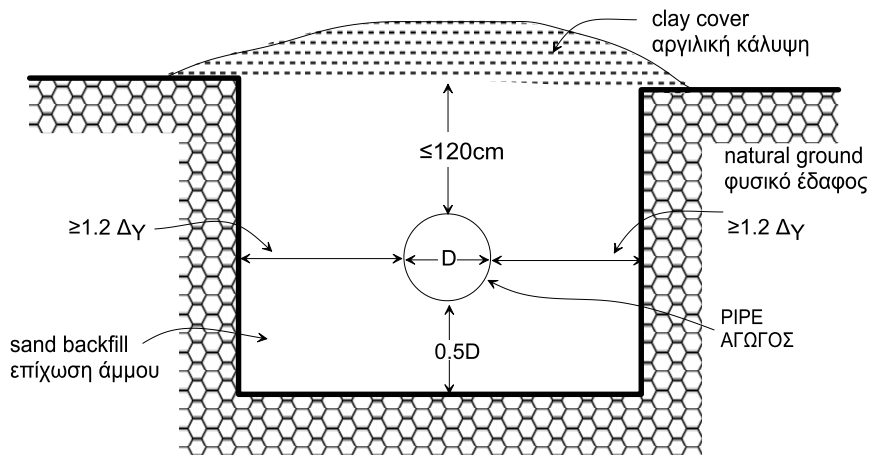


**Figure 6.1:** Area of the trench's section

Finally, it was assumed that the pipeline can be protected from permanent soil displacements due to a rupture of a strike slip by constructing an underground prefabricated box (culvert) made of reinforced concrete (See. Figure 6.2) of suitable dimensions, within which the pipeline can be move freely. Essentially speaking the construction consists of a number of prefabricated boxes which surround the pipeline. These boxes abut against each other and in case of a rupture they are able to move relative to one another and receive the movement of the fracture. The pipeline in this case is asked to only take the elongation  $\Delta x$  due to the movement. To calculate the

elongation it was used the analytical methodology of Karamitros et al. (2011) for continuous pipe of outside diameter  $D = 0.762\text{m}$ , thickness  $t = 12.5\text{mm}$  and steel API 5L Grade X65. However it should be mentioned at this point that it was only imposed the horizontal component of positive movement along the axis  $x$  (along the pipeline), to determine to what positive move's extend this particular component causes deformations due to axial forces equal to the limit of 0.5%. These deformations are expected to grow at the ends of the length of the pipeline which is being protected by the culvert boxes, which were assumed that coincided with the curved length of the pipeline, as that is where large axial forces develop. Note that analysis were only made for an angle of  $60^\circ$ , since in the case where the angle is  $90^\circ$  the horizontal elongation is very small, and is due solely to the curvature of the pipeline ( $\Delta x$  due to the fault rupture is negligible). It is therefore not expected to have substantial deformation in the pipeline in this case and for the purposes of comparison was assumed a stable low value.

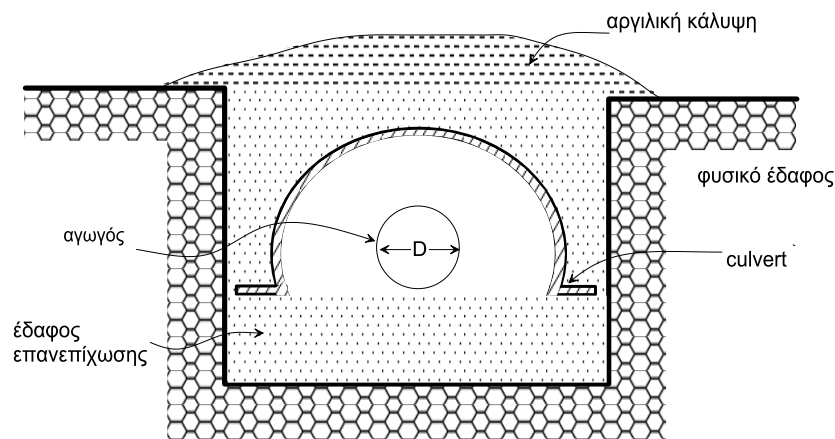


**Figure 6.2:** Segment of an underground prefabricated box (Culvert)

The prefabrication, transportation and installation costs of the circular prefabricated box (culvert) of reinforced concrete which is assumed to be 15cm thick and with a radius of 130cm are around 200€/m. However, in addition to this cost it was also need to consider the costs of trench excavation mining in order to allow the placement of the oversized box. Although this cost depends on the excavation material, a medium mining cost for a normal combination of soils (soil, semi rock, rock) is approximately 50 €/m and includes transportation and disposal of soil material. It should be noted that these mining's are additional routines on top of the ones that take place anyway in

areas active faults, whose cost will not be considered. In addition to the above, the cost of backfill with classified material must be added, which is around 30 € / m. Therefore the total cost is considered equal to 280 € / m and concerns semi-cylindrical shells of radius 130cm. This container is considered to be effective for the case of a fault displacement around 1D, so that there is a safety margin between the pipe and the culvert. So in the case of larger displacements, in order to give the total cost of the process it was multiplied the amount of 280 € / m by the ratio of positive movement to the diameter of the pipeline,  $D_f / D$ , while also adding the purchasing cost of the external pipe with diameter  $D = 0.762\text{m}$ , thickness  $t = 12.5\text{mm}$  and steel API 5L Grade X65. Note that this cost is very low because it concerns prefabricated circular boxes and was assumed that it increases linearly (favourable assumption for the cost). In the case where these are not sufficient and a box needs to be constructed by conventional means (by using molds) the cost increases significantly.

For the application of the method using flexible joints, the analytical methodology presented in Chapter 3 was used, for the case where the distance between the joints ranges from 6m to 8m, and these are considered as the most effective distances. The analysis was made for pipeline of outer diameter  $D = 0.762\text{m}$ , thickness  $t = 12.5\text{mm}$  and steel API 5L Grade X65 for intersection with the pipe just after the 4<sup>th</sup> flexible joint (because this is considered as a worse case than having the intersection right in the middle of the pipeline). The analysis showed the value of the imposed displacement at which deformations exceeding the limit of 0.5% are developed.

To estimate the cost of this solution, offers of the company BOA Group were taken into account and an indicative joint value was used equal to €3653 each, which involves nodes with the necessary geometric characteristics (type 7510 and heading DN800). The cost of the process was divided by the total length of the application of the seven joint (three nodes on either side of the intersection with the fault), and then it was added to it the pipe procurement costs on a per meter basis. This offer is related to retail prices and hence is disadvantageous in terms of cost.

It should be noted that for the cost analysis in this chapter, it was assumed that we know exactly the position of the fault trace. In case of uncertainty in the position of the fault trace, all methods should be applied to a greater length, but the resulting relationship between cost per meter will remain approximately constant.



In addition, I performed a comparison of the conventional methods of dealing with permanent soil displacement due to the rupture of active rifts as this was described above with the method of flexible nodes, based on their effectiveness and their cost.

### **6.3 Methodologies' evaluation concerning the effectiveness and the cost of each one**

In addition, it was performed a comparison of the conventional methods of dealing with permanent soil displacement due to the rupture of active fault as this was described above with the method of flexible joints, based on their effectiveness and their cost.

Specifically Figure 6.3 shows the diagram of the maximum axial pipe's deformations as functions of the ratio of the fault displacement to the diameter of the pipeline,  $D_f / D$  for the case of the fault crossing the pipe at  $90^\circ$ , for each alternative method, so as to assess the effectiveness and efficiency of each method. At the same time it was correlated the costs to the length of curvature of each method with the ratio  $D_f / D$ , to determine in which field of ground displacement each alternative methodology is economically advantageous. In Figure 6.4, the corresponding diagrams are shown for the case of the fault crossing the pipe at  $60^\circ$ .

In both Figures one can observe that increasing the thickness of the pipeline wall, although practically is the predominant way of addressing aggravated deformations due to the rupture of faults, has not been a particularly favourable influence on elimination of pipeline deformations, as it does not cover the cases of very large imposed displacements (larger than  $3.6D$  for fault intersection at  $90^\circ$  and bigger than  $3.35D$  to fault intersection at  $60^\circ$ ). Moreover it is evident that even for such small displacements, the cost is increased by 16% for steel grade API 5L Grade X65, and 35% for steel grade API 5L Grade X70 by increasing the thickness of the cross section of the pipeline from  $t = 12.5\text{mm}$  at  $t = 20\text{mm}$ .

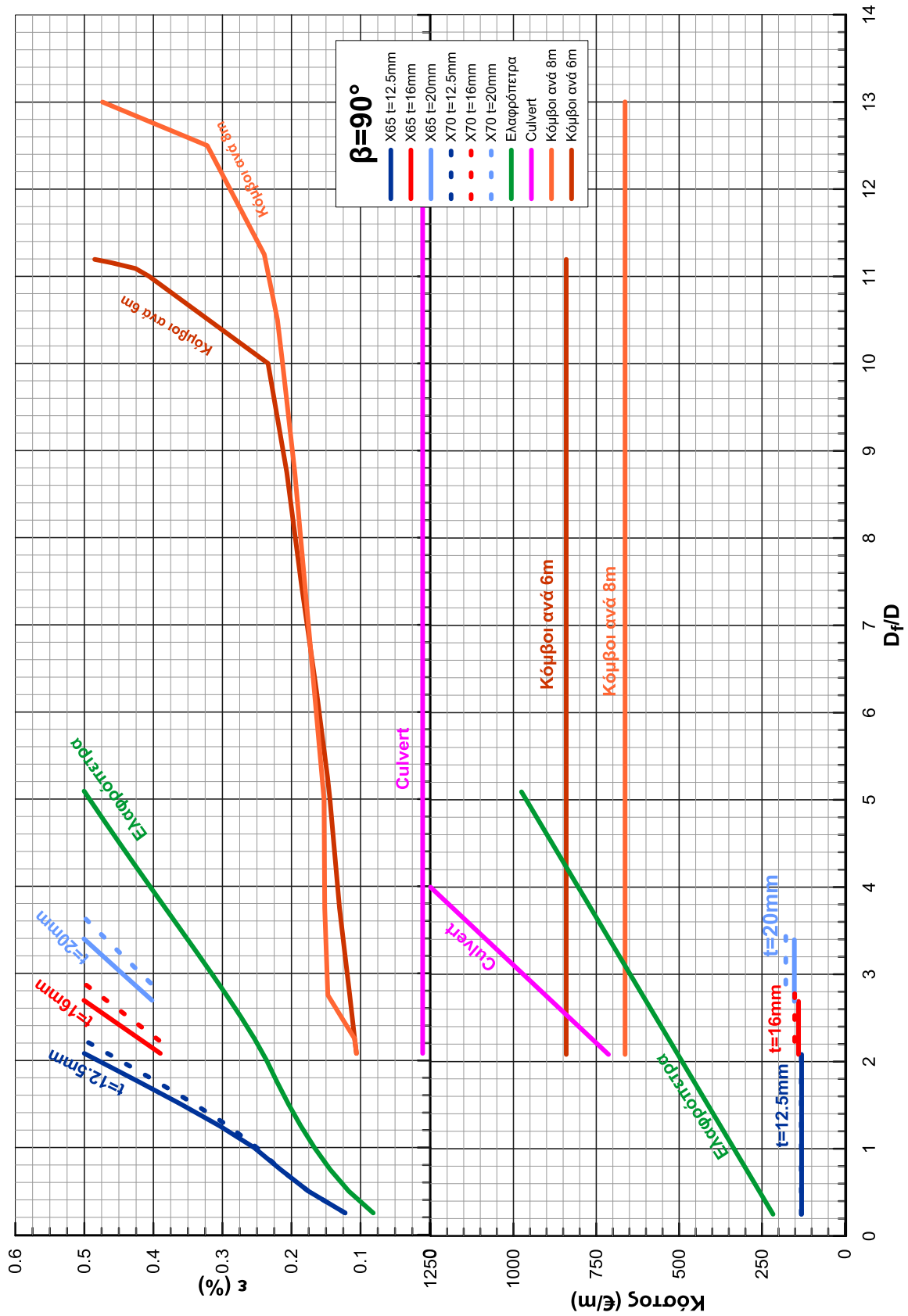


Figure 6.3: Diagram illustrating the maximum axial deformation and the cost according to the ratio of fault displacement to the diameter of a pipeline for each method separately for intersection angle with the fault at 90°

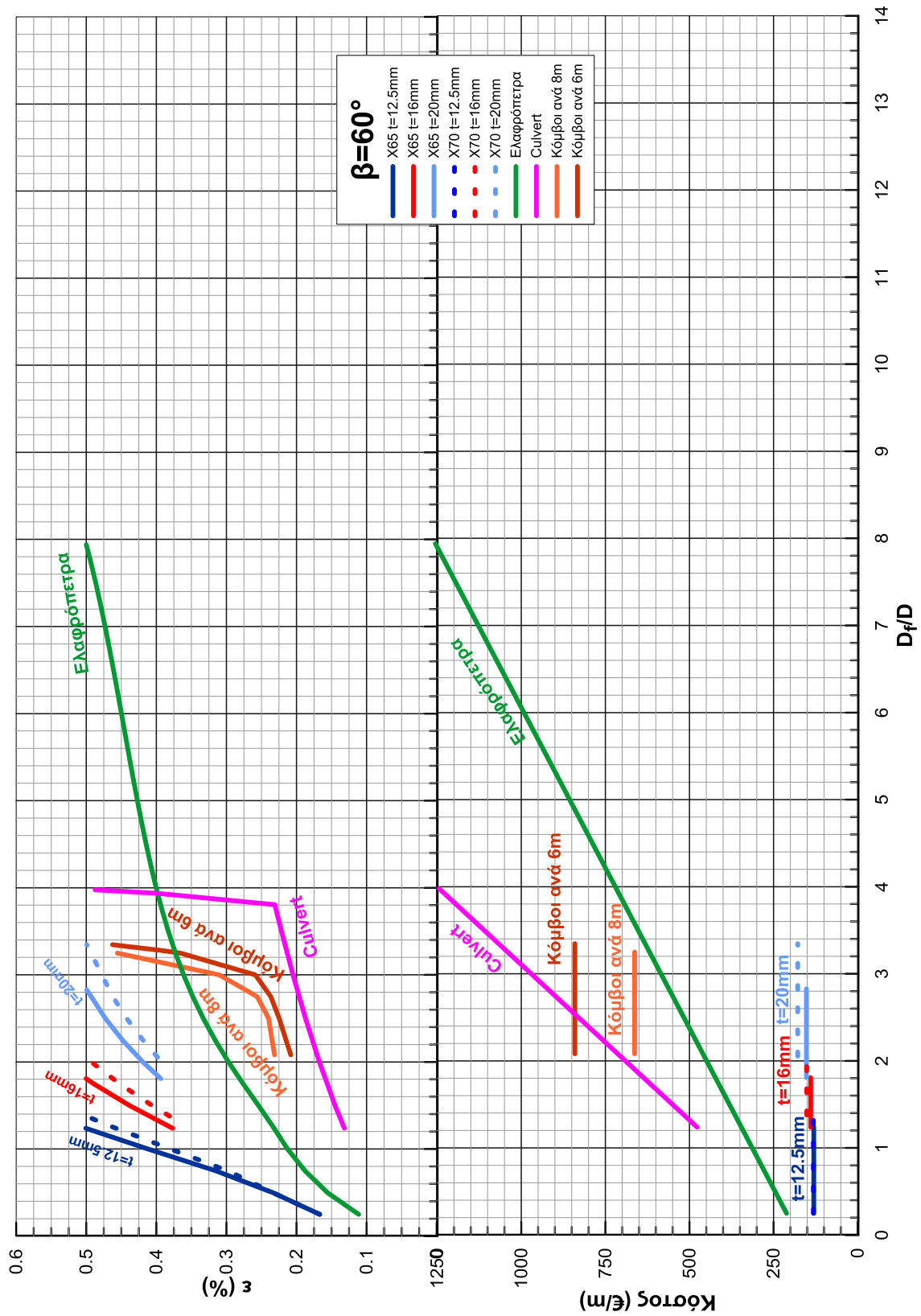


Figure 6.4: Diagram illustrating the maximum axial deformation and the cost according to the ratio of fault displacement to the diameter of a pipeline for each method separately for intersection angle with the fault at 60°

As far as it concerns the upgrading of the quality of the steel API 5L X65 to X70 it is noticeable that it consists a measure with little effect, with disproportionately high costs.

According to the Figure 6.3 for a crossing angle of the fracture with the pipe equal to  $90^\circ$ , the use of pumice for backfilling the trench is noticed to have a moderate effect on the impairment of deformations, as it protects the pipe from imposed displacements up to approximately  $5D$ . However it is difficult to be obtained in large quantities and it is a financially expensive solution (in relation to performance and cost of the flexible joints) for moderate displacements. Unlike the case of fault intersection with a pipe at  $60^\circ$ , the use of pumice appears to be the solution allowing the receipt of the maximum deformations to fail since the fault displacement which causes the pipeline reaches up  $7.95D$  however is a moderately expensive solution. Due to the pumice, the axial forces are absorbed due to the capacity it has to reduce the friction between the pipeline and the ground, something that is not achieved so strongly with flexible joints. Besides, their design was not originally made to receive the axial forces.

The use of flexible joints per 6m and 8m seems to have the greater efficiency (excluding the culvert construction) for the case of the strike slip fault crossing the pipeline at  $90^\circ$  (Figure 6.3), since the imposed fault displacement reach up to  $13D$  when the joints are placed per 8m, and  $11.2D$  when the joints are placed at every 6m. However the cost is smaller when compared to the performance and the cost of other methods.

In the case of fault cross pipeline at  $60^\circ$ , when the joints are spaced for 8m and 6m the positive movement that the pipe can safely withstand reaches  $3.25D$ , and  $3.35D$  respectively. It is observed that the angle that we are using the flexible joints has a limit to the movement that the pipeline can receive securely without fail, while the cost is generally greater than the case where pumice is used.

The protection of the pipeline from underground boxes (culvert) of reinforced concrete of appropriate width corresponding to the expected displacement of the fault consists of a moderately efficient method, as shown in Figure 6.4. In the case the pipeline crosses at  $60^\circ$  it can be applied up to a fault displacement equal to  $4D$ . The

cost, however, is much higher than the cost of implementing the methods using pumice or flexible nodes. Regarding the use of culvert in case the fault intersects the pipeline at  $90^\circ$  (Figure 6.3), it is shown to be the most expensive solution, but the substance can be applied regardless of the fault displacement.

It should be noted that the relatively low cost per meter length that was taken into account in the diagrams for the case of culvert, concerns prefabricated circular boxes and is considered to have a mere linear increase in the size of the displacement. In fact in the case of large displacements the outer casing (culvert) will be built with conventional casting methods (usage of mold) thus increasing the cost. Moreover, the cost for required backfill to position the box disproportionately increases with the increase of the diameter of the outer shell.

In summary, increasing the thickness is shown to be the optimal solution for small and medium fault's displacement (less than about  $3.5D$ ). The use of flexible joints appears to be optimal for strike slip faults when the pipelines crosses the fault at  $90^\circ$  by placing the joint at every 8m to be more effective at a reduced cost compared to the use of pumice stone, which is the third most prevalent solution. The use of culvert may be considered a safe solution, but it is not economically advantageous, since by increasing the positive displacement, the cost of the solution is increased significantly as well.

Concerning the performance of the flexible joints in relation to the costs in the case where the intersection of the fault to the pipe is at  $60^\circ$ , it is not the optimal solution since the use of pumice sufficiently reduces deformation and costs less. Of course the use of flexible nodes is in this case an alternative way of designing in areas where it is not easy or cost effective to transfer the pumice.

# 7

## Conclusions

---

The seismically imposed permanent ground displacement, such as those caused by the rupture of active faults, consist the most serious threat that the underground oil pipelines or gas are facing. Moreover, the usual "conventional" methodologies for dealing with such permanent ground displacement are generally effective for small to medium displacement of the fault (up to 2.5-3.0 diameters of the pipeline). An exception to this is the manufacturing method of a "sacrificial" reinforces concrete structure (culvert), but the cost of this is increased excessively as the expected displacement of the fault grows.

Keeping in mind what was mentioned above; the Department of Geotechnical Engineering of NTUA studied the alternative design of pipelines in areas of large ground deformation, using flexible joints through numerical analysis and small-scale experiments. Within this research, a new analytical method for assessing the influence of the flexible joints in basic design parameters that are developed in the pipeline.

As part of this broader research in this thesis, it was also assessed the accuracy of the proposed analytical methodology for pipes with flexible joints that cross strike slip faults. In parallel to the latter, an economical evaluation of this design method against the 'conventional' methods was performed in order to define the conditions of application in practice.

After extensive comparison with numerical analysis being carried out it is evident that the proposed analytical methodology is sufficiently close to the mechanism of the phenomenon and gives remarkable results in almost all the cases examined. Additionally, by comparing the results of analytical and numerical resolutions and the

corresponding errors of each of the sizes, the following limits were established for the proposed analytical methodology:

- Transverse displacement of the fault greater than twice the diameter of the pipeline ( $D_f > 2D$ )
- Intersection angle with the fault of not less than  $60^\circ$ .

It is clarified that those limits are not a practical limitation to the use of the analytical method, since the use of flexible joint is interesting to us only in cases of large ground deformation ( $> 2.5-3.0 D$ ), while when the pipe crosses the fault at a small angle, the use of joints is no longer appropriate, since deformations in the pipe are primarily due to axial displacements and therefore the use of bellows joints does not substantially eliminate the developing deformations.

Based on the economical comparison of the proposed design method with flexible joints against "conventional" methods, it was found that to have a maximum effectiveness through the use of flexible joints, the pipe must intersect perpendicularly the fault trace. Additionally, it was found that their use is favourable for the pipeline and impairs developing deformations under the fair limit of 0.5% even when the ground displacement go up to  $3.3D$  for the cases that it intersects the pipeline with an angle of  $60^\circ$  and up to  $10D$ , in the cases of vertical intersections. Therefore, this method has the most favourable influence out of all the "conventional" methods, excluding the culvert. Regarding the cost, the use of flexible joints either per 6m or per 8m even though it is a more expensive solution for medium ground displacement than using pumice or then the method of increasing the thickness of the conduit, but on the other hand increased thickness has application limits up to approximately  $3.5D$  while using pumice has limitations of up to about  $5.1D$ . In addition, the use of flexible nodes is in most cases cheaper than the culvert, while the construction needs no additional provision since the joints are simply welded in the positions, just like the other parts of the pipeline.

In summary, we conclude that in the case of vertical intersection of the fault, the increase of the wall thickness of the pipeline is appropriate for ground displacement  $df \leq 3.5D$ , where  $D$  is the diameter of the pipeline. The use of flexible joint is the most effective and efficient solution for larger imposed displacements  $3.5D < df \leq 10D$

while for even greater imposed displacement  $df > 10D$ , the protection of the pipe by culvert is recommended.

For the case of intersection angle, increasing the wall thickness of the pipe is indicated for imposed ground displacement  $df \leq 3.0D$ , where  $D$  is the diameter of the pipeline. However for larger displacements the use of pumice is the optimal solution, since it reduces deformations sufficiently and costs less.





# 8

## References

---

1. American Lifeline Alliance -ALA- (2005), "Design Guidelines for Seismic Resistant Water Pipeline Installations", FEMA, 255p.
2. American Lifeline Alliance -ALA/ASCE- (2001), "Guidelines for the Design of Buried Steel Pipe", ASCE, (with addenda through February 2005) 76p.
3. American Society of Civil Engineers -ASCE- (1984), "Guidelines for the Seismic Design of Oil and Gas Pipeline Systems", Committee on Gas and Liquid Fuel Pipelines, ASCE, 473p.
4. Ballantyne, D., (1992), "Thoughts on a Pipeline Design Standard Incorporating Countermeasure for Permanent Ground Deformation," Proceedings of the Fourth Japan-U.S. Workshop on Earthquake Resistant Design of Lifeline Facilities and Countermeasures for Soil Liquefaction, Honolulu, Hawaii, Technical Report NCEER-92-0019, MCEER, Buffalo, New York, pp. 875-887.
5. Cheng L. (2001), "Seismic Design of Water Pipelines at Fault Crossing", Proceeding of The 2 Japan and U.S. Workshop on Seismic Measures for Water Supply, AWWA, Tokyo, Japan, August 2001.
6. ElHmadi K. & O'Rourke M.J. (1990), "Seismic damage to segmented buried pipelines", Earthquake Engineering and Structural Dynamics, Vol. 19, pp. 529-539.
7. Ford, D.B., (1983), "Joint Design for Pipelines Subjected to Large Ground Deformations,"Earthquake Behavior and Safety of Oil and Gas Storage Facilities, Buried Pipelines and Equipment, PVP-77, ASME, New York, June, pp. 160-165.
8. Isenberg, J. and Richardson, E., (1989), "Countermeasures to Mitigate Damage to Pipelines," Proceedings of the Second U.S.-Japan Workshop on Liquefaction, Large Ground Deformation and Their Effects on Lifelines, Buffalo, New York, Technical Report NCEER-89-0032, MCEER, Buffalo, New York, pp. 468-482.

9. Karamitros D. K., Bouckovalas G. D. & Kouretzis G. P., (2007), "Stress analysis of buried steel pipelines at strike-slip fault crossings", *Soil Dynamics and Earthquake Engineering* 27, pp. 200–211.
10. Karamitros D.K., Bouckovalas G.D., Kouretzis G.P. & Gkesouli V. (2011), "An analytical method for strength verification of buried steel pipelines at normal fault crossings", *Soil Dynamics and Earthquake Engineering* 31, pp. 1452–1464.
11. Kenedy R.P., Chow A.W. & Williamson R.A. (1977), "Fault movement effects on buried oil pipeline", *Transport Engineering Journal, ASCE*, 103, pp. 617-633.
12. Newmark N.M. & Hall W.J. (1975), "Pipeline design to resist large fault displacement", *Proceedings of the US National Conference on Earthquake Engineering*. University of Michigan, pp. 416-425.
13. O'Rourke T.D. & Trautmann C.H. (1981), "Earthquake Ground Rupture Effects on Jointed Pipe", *Proceedings of the Second Specialty Conference of the Technical Council on Lifeline Earthquake Engineering, ASCE*, August, pp. 65-80.
14. O'Rourke, M.J. and Liu, X.J., (1994), "Failure Criterion for Buried Pipe Subjected to Longitudinal PGD: Benchmark Case History," *Proceedings of the Fifth U.S.- Japan Workshop on Earthquake Resistant Design for Lifeline Facilities and Countermeasures Against Soil Liquefaction*, Snowbird, Utah, Technical Report NCEER-94-0026, MCEER, Buffalo, New York, pp. 639-652.
15. O'Rourke M.J. & Liu J.X. (2012), "Seismic Design of Buried and Offshore Pipelines", *Monograph MCEER-12-MN04*, November 2012.
16. O'Rourke T.D., Jezerski J.M., Olson N.A., Bonneau A.L., Palmer M.C., Stewart H.E., O'Rourke M.J. & Abdoun T. (2009), "Geotechnics of Pipeline System Response to Earthquakes", *Geotechnical Earthquake Engineering and Soil Dynamics IV Congress 2009*.
17. Takada S. (1984), "Model Analysis and Experimental Study on Mechanical Behavior of Buried Ductile Iron Pipelines Subjected to Large Ground Deformations", *Proceedings of the Eighth World Conference on Earthquake Engineering*, San Francisco, California, Vol. VII, pp. 255-262.
18. Takada S., Hassani N. & Fukuda K. (2001), "A new proposal for simplified design of buried steel pipes crossing active faults", *Earthquake Engineering and Structural Dynamics* 30, p. 1243–57.

19. Tan R.Y. & Yang C.H. (1988), "Structural Responses of Underground Pipelines to Dynamic Loadings", *Mech. Struct. & Mach.*, 16 (1), pp.103-122.
20. Trifonov O.V. & Cherniy V.P. (2010), "A semi-analytical approach to a nonlinear stress-strain analysis of buried steel pipelines crossing active faults", *Soil Dynamics and Earthquake Engineering*, 30 (11): pp. 1298-1308.
21. Wang L.R.L. & Yeh Y. (1985), "A refined seismic analysis and design of buried pipeline for fault movement", *Earthquake Eng Struct Dyn*, 13: pp.75-96.
22. Wang L.R.L. (1996), "Some aspects of prioritization for rehabilitation of buried lifelines", *Eleventh World Conference on Earthquake Engineering*, Paper No. 1902, Elsevier Science Ltd.
23. Wilson J.F. (1984), "Mechanics of Bellows: A critical Survey", *Int.J.Mech.Sci.* Vol. 26, No. 11/12, pp. 593-605, 1984.



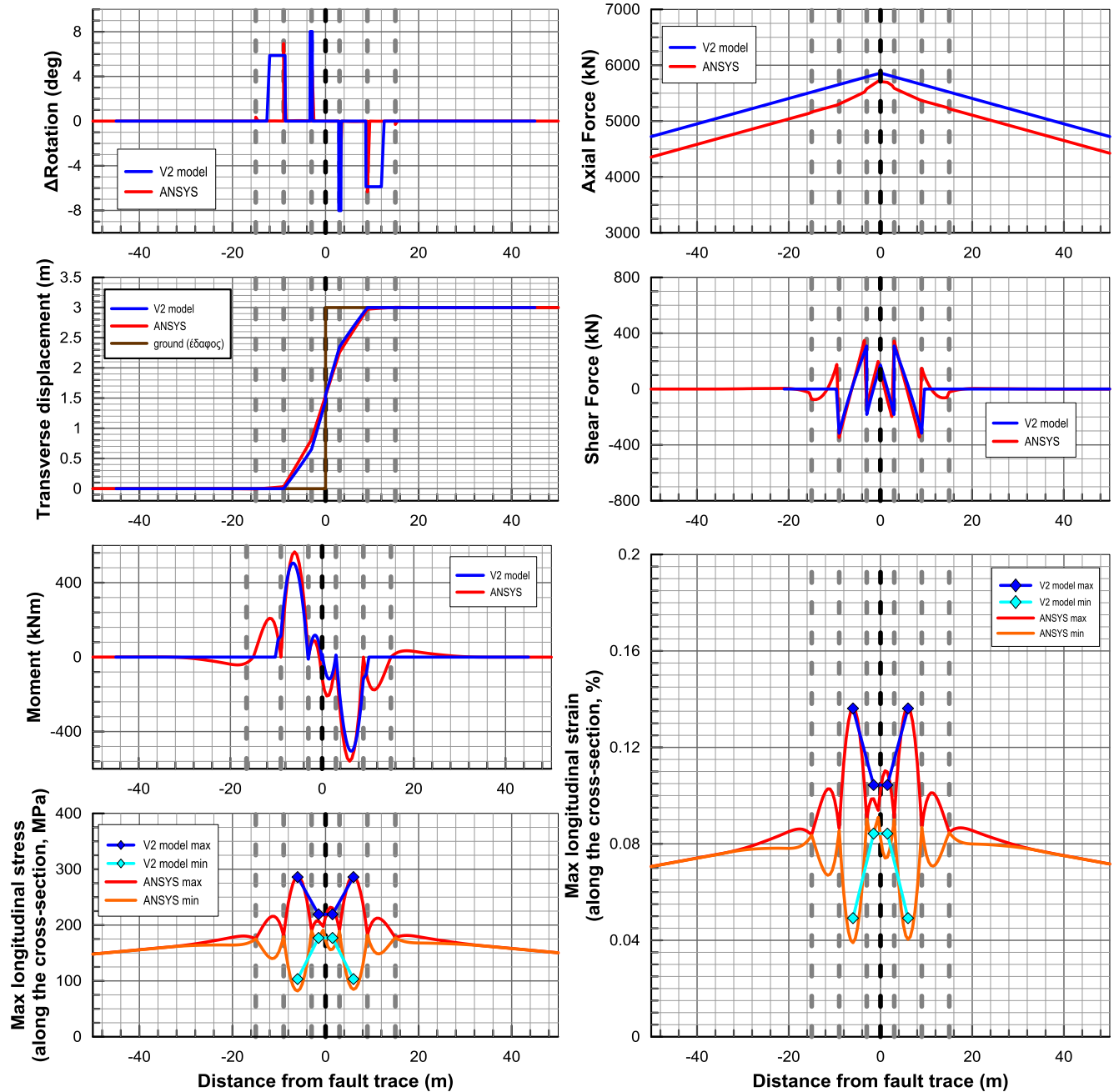
# **Appentix A'**

---

**Parametric Numerical Analyses for strike slip faults**

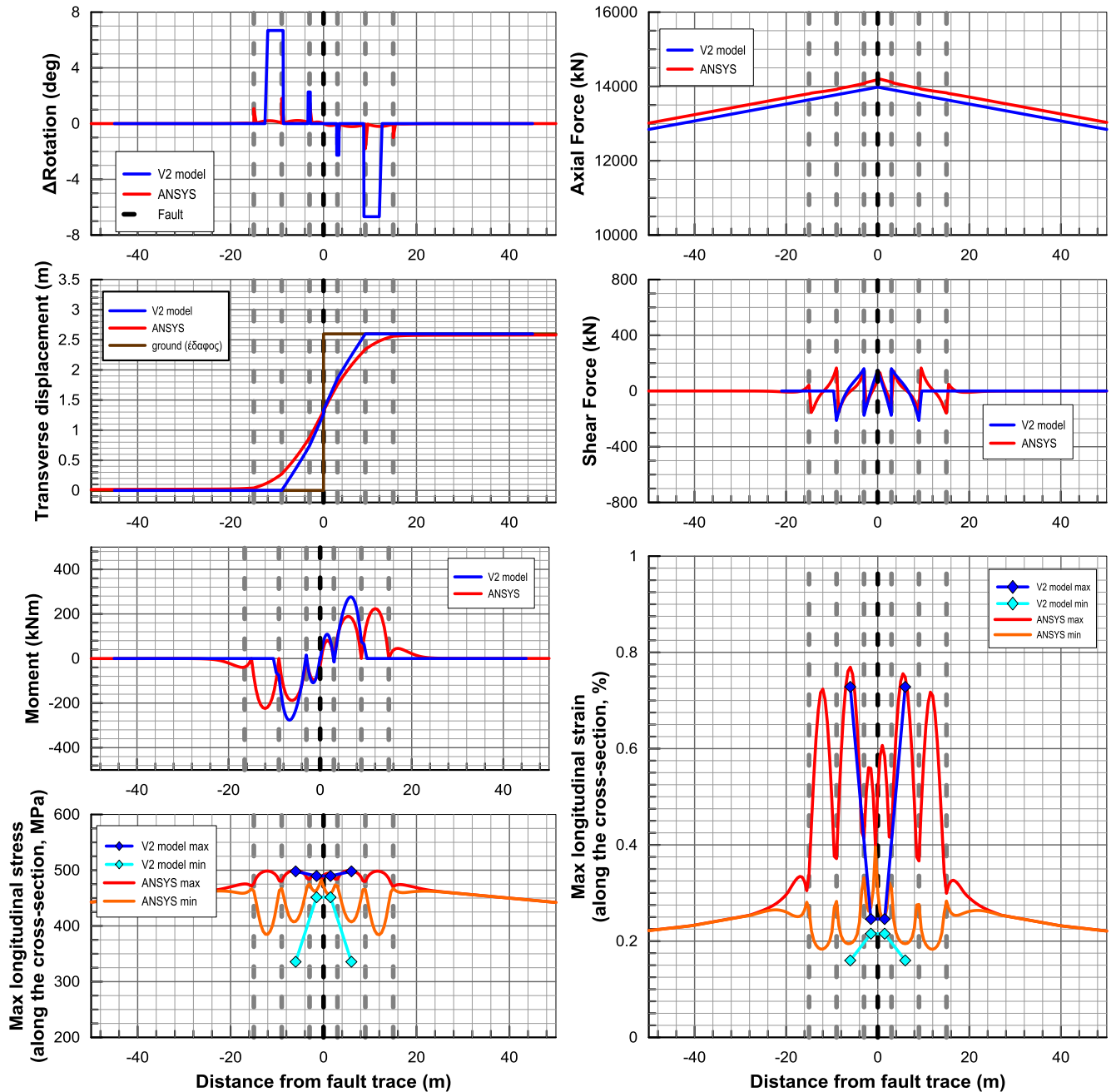


# A1) Flexible joints placed at 6m – Strike slip fault in the middle between two subsequent joints – $D_f=3m$ $\beta=90^\circ$

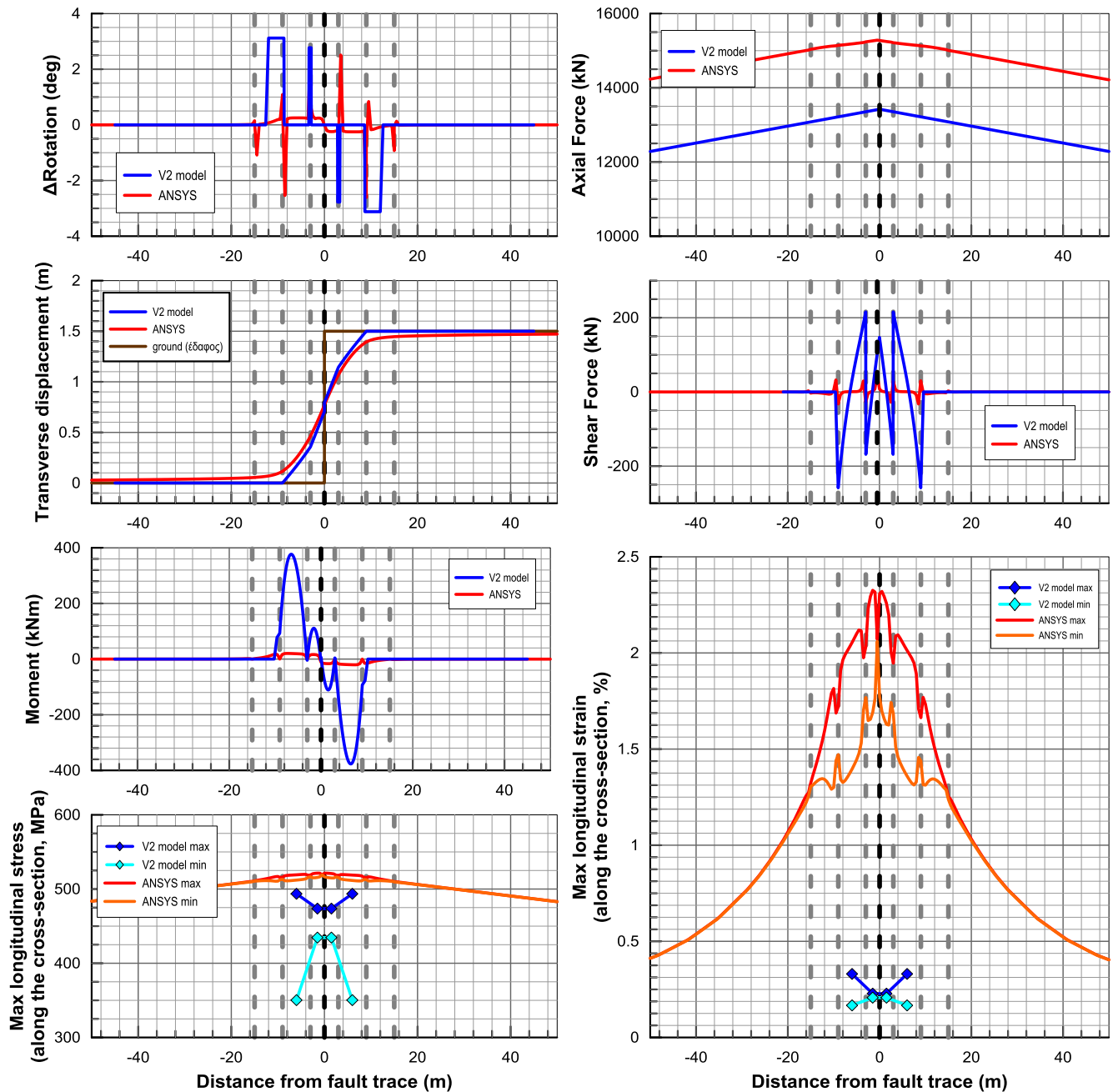




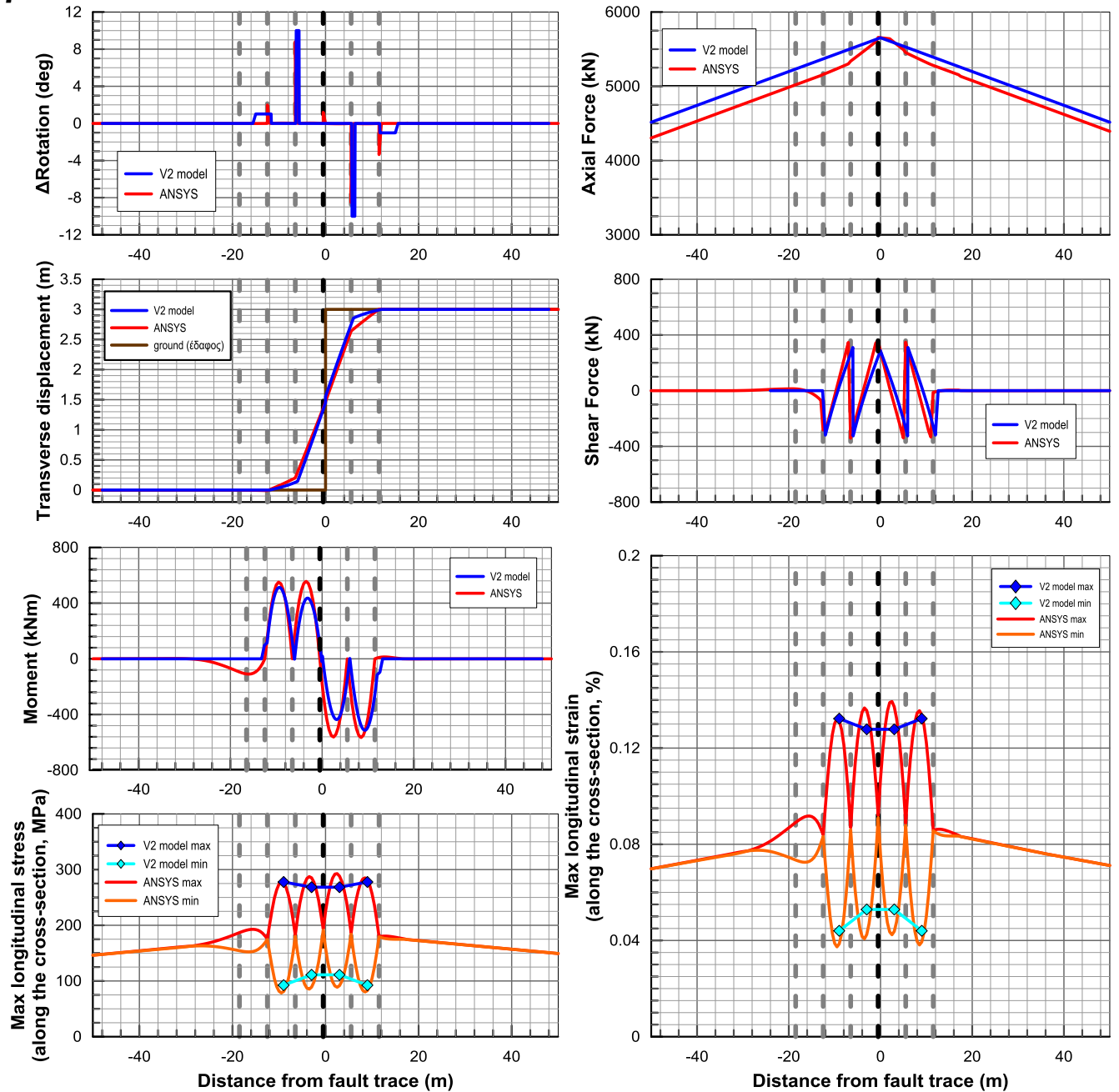
## A2) Flexible joints placed at 6m – Strike slip fault in the middle between two subsequent joints – $D_f=3m$ $\beta=60^\circ$



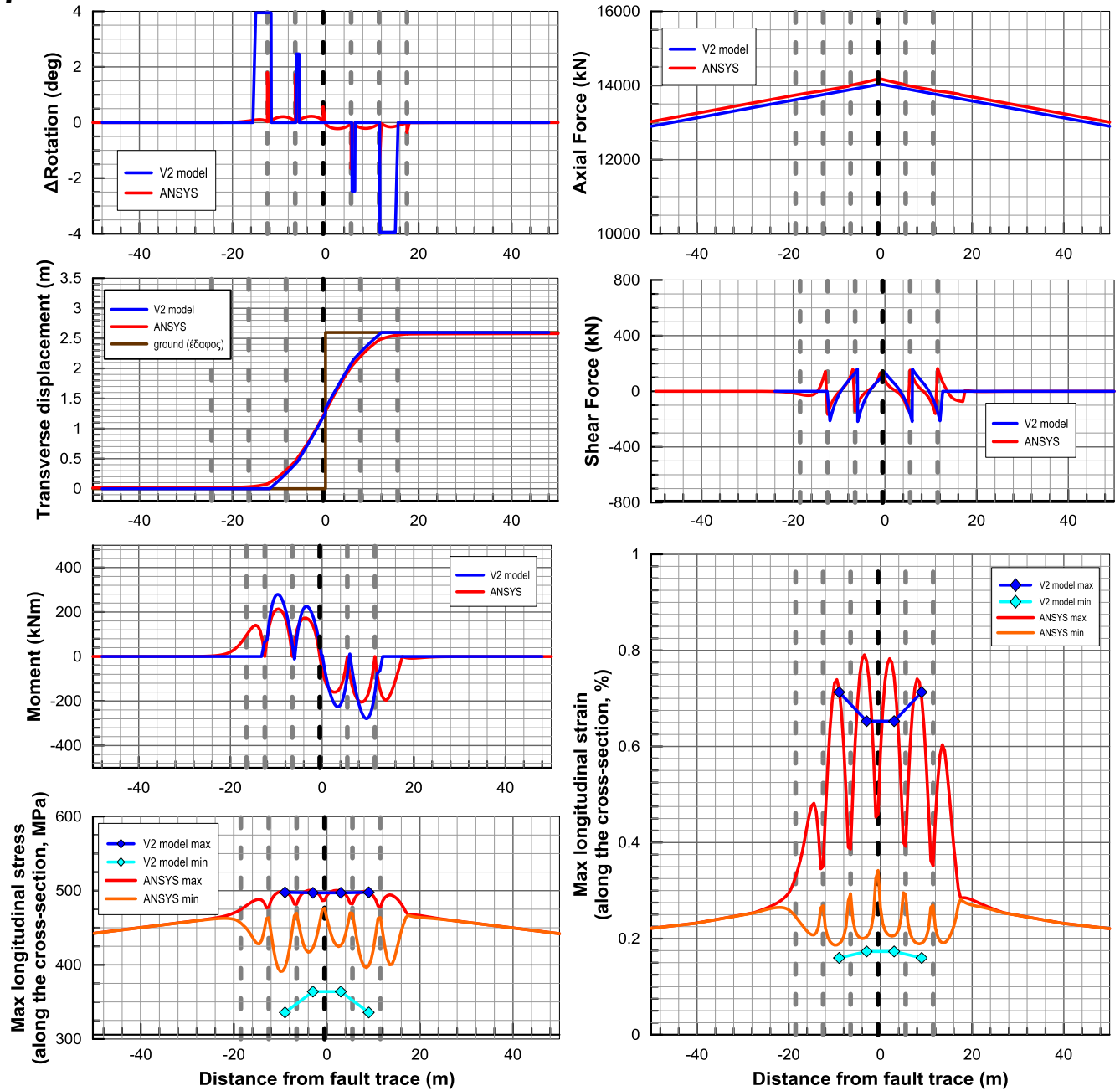
### A3) Flexible joints placed at 6m – Strike slip fault in the middle between two subsequent joints – $D_f=3m$ $\beta=30^\circ$



### A4) Flexible joints placed at 6m – Strike slip fault adjacent to the joint – $D_f=3m$ $\beta=90^\circ$

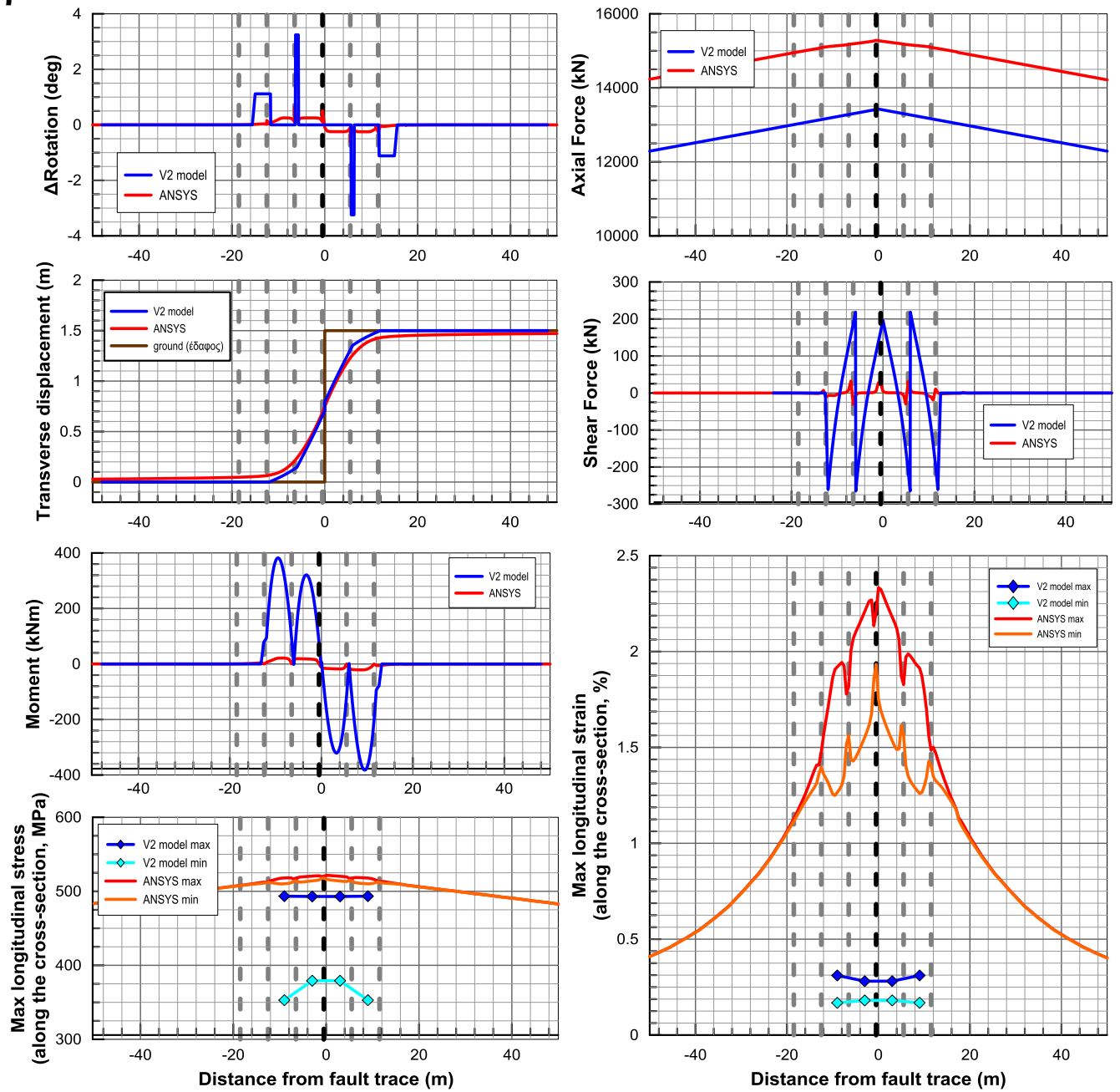


## A5) Flexible joints placed at 6m – Strike slip fault adjacent to the joint – $D_f=3m$ $\beta=60^\circ$

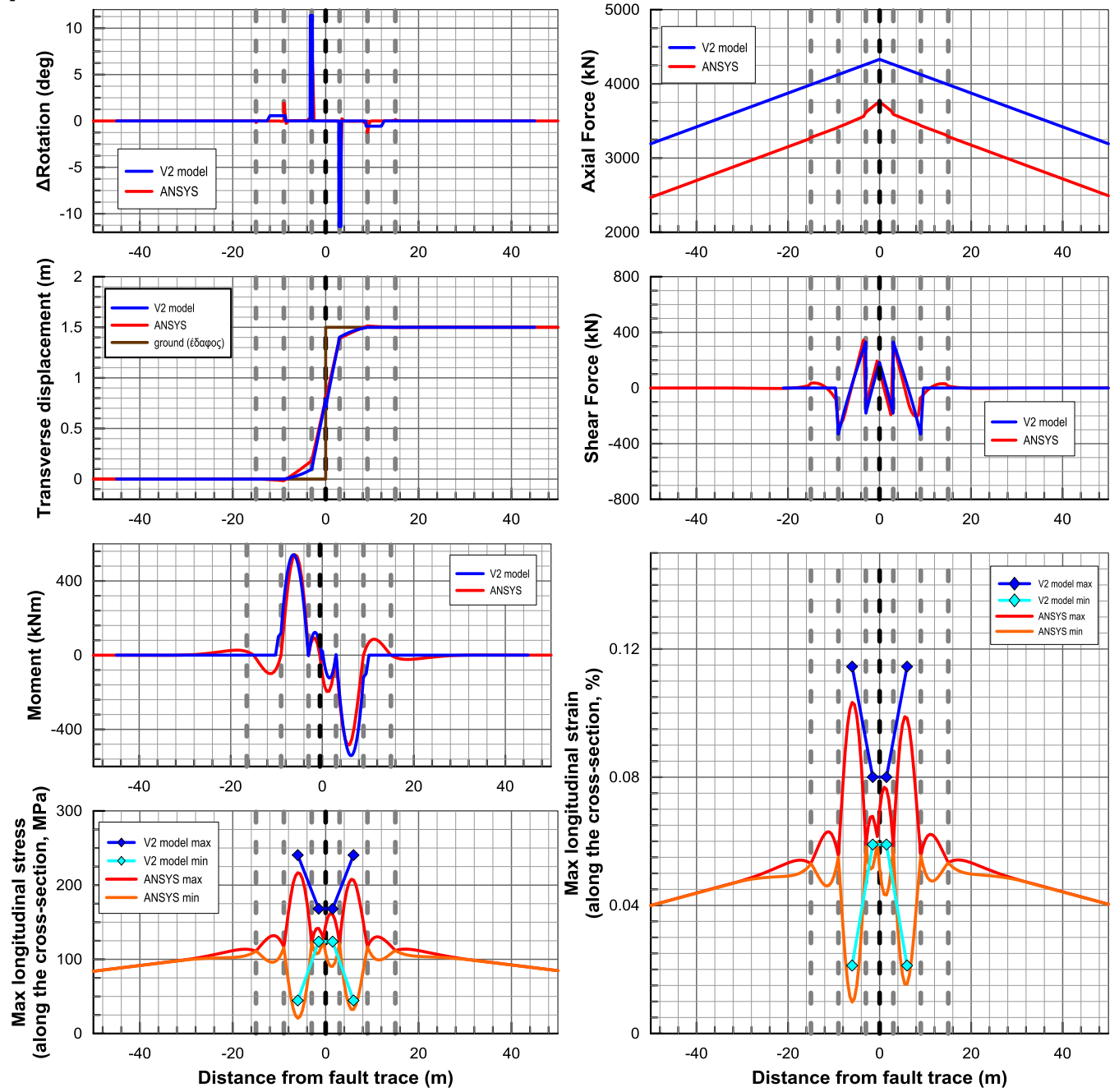


## A6) Flexible joints placed at 6m – Strike slip fault adjacent to the joint – $D_f=3m$

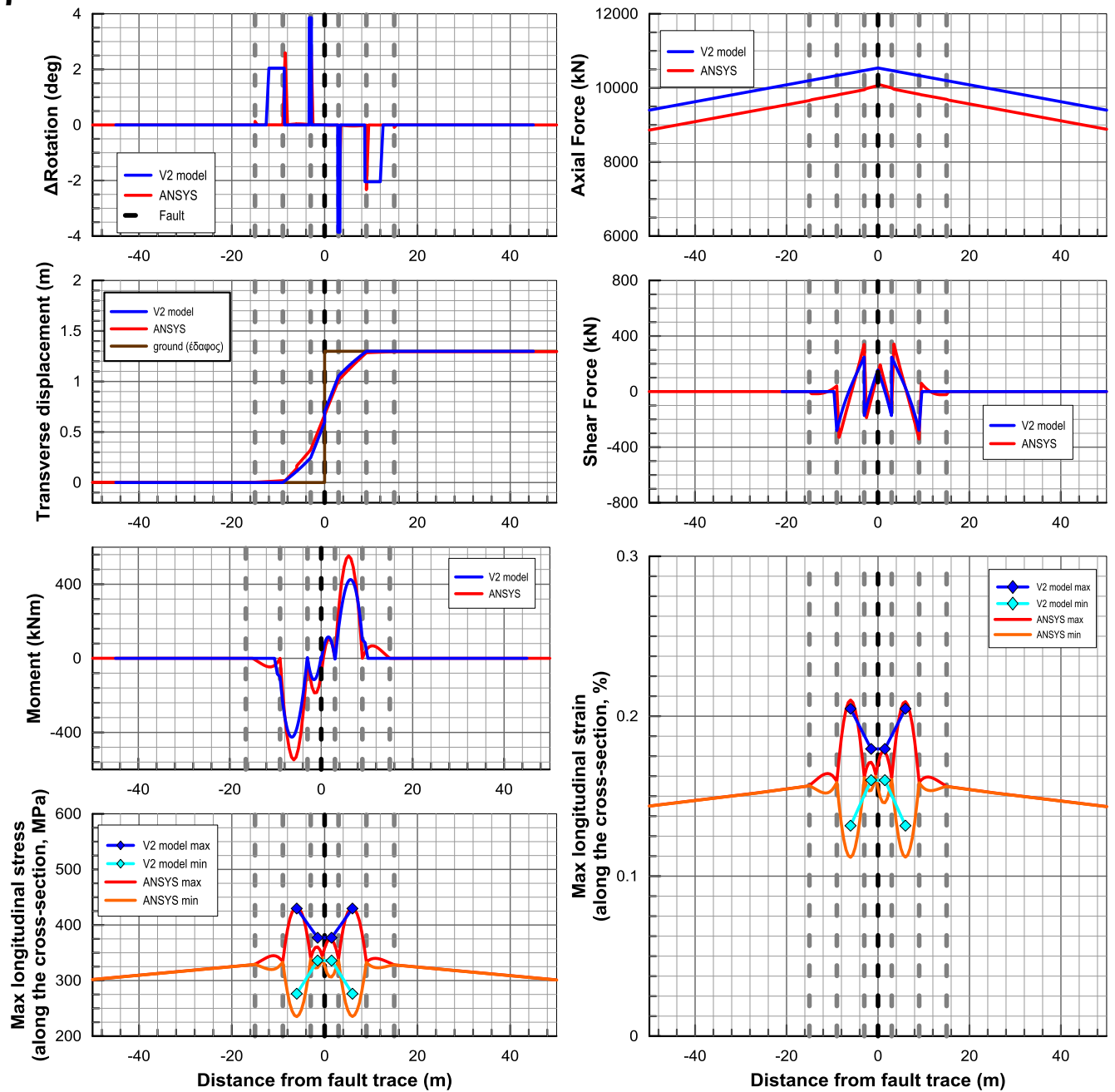
$\beta=30^\circ$



## A7) Flexible joints placed at 6m – Strike slip fault in the middle between two subsequent joints – $D_f=1.5m$ $\beta=90^\circ$

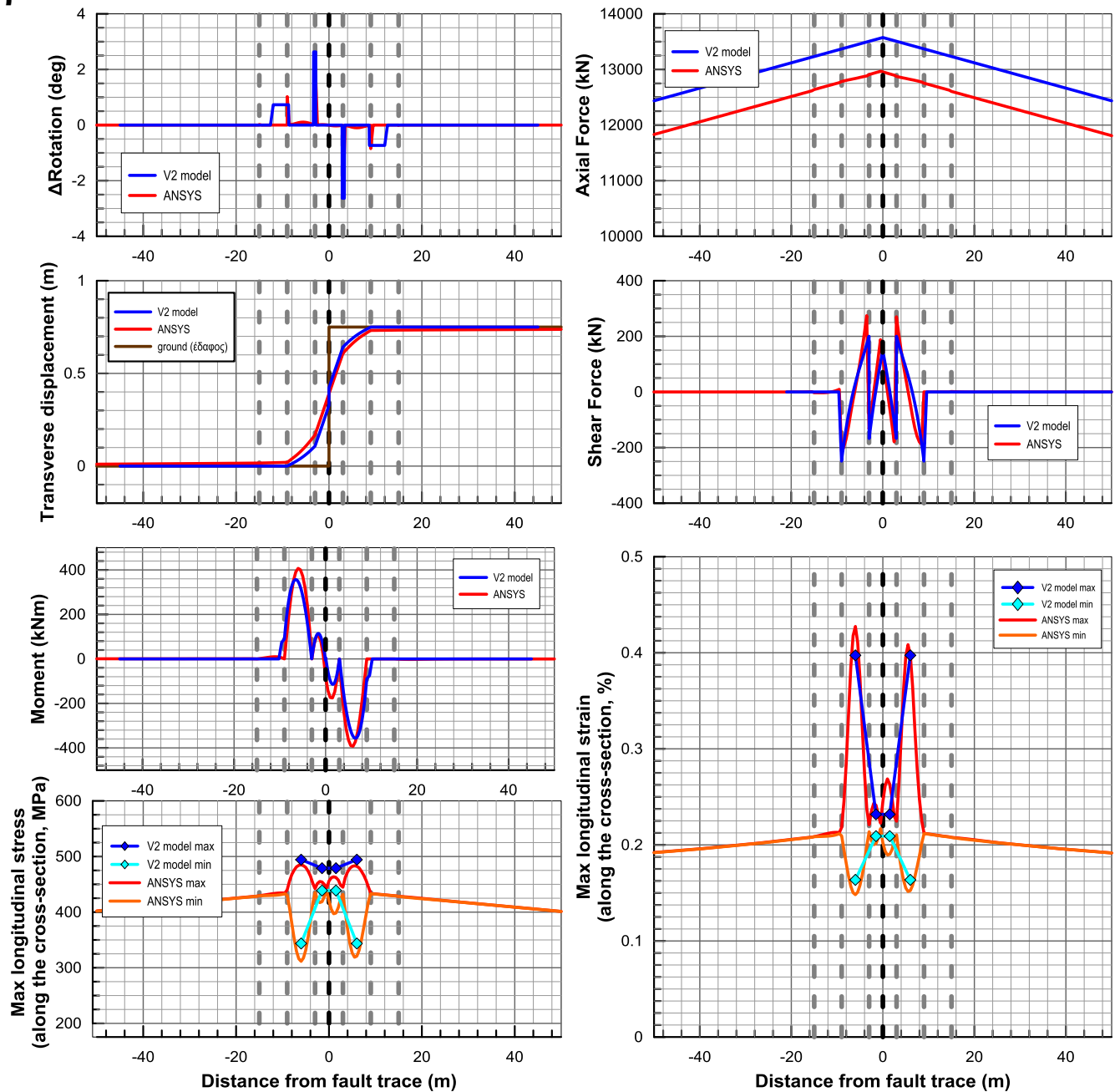


## A8) Flexible joints placed at 6m – Strike slip fault in the middle between two subsequent joints – $D_f=1.5m$ $\beta=60^\circ$



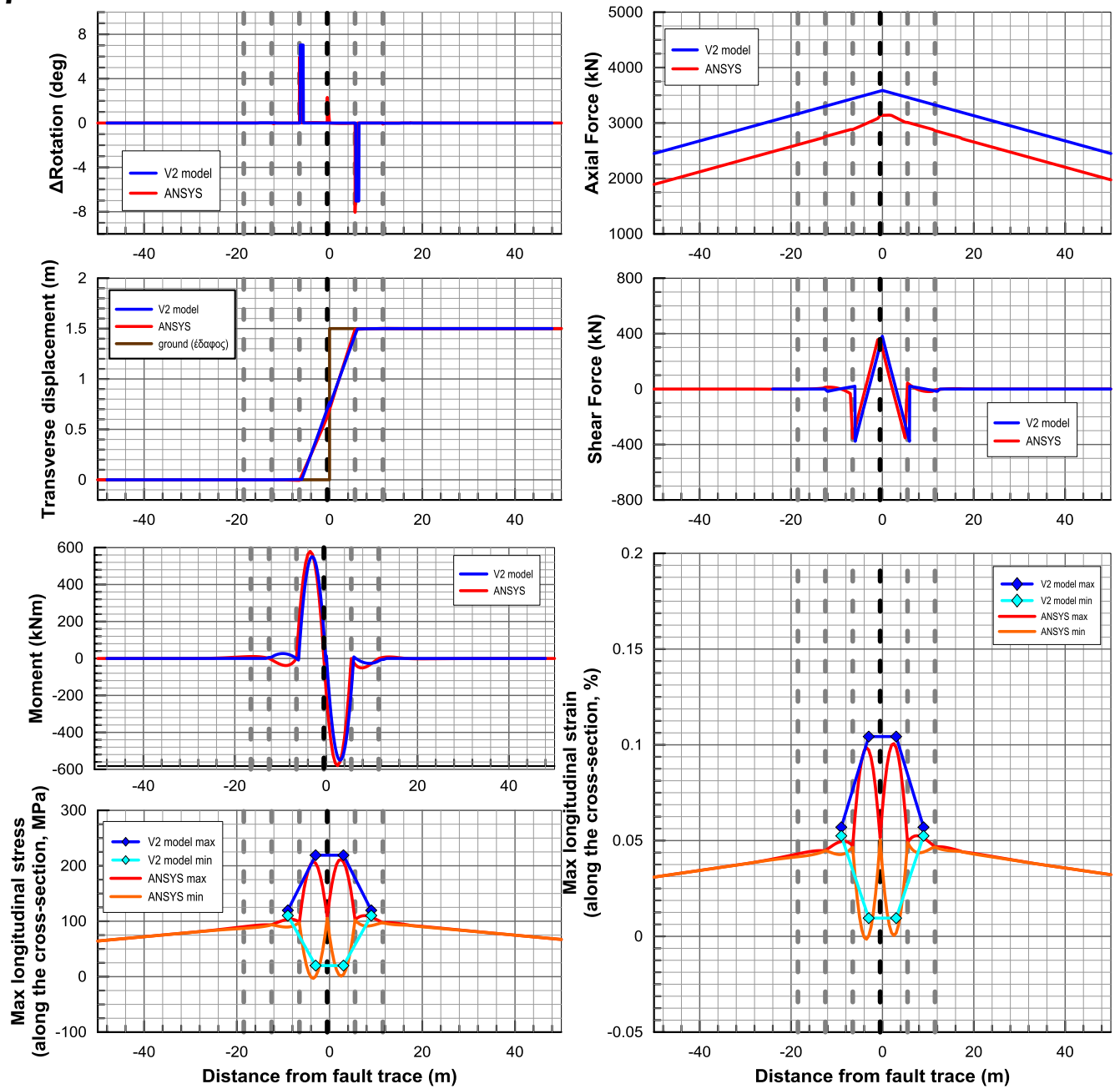
## A9) Flexible joints placed at 6m – Strike slip fault in the middle between two subsequent joints – $D_f=1.5m$

$\beta=30^\circ$

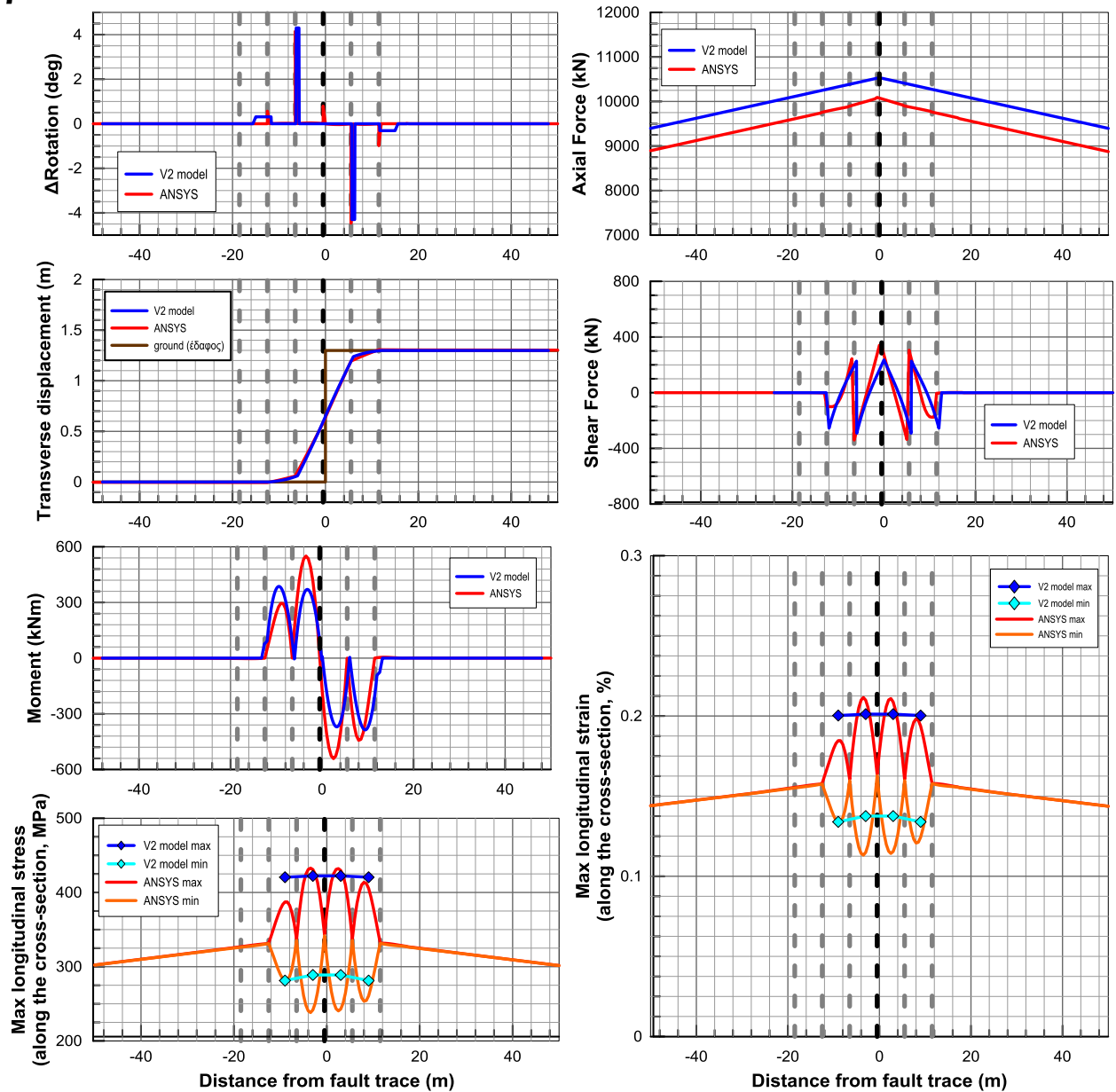




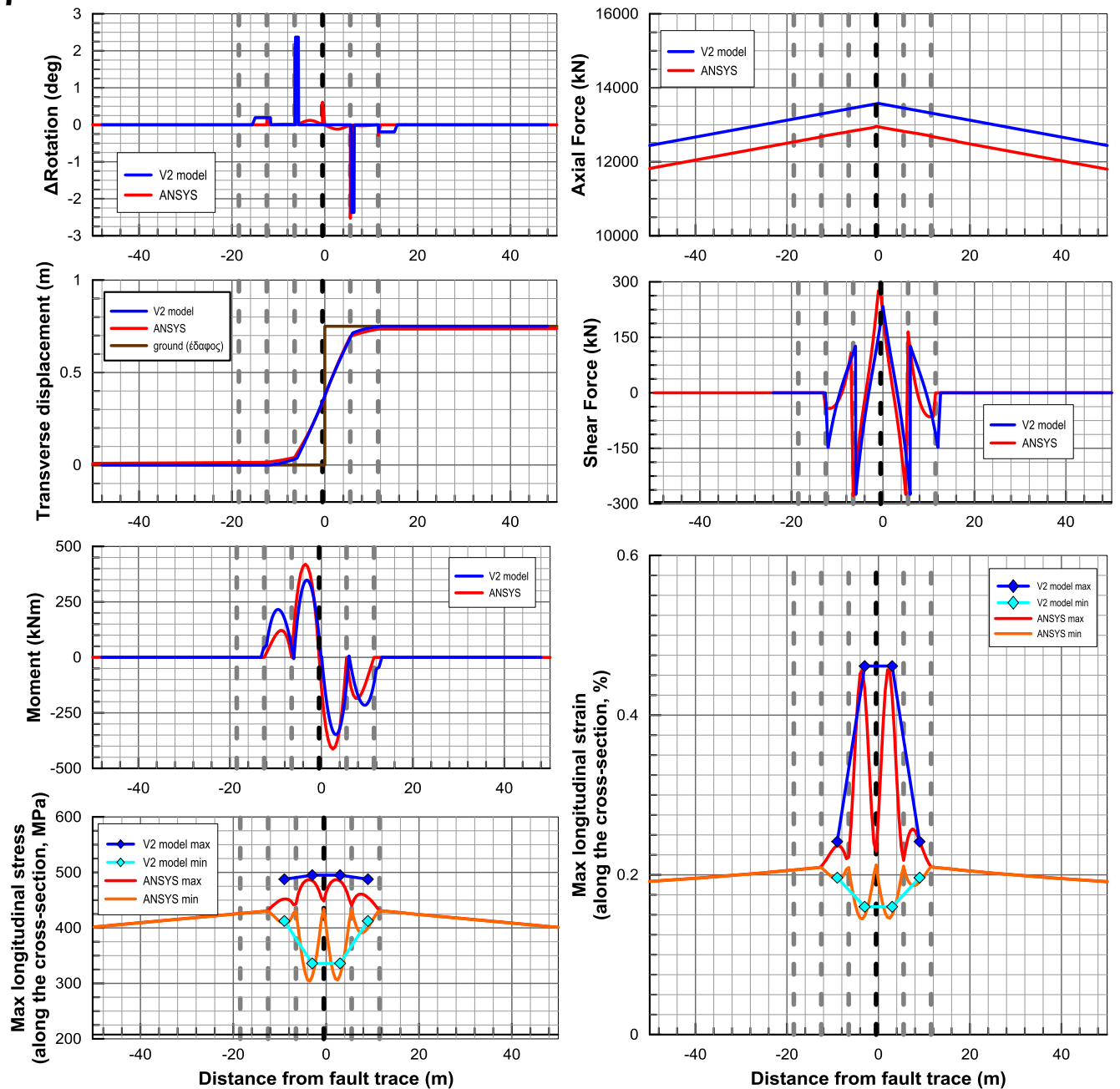
# A10) Flexible joints placed at 6m – Strike slip fault adjacent to the joint – $D_f=1,5m$ $\beta=90^\circ$



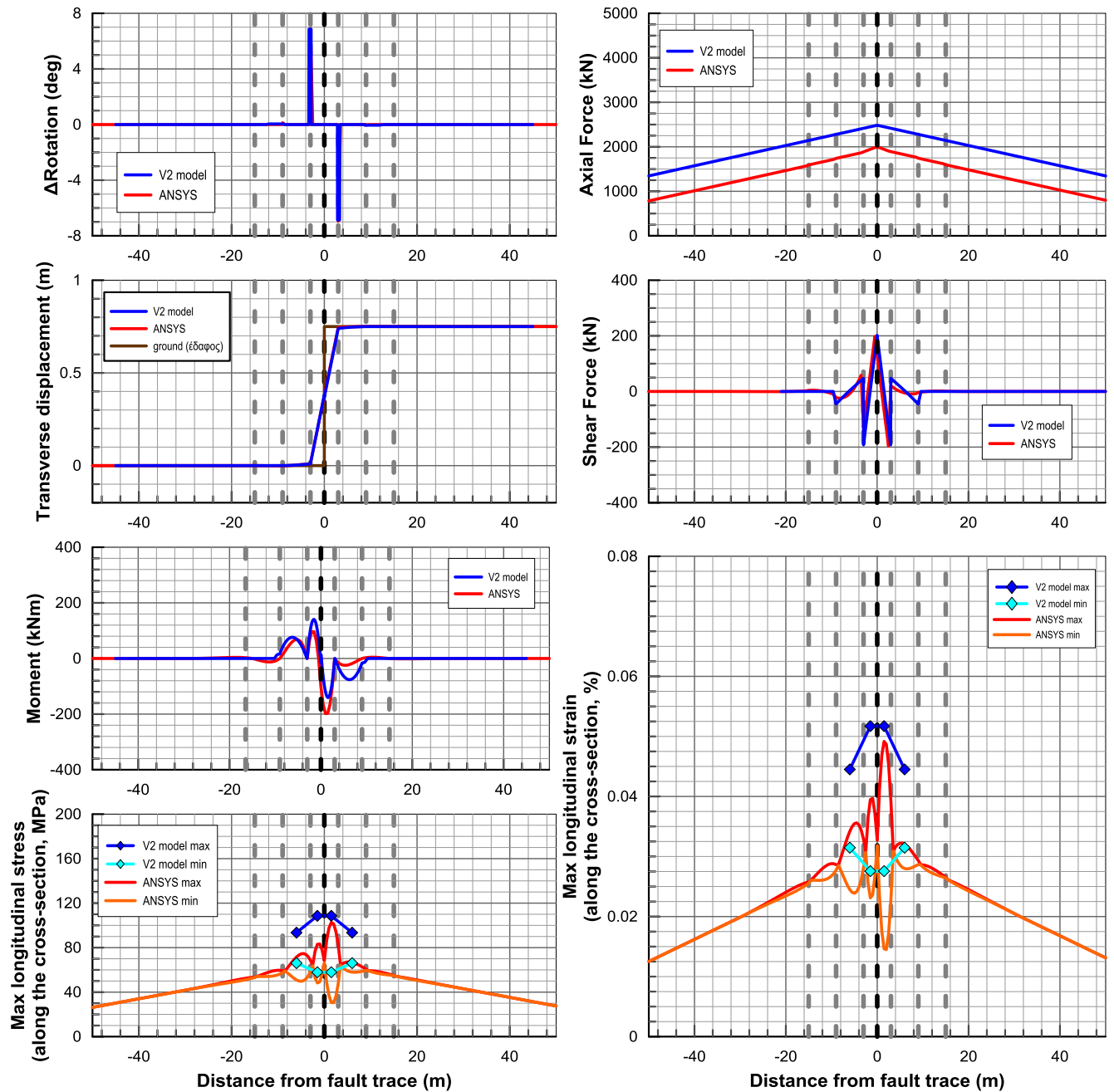
# A11) Flexible joints placed at 6m – Strike slip fault adjacent to the joint – $D_f=1,5m$ $\beta=60^\circ$



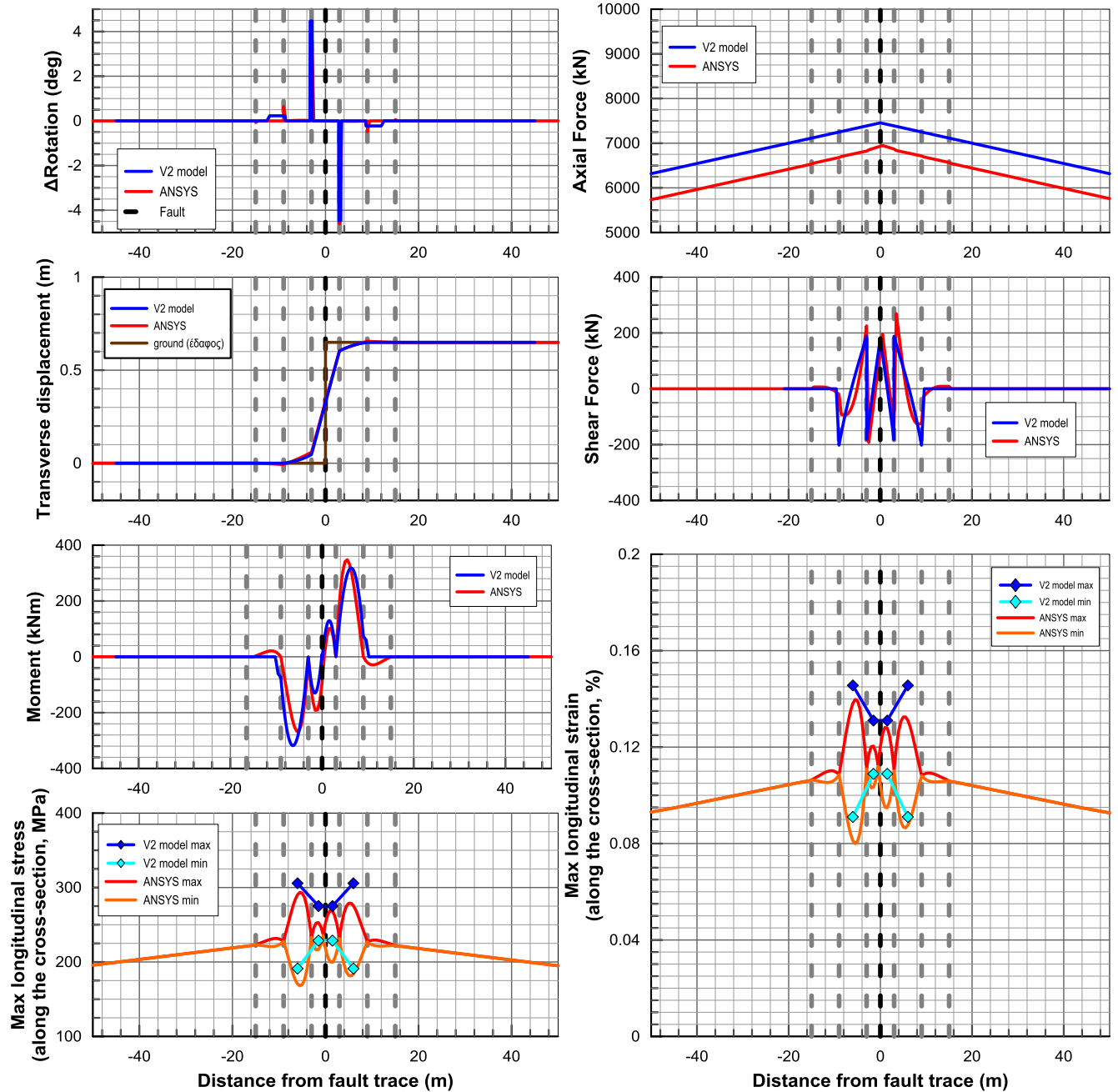
## A12) Flexible joints placed at 6m – Strike slip fault adjacent to the joint – $D_f=1,5m$ $\beta=30^\circ$



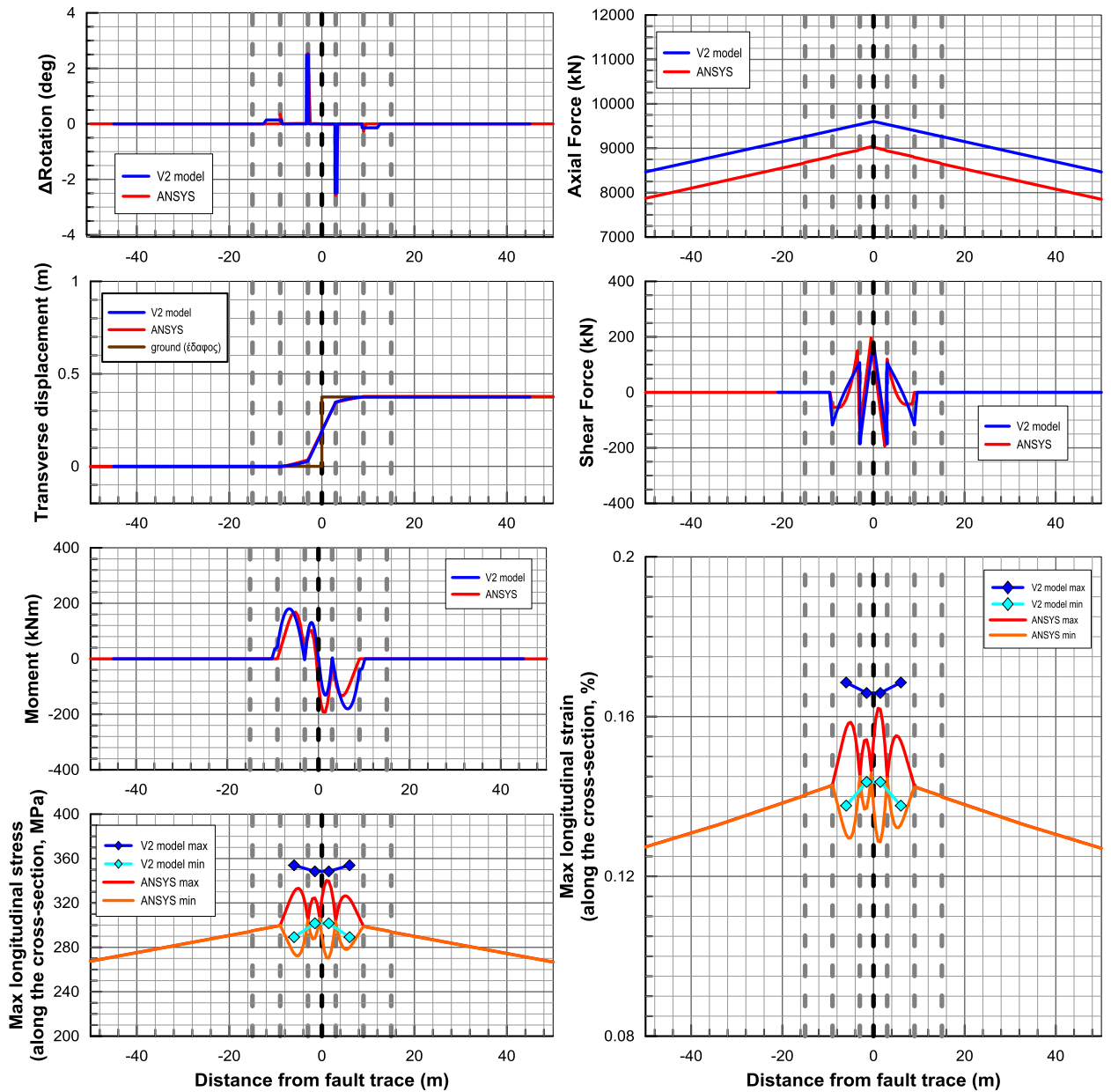
### A13) Flexible joints placed at 6m – Strike slip fault in the middle between two subsequent joints – $D_f=0.75m$ $\beta=90^\circ$



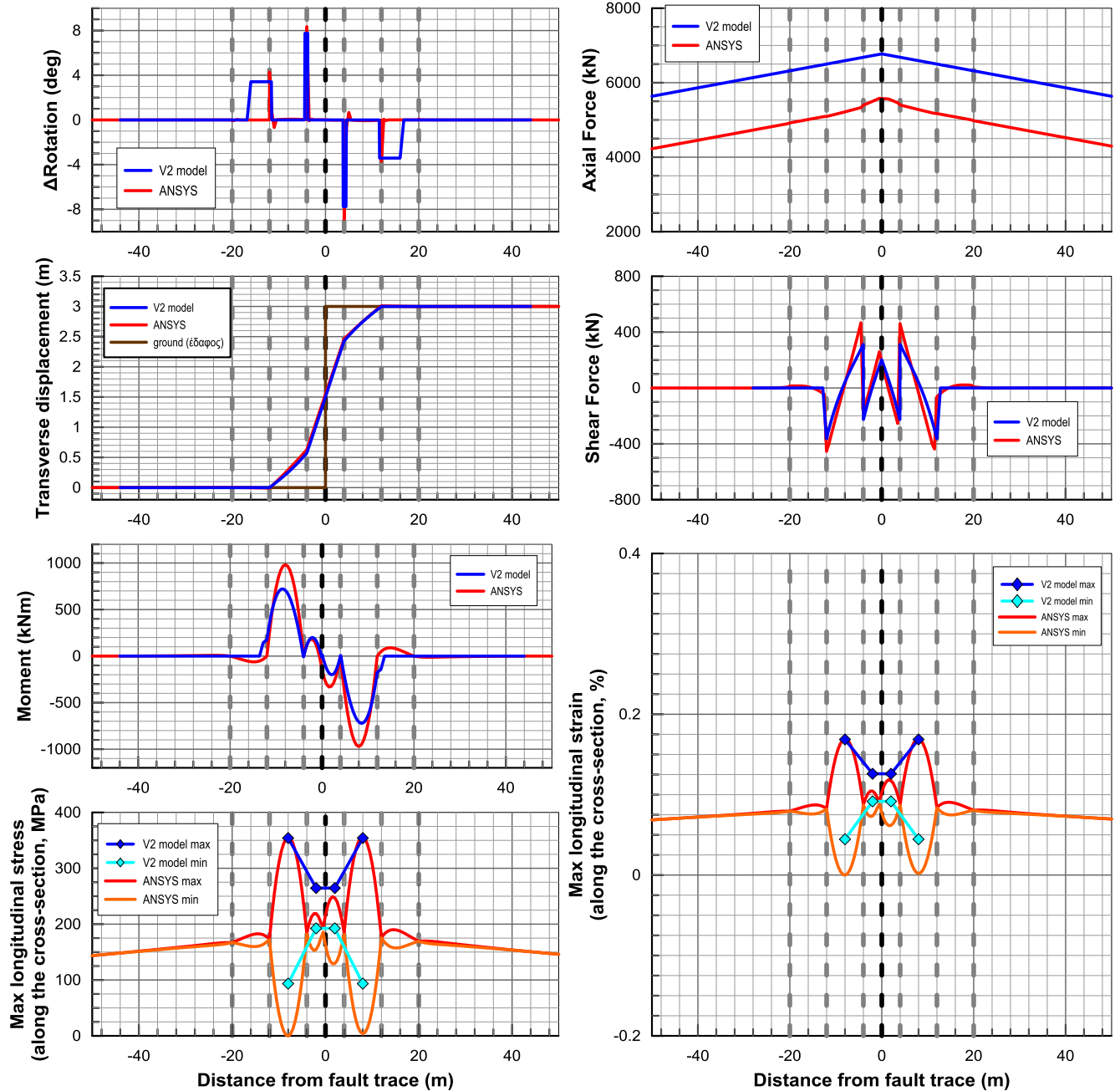
# A14) Flexible joints placed at 6m – Strike slip fault in the middle between two subsequent joints – $D_f=0.75m$ $\beta=60^\circ$



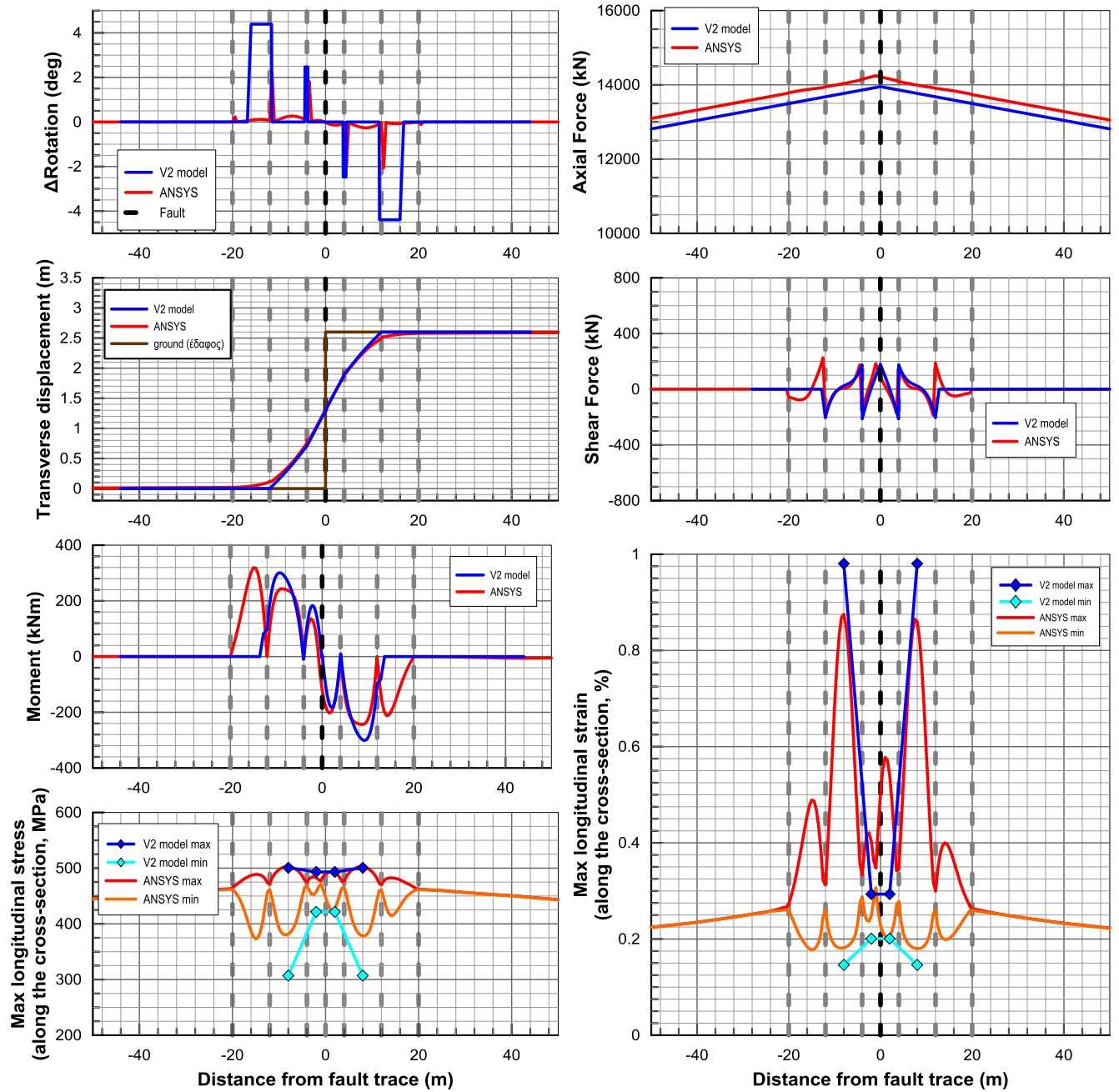
## A15) Flexible joints placed at 6m – Strike slip fault in the middle between two subsequent joints – $D_f=0.75m$ $\beta=30^\circ$



# A16) Flexible joints placed at 8m – Strike slip fault in the middle between two subsequent joints – $D_f=3m$ $\beta=90^\circ$

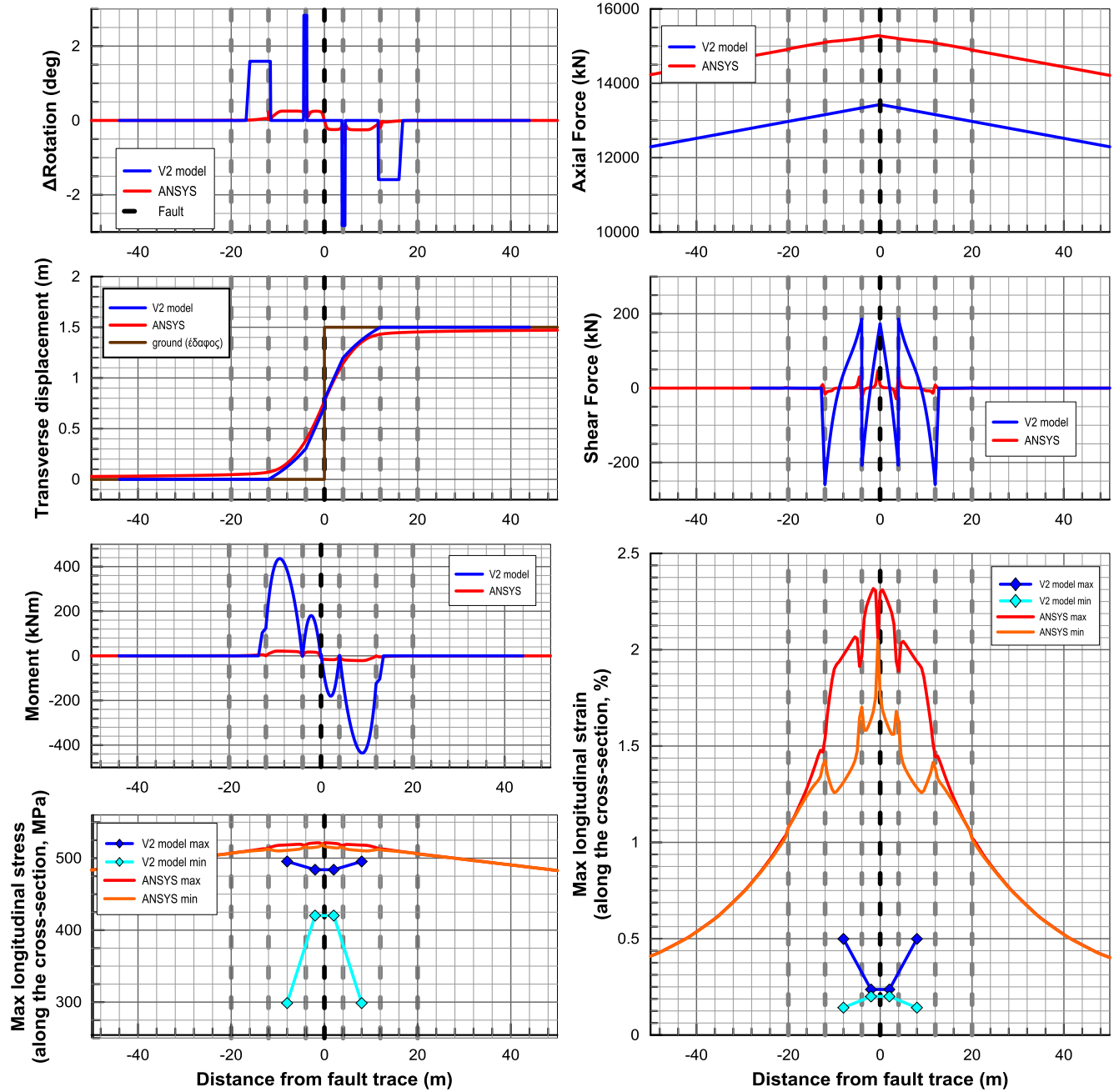


# A17) Flexible joints placed at 8m – Strike slip fault in the middle between two subsequent joints – $D_f=3m$ $\beta=60^\circ$

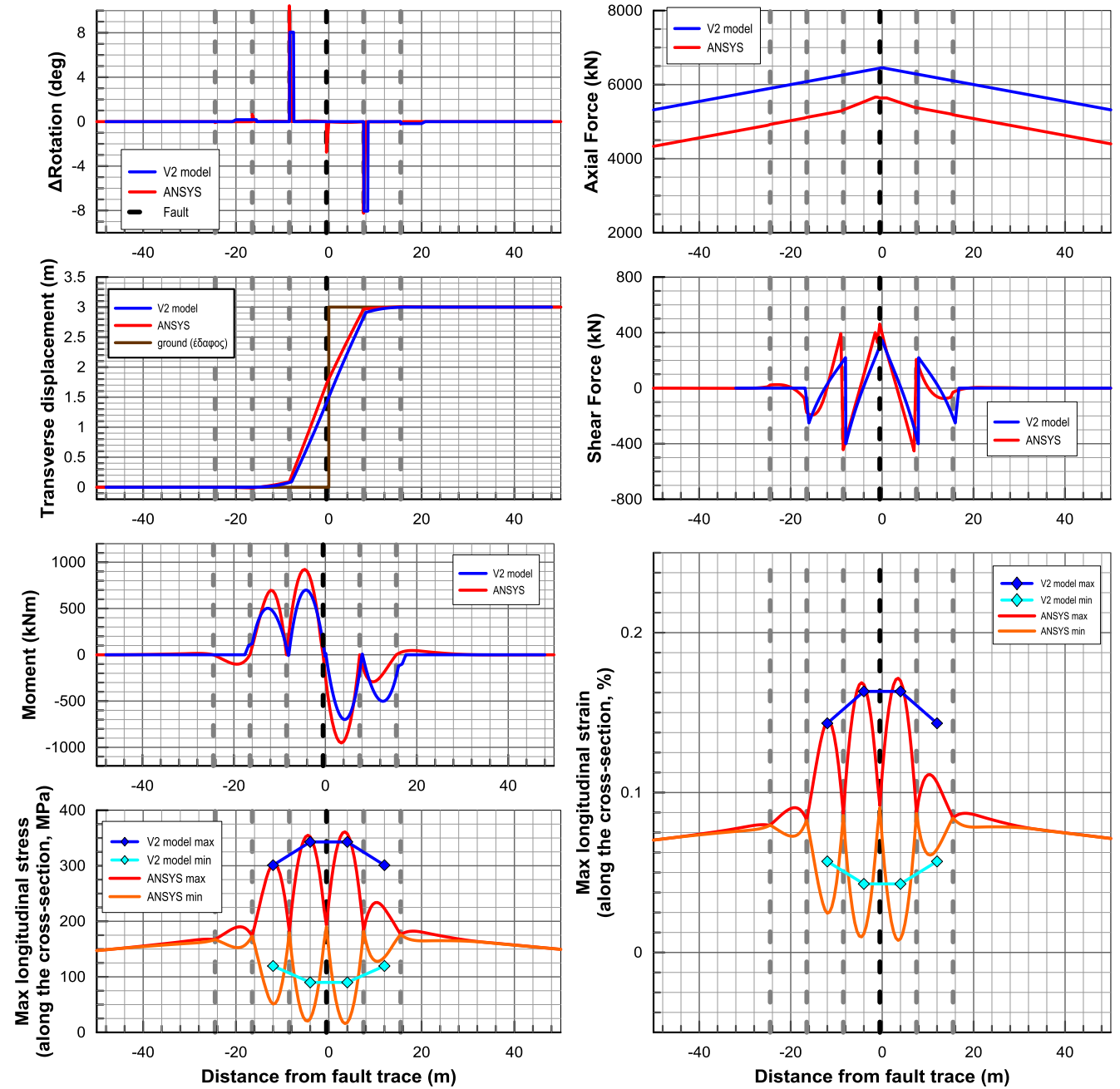




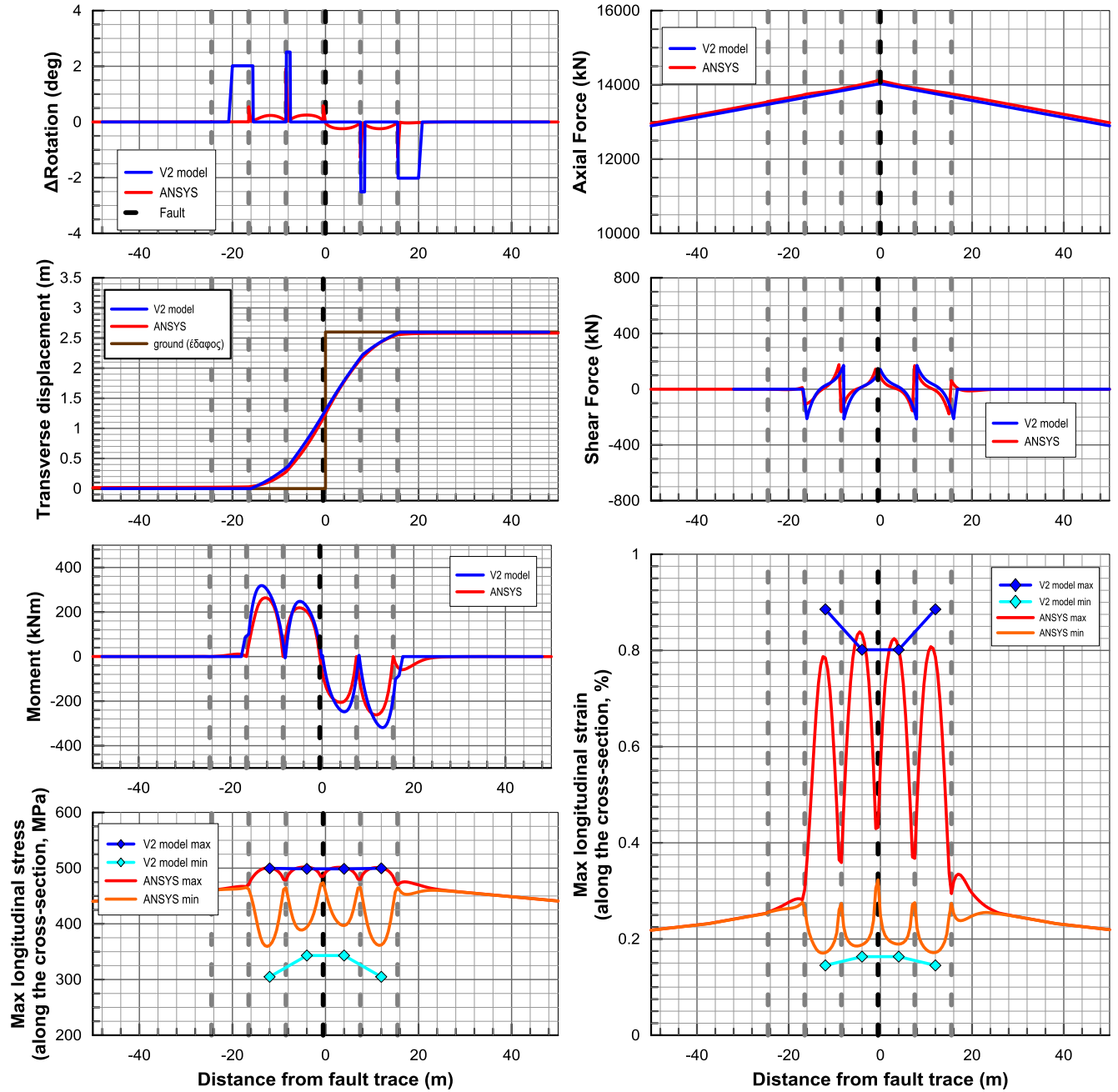
# A18) Flexible joints placed at 8m – Strike slip fault in the middle between two subsequent joints – $D_f=3m$ $\beta=30^\circ$



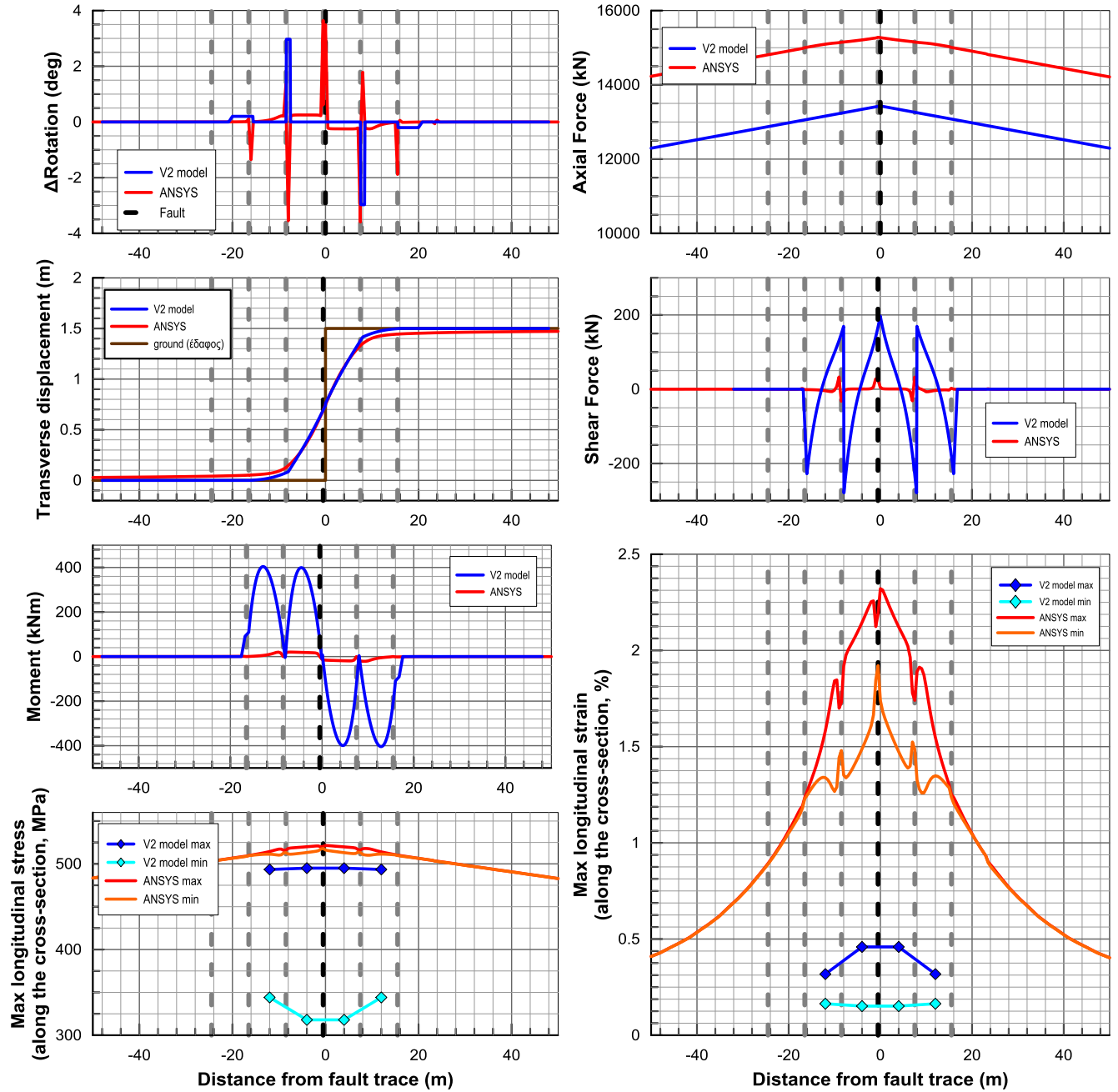
# A19) Flexible joints placed at 8m – Strike slip fault adjacent to the joint – $D_f=3m$ $\beta=90^\circ$



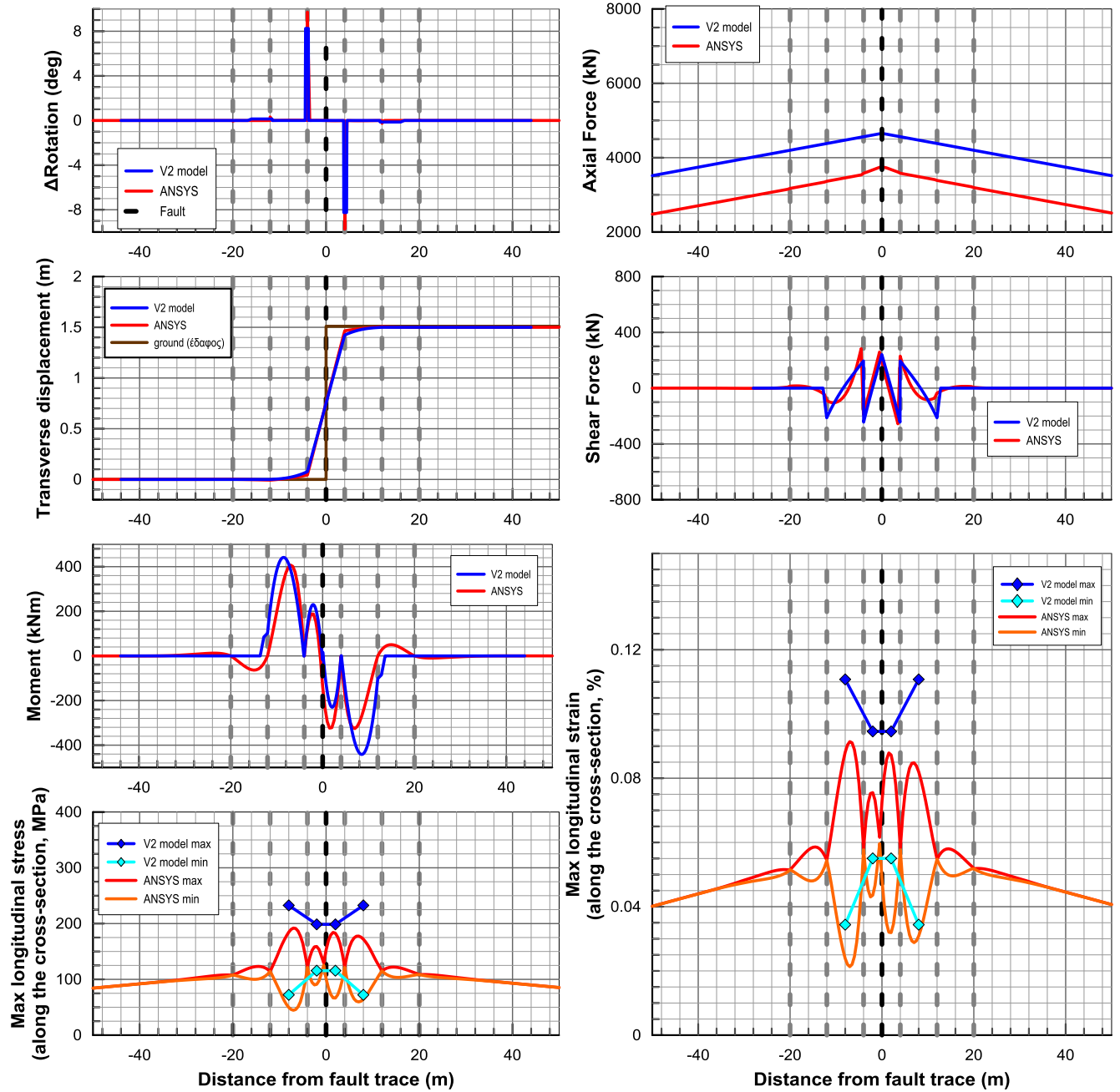
## A20) Flexible joints placed at 8m – Strike slip fault adjacent to the joint – $D_f=3m$ $\beta=60^\circ$



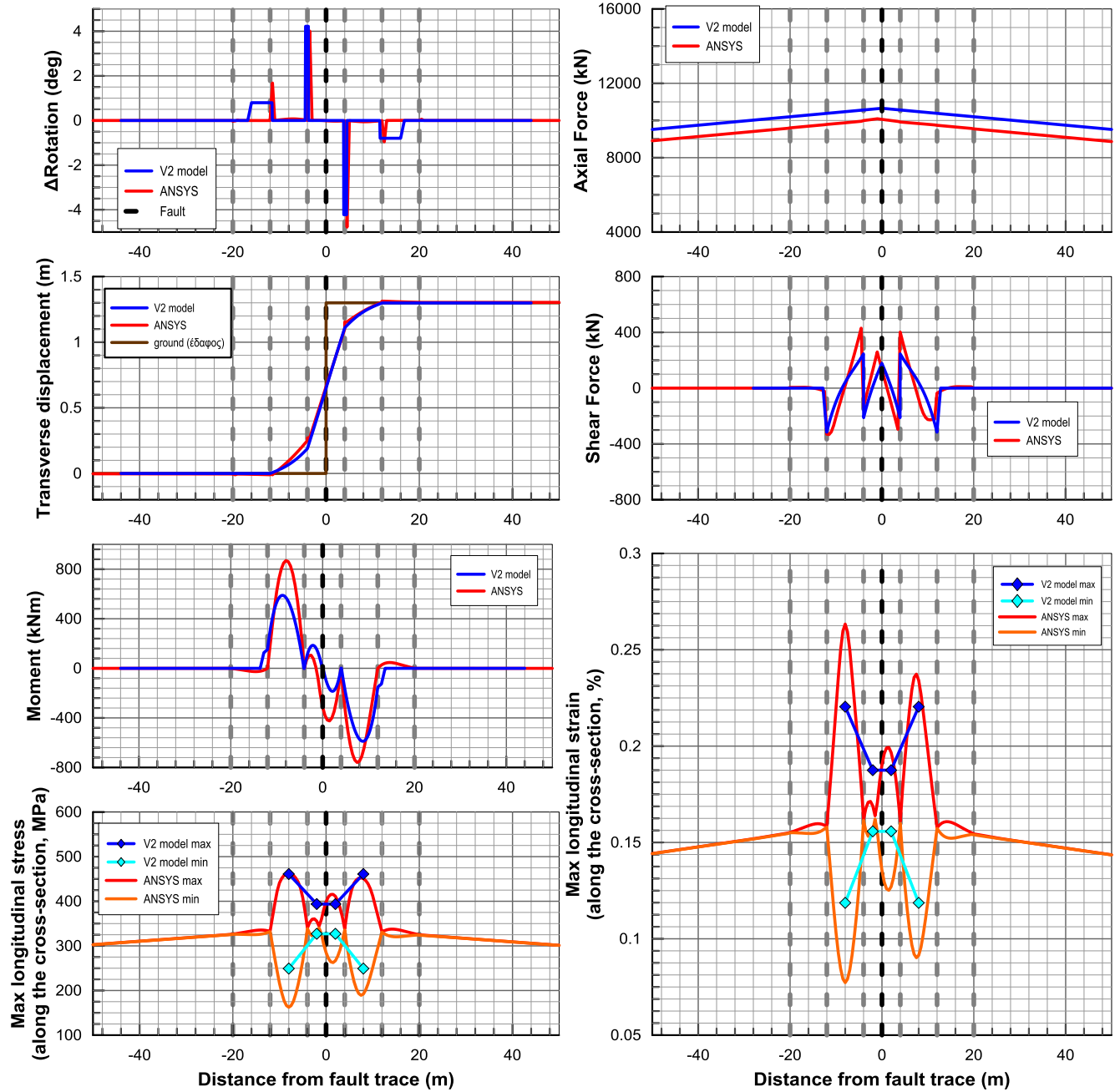
## A21) Flexible joints placed at 8m – Strike slip fault adjacent to the joint – $D_f=3m$ $\beta=30^\circ$



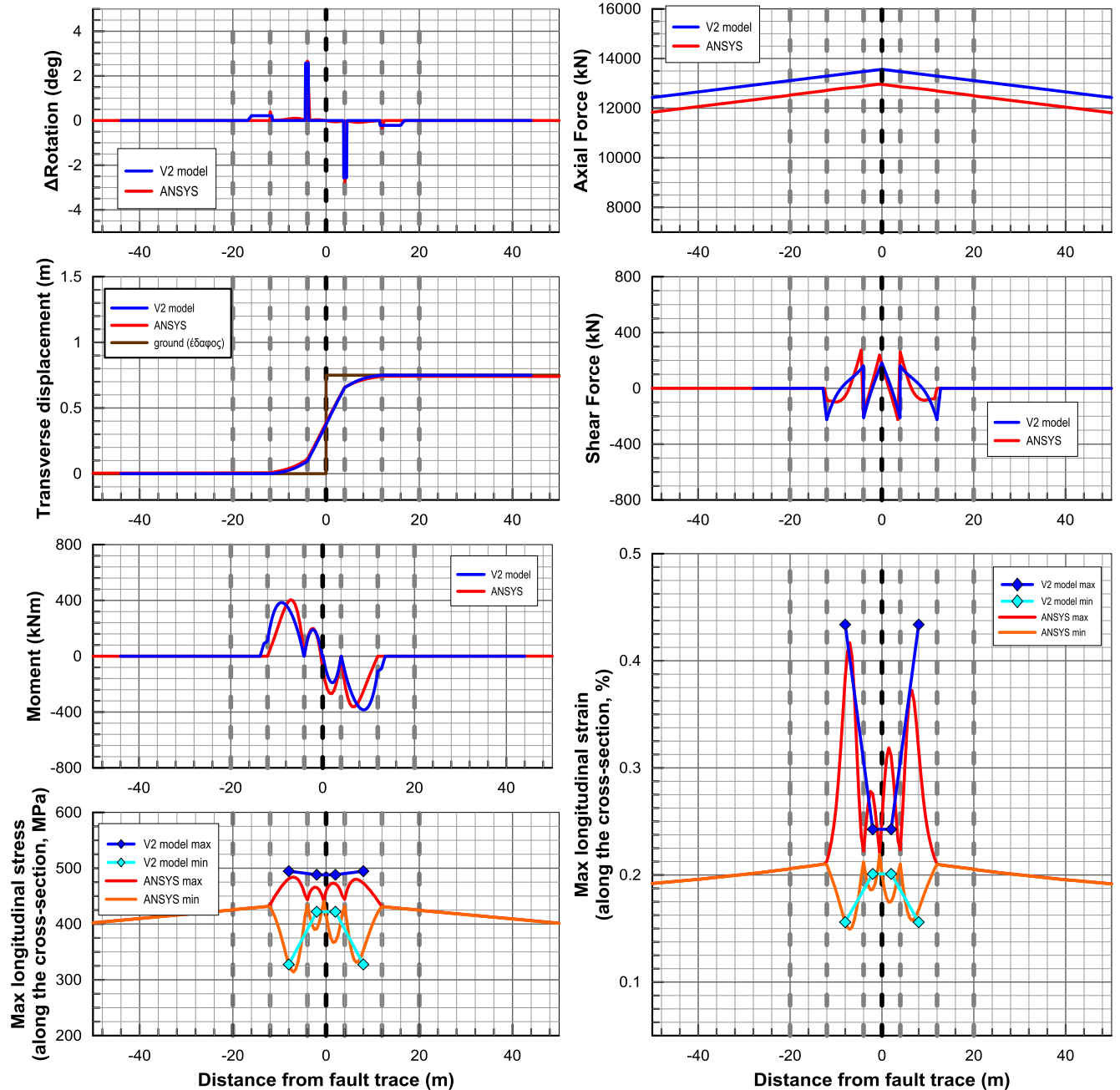
## A22) Flexible joints placed at 8m – Strike slip fault in the middle between two subsequent joints – $D_f=1,5m$ $\beta=90^\circ$



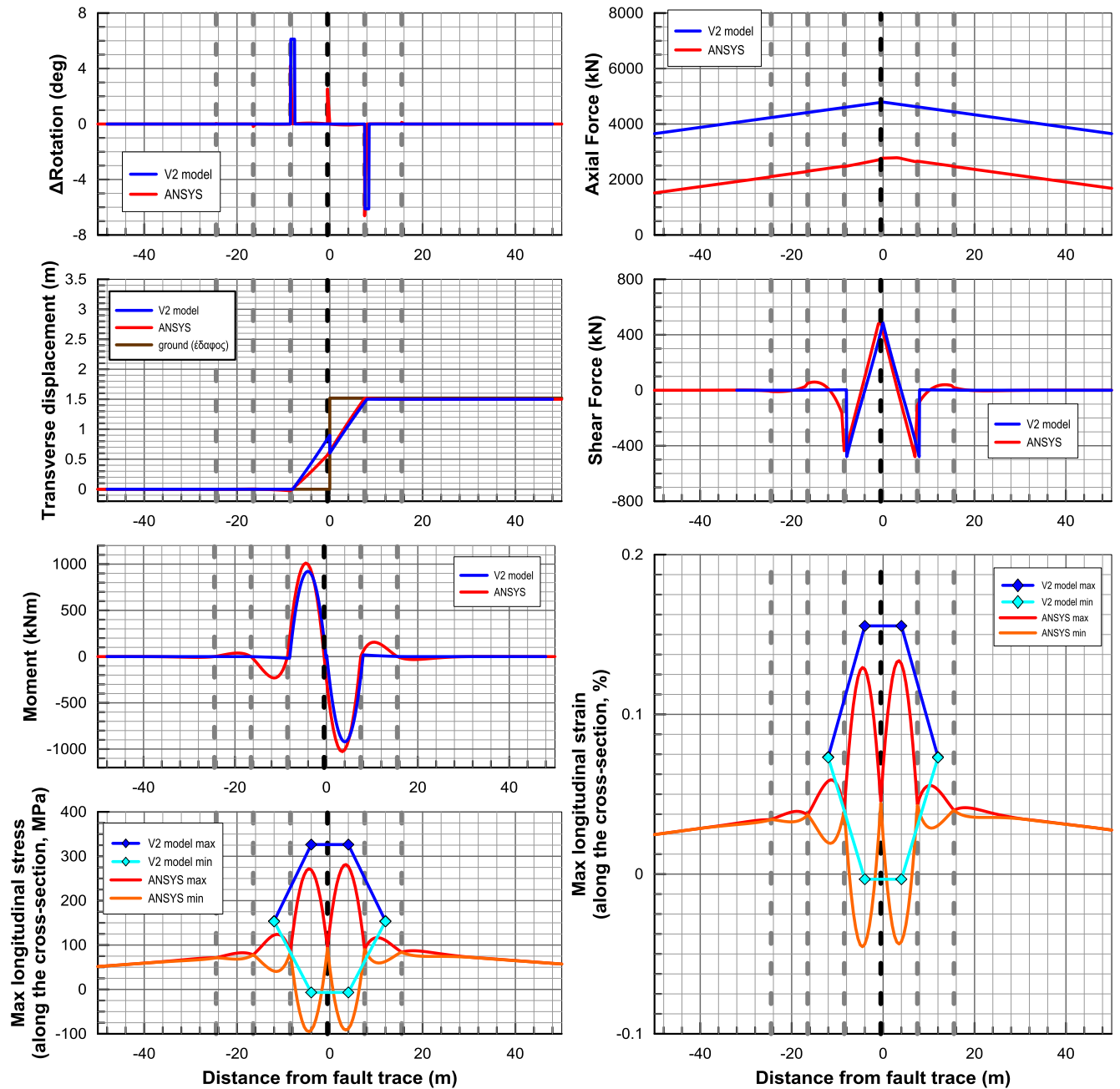
## A23) Flexible joints placed at 8m – Strike slip fault in the middle between two subsequent joints – $D_f=1,5m$ $\beta=60^\circ$



## A24) Flexible joints placed at 8m – Strike slip fault in the middle between two subsequent joints – $D_f=1,5m$ $\beta=30^\circ$

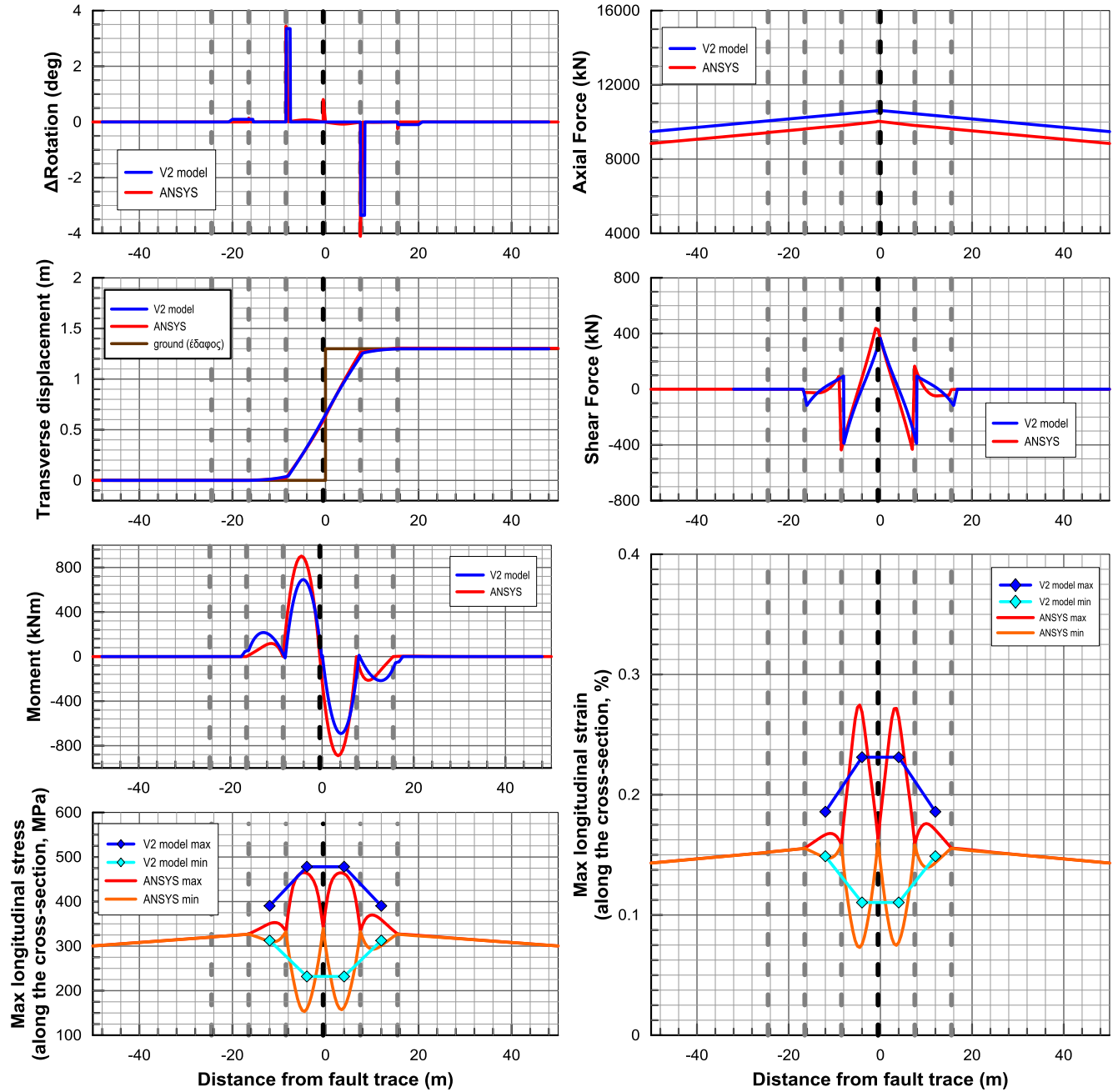


## A25) Flexible joints placed at 8m – Strike slip fault adjacent to the joint – $D_f=1,5m$ $\beta=90^\circ$

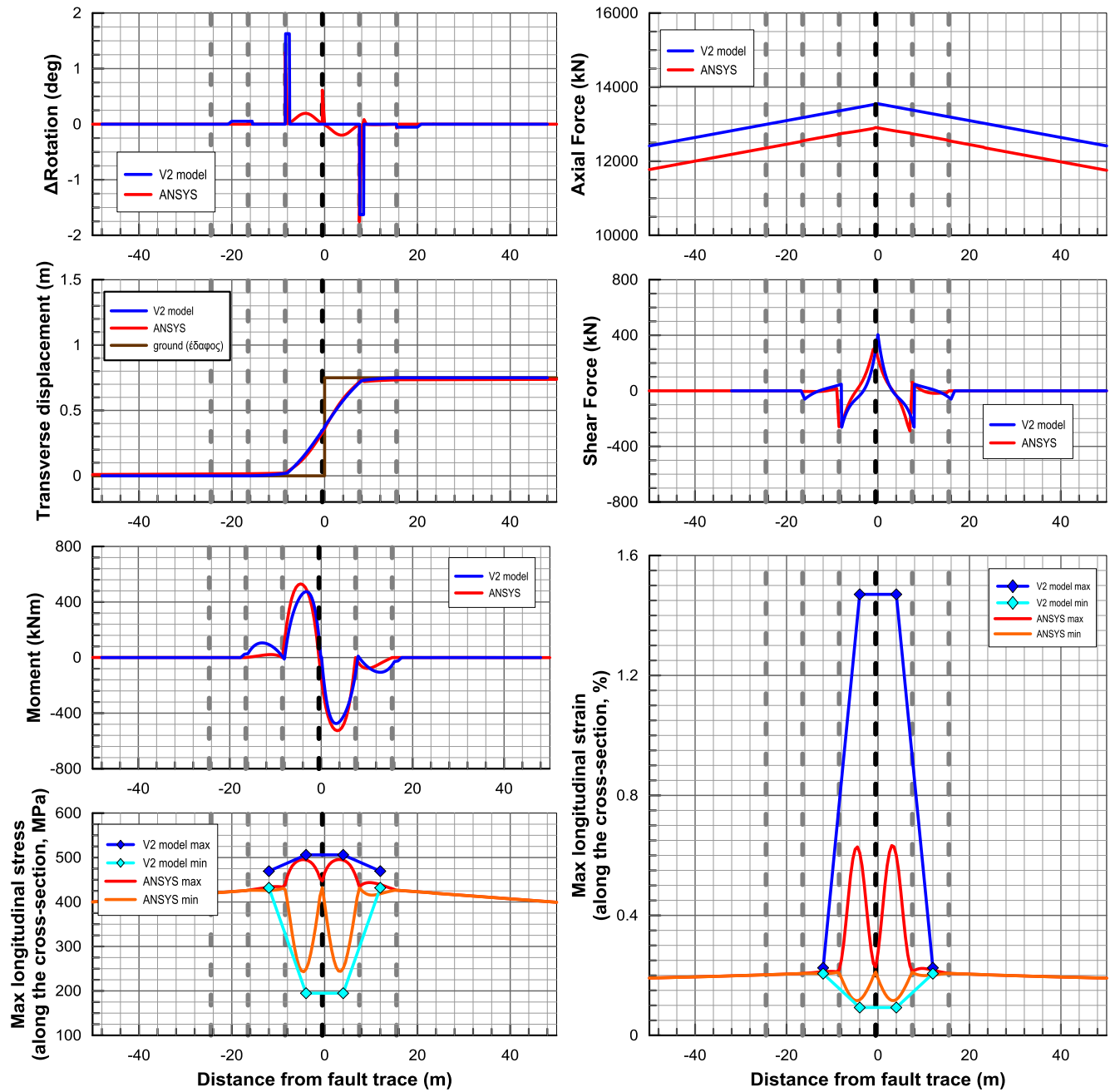




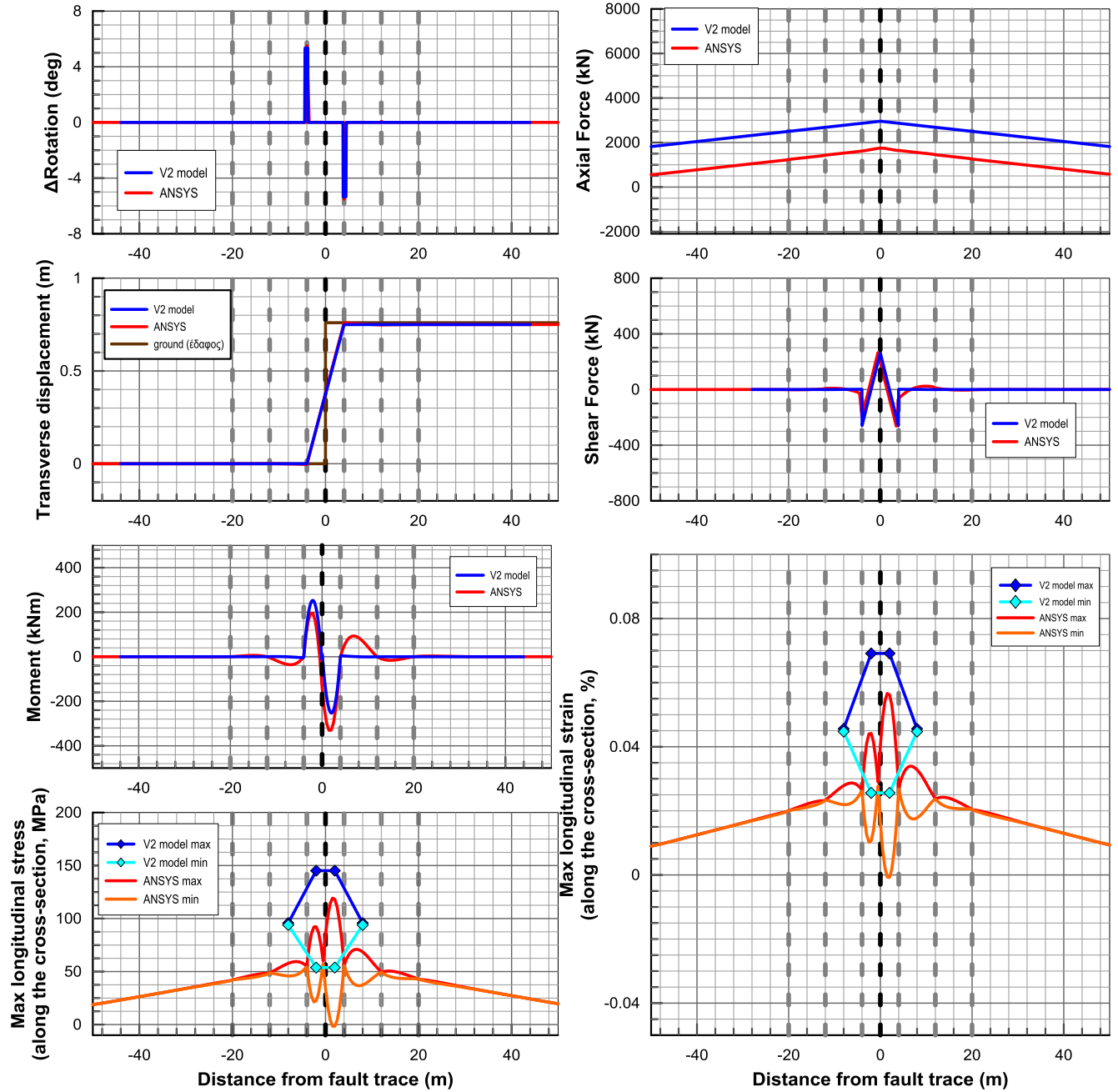
## A26) Flexible joints placed at 8m – Strike slip fault adjacent to the joint – $D_f=1,5m$ $\beta=60^\circ$



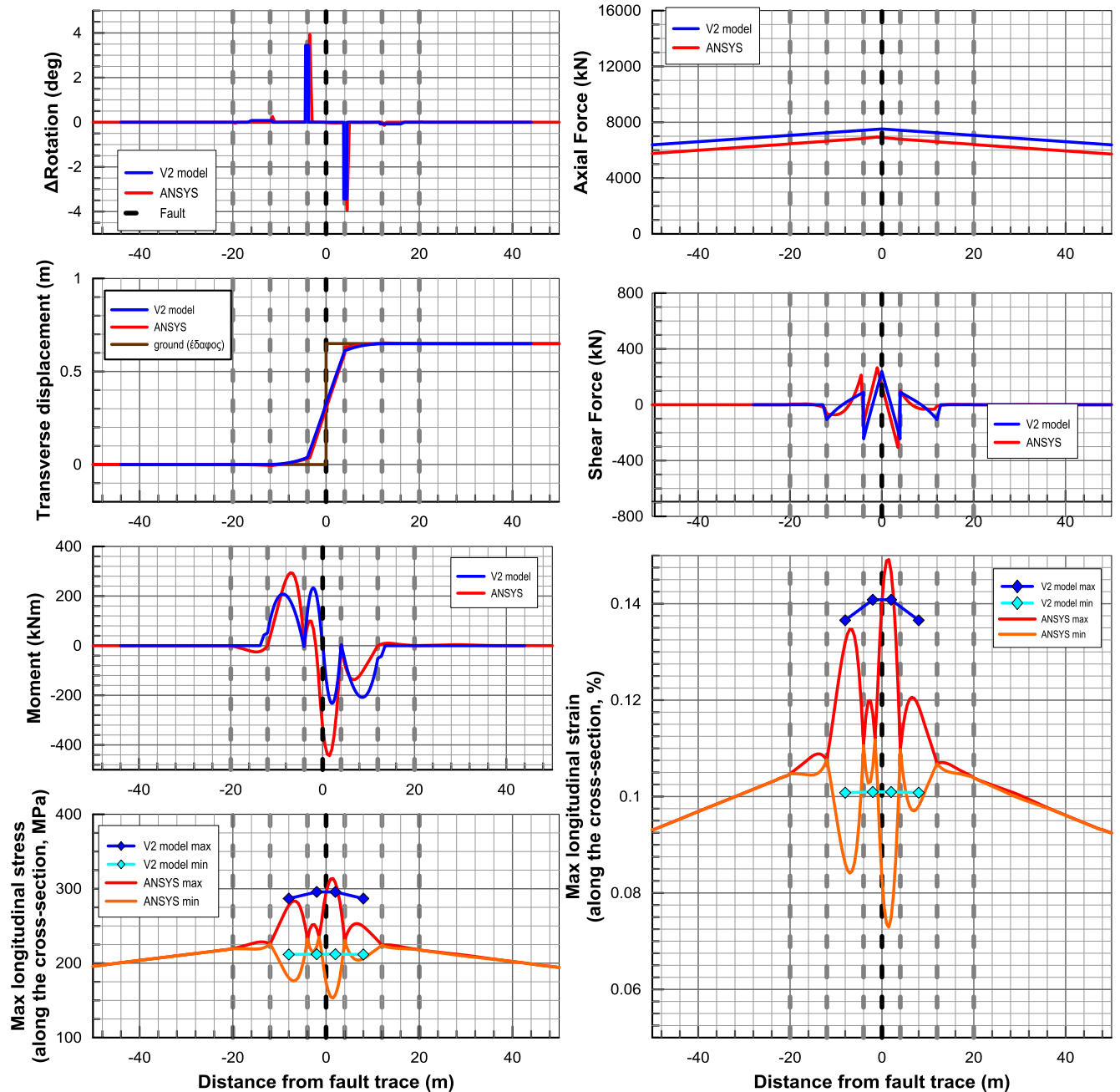
## A27) Flexible joints placed at 8m – Strike slip fault adjacent to the joint – $D_f=1,5m$ $\beta=30^\circ$



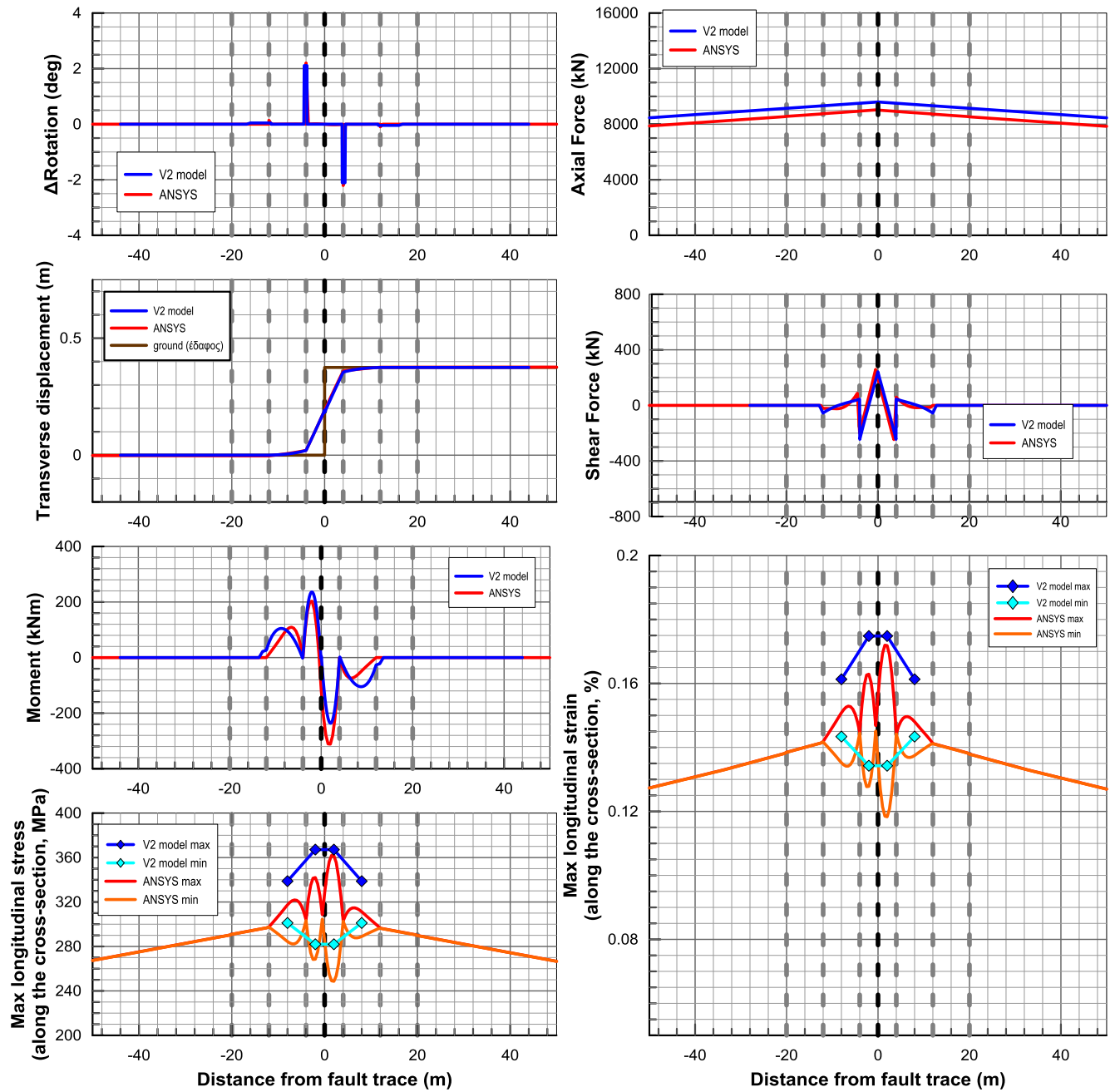
## A28) Flexible joints placed at 8m – Strike slip fault in the middle between two subsequent joints – $D_f=0,75m$ $\beta=90^\circ$



## A29) Flexible joints placed at 8m – Strike slip fault in the middle between two subsequent joints – $D_f=0,75m$ $\beta=60^\circ$

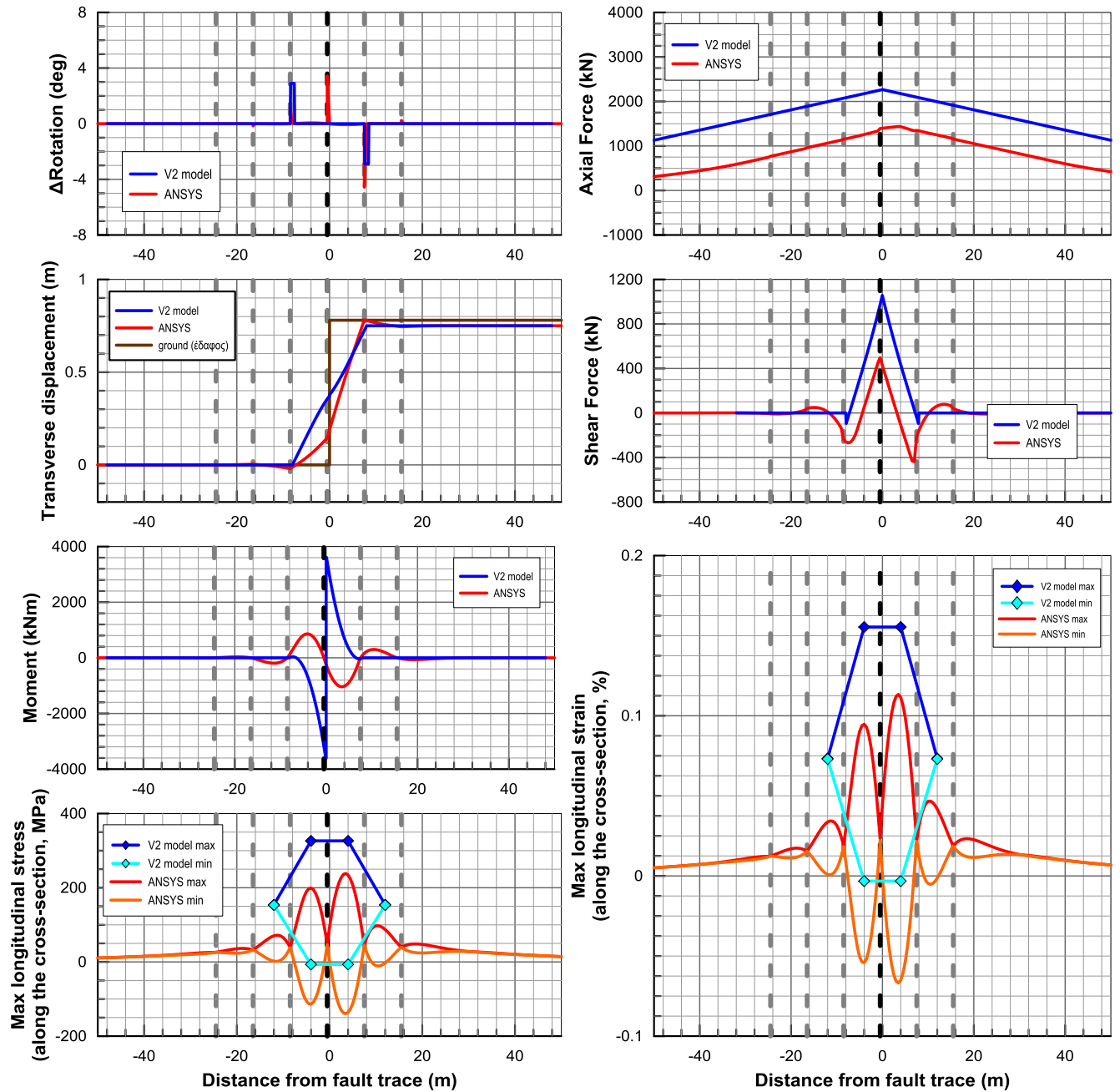


### A30) Flexible joints placed at 8m – Strike slip fault in the middle between two subsequent joints – $D_f=0,75m$ $\beta=30^\circ$

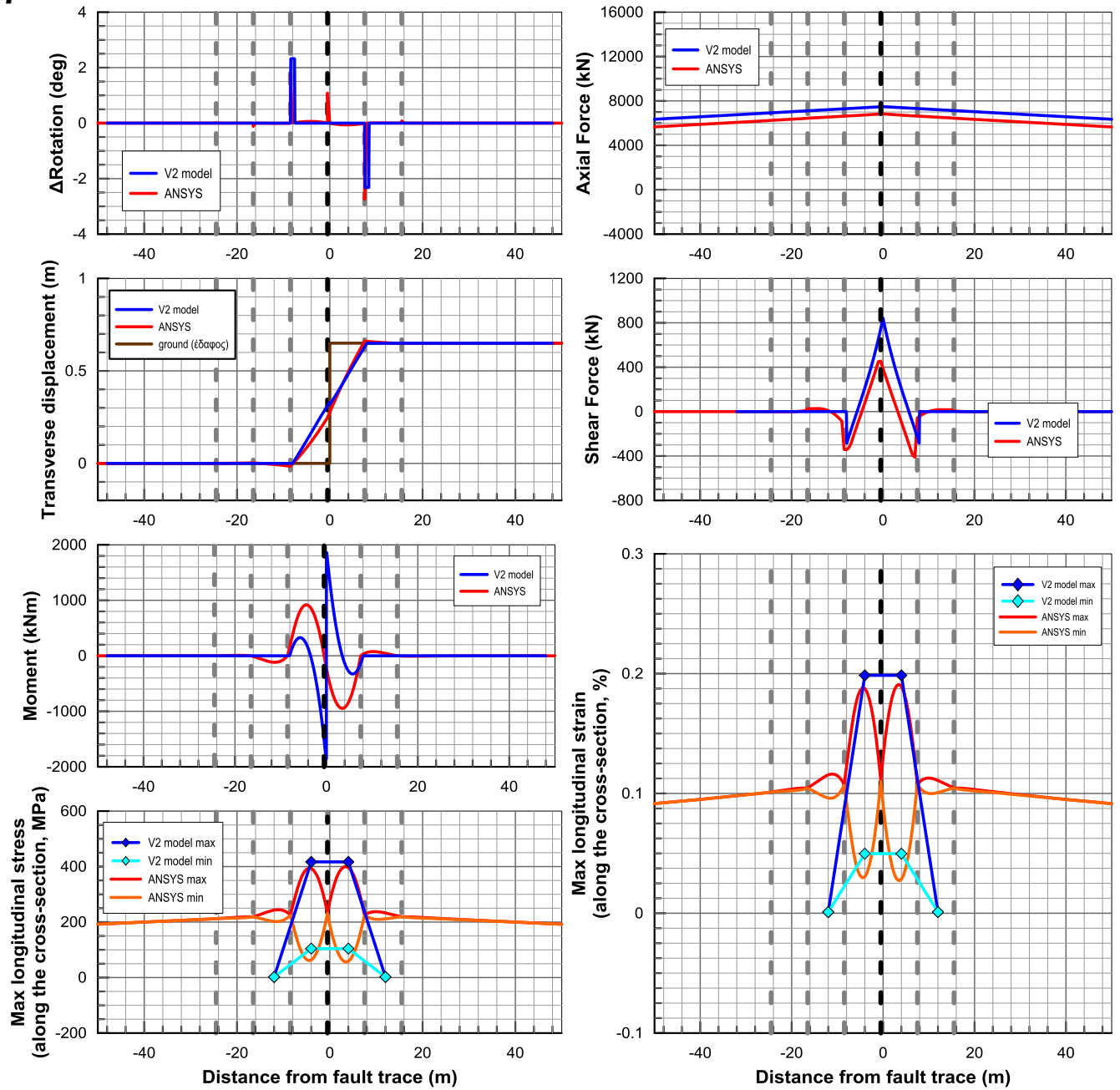


# A31) Flexible joints placed at 8m – – Strike slip fault adjacent to the joint –

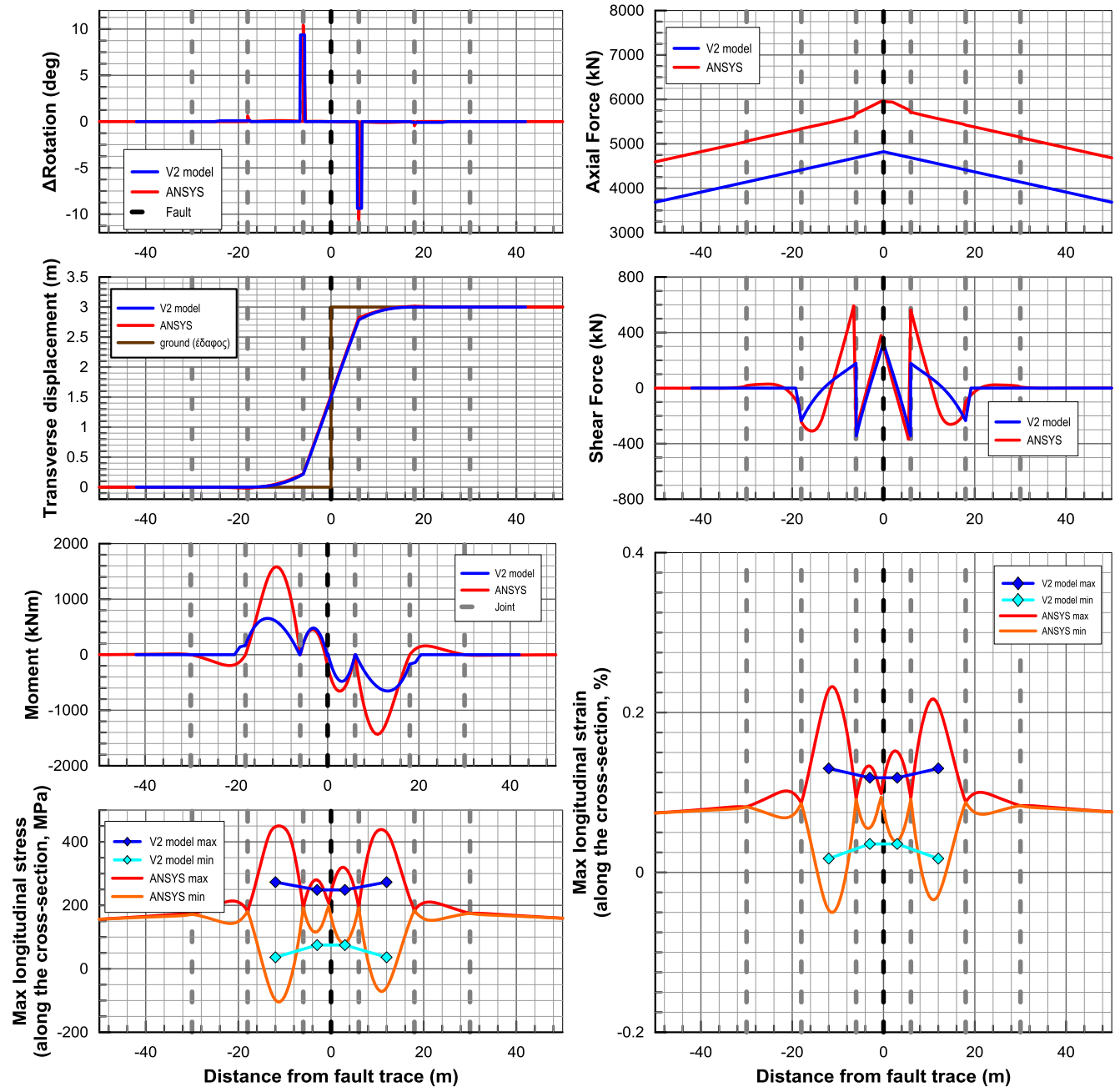
$D_f=0,75m$   
 $\beta=90^\circ$



## A32) Flexible joints placed at 8m – – Strike slip fault adjacent to the joint – $D_f=0,75m$ $\beta=60^\circ$

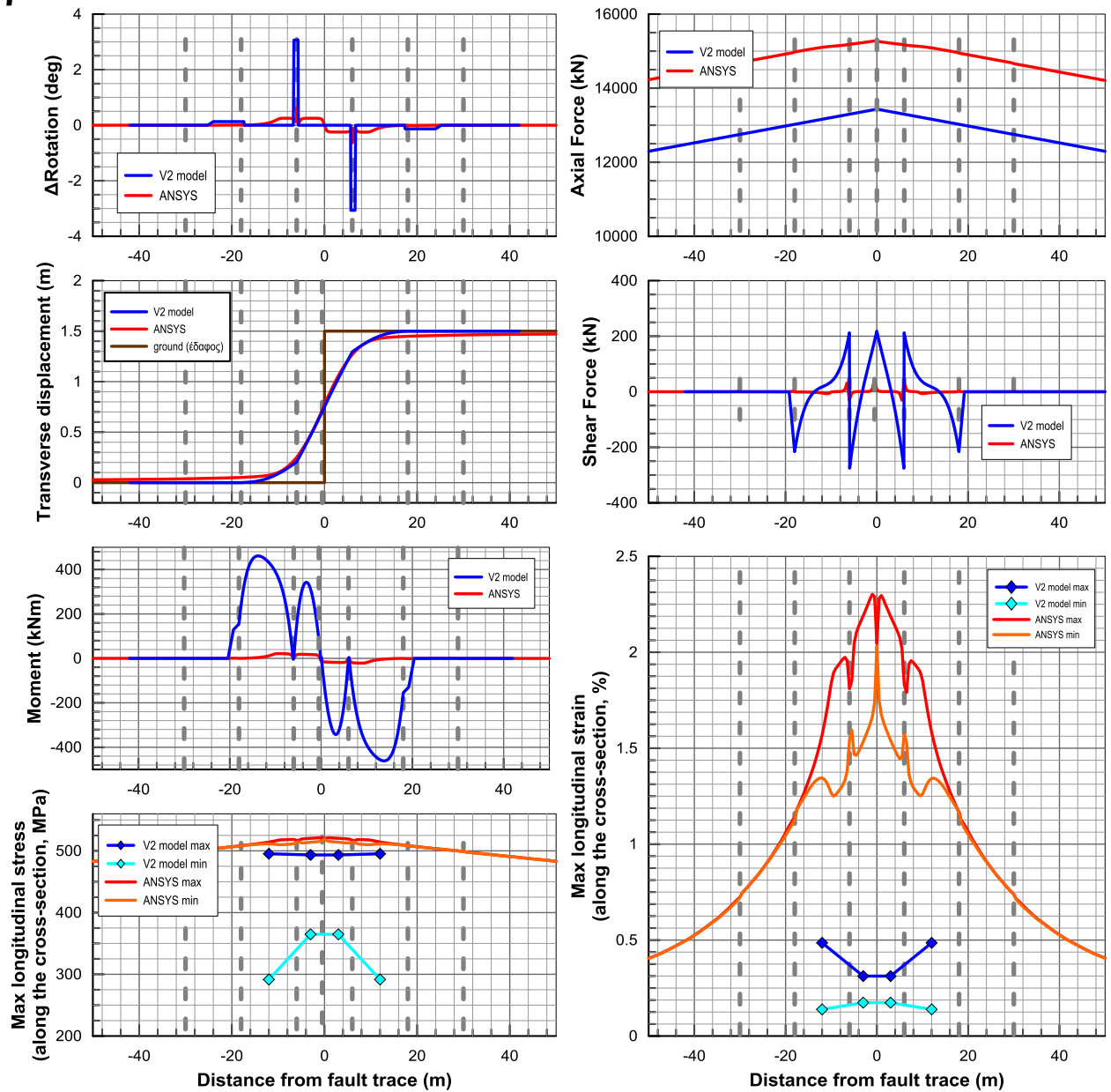


### A33) Flexible joints placed at 12m – Strike slip fault in the middle between two subsequent joints – $D_f=3m$ $\beta=90^\circ$

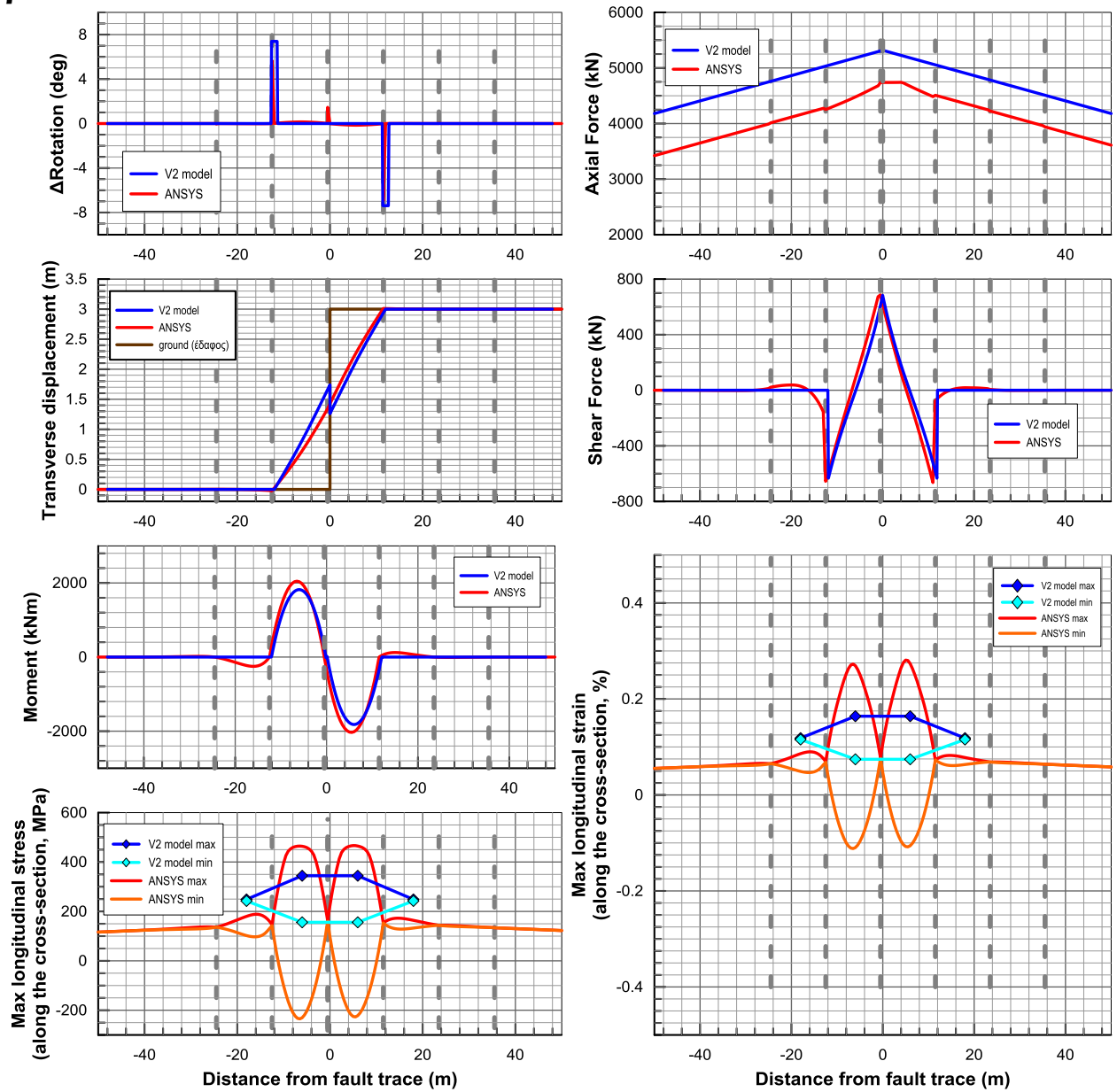




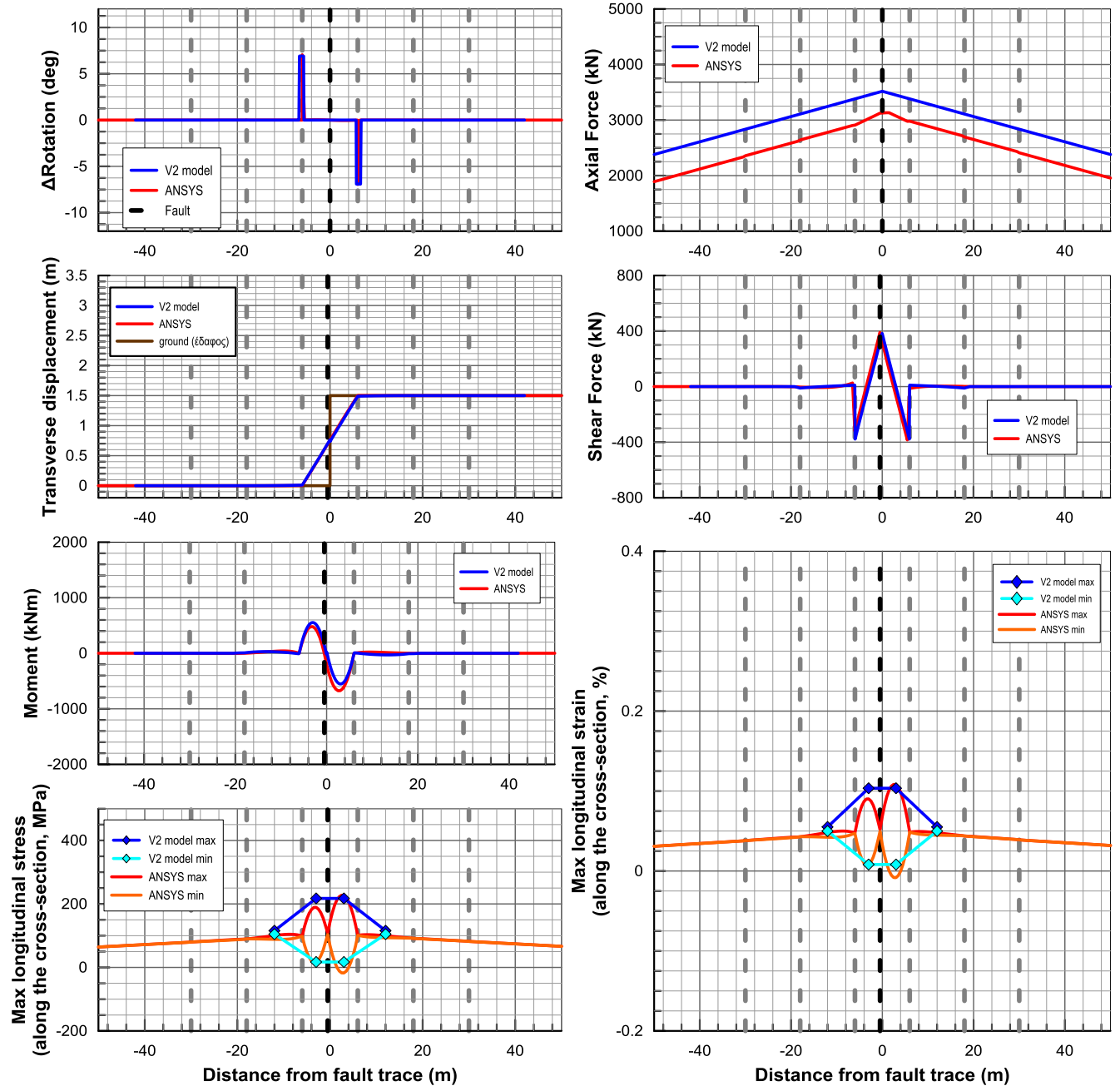
### A34) Flexible joints placed at 12m – Strike slip fault in the middle between two subsequent joints – $D_f=3m$ $\beta=30^\circ$



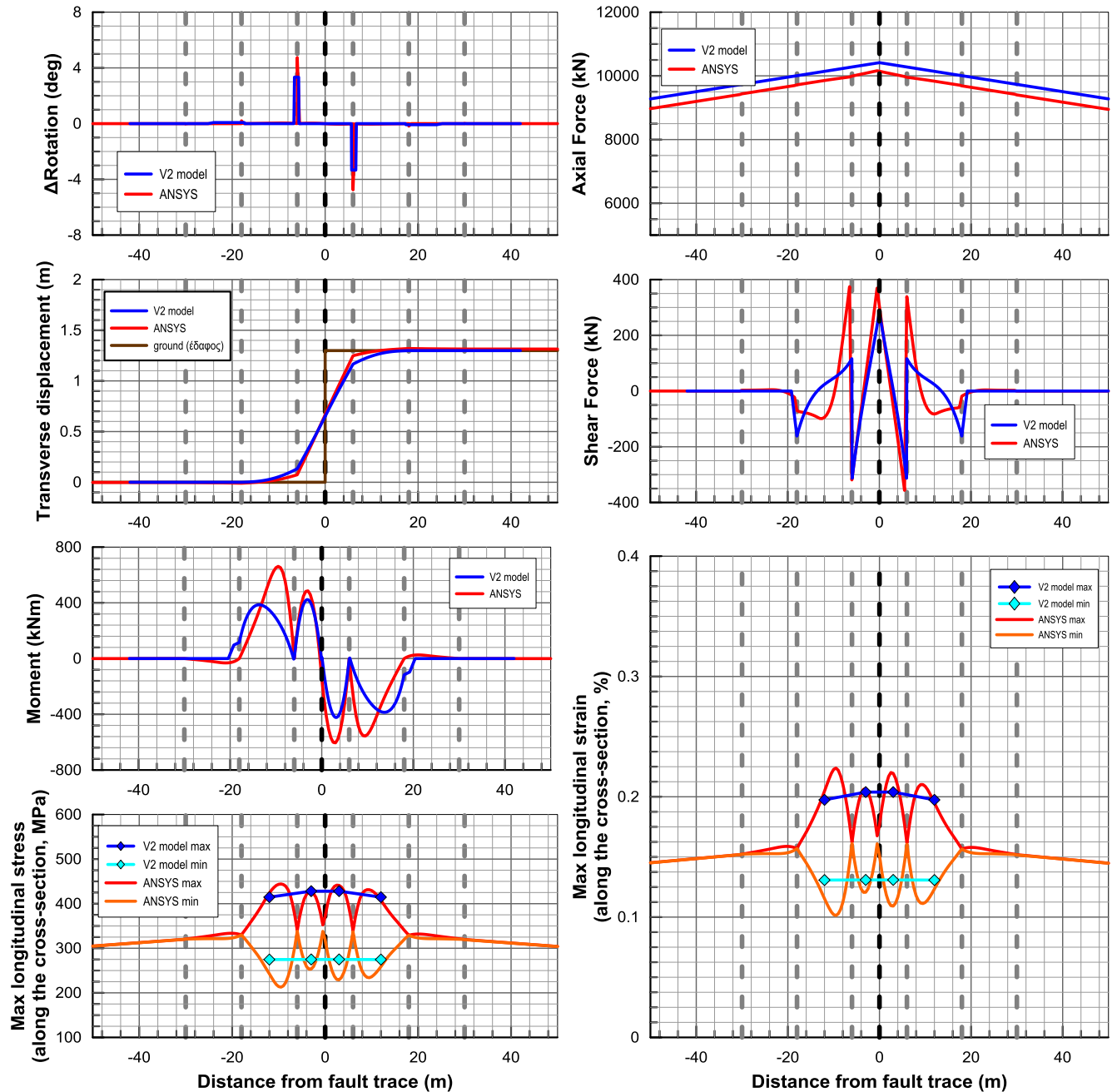
## A35) Flexible joints placed at 12m – Strike slip fault adjacent to the joint – $D_f=3m$ $\beta=90^\circ$



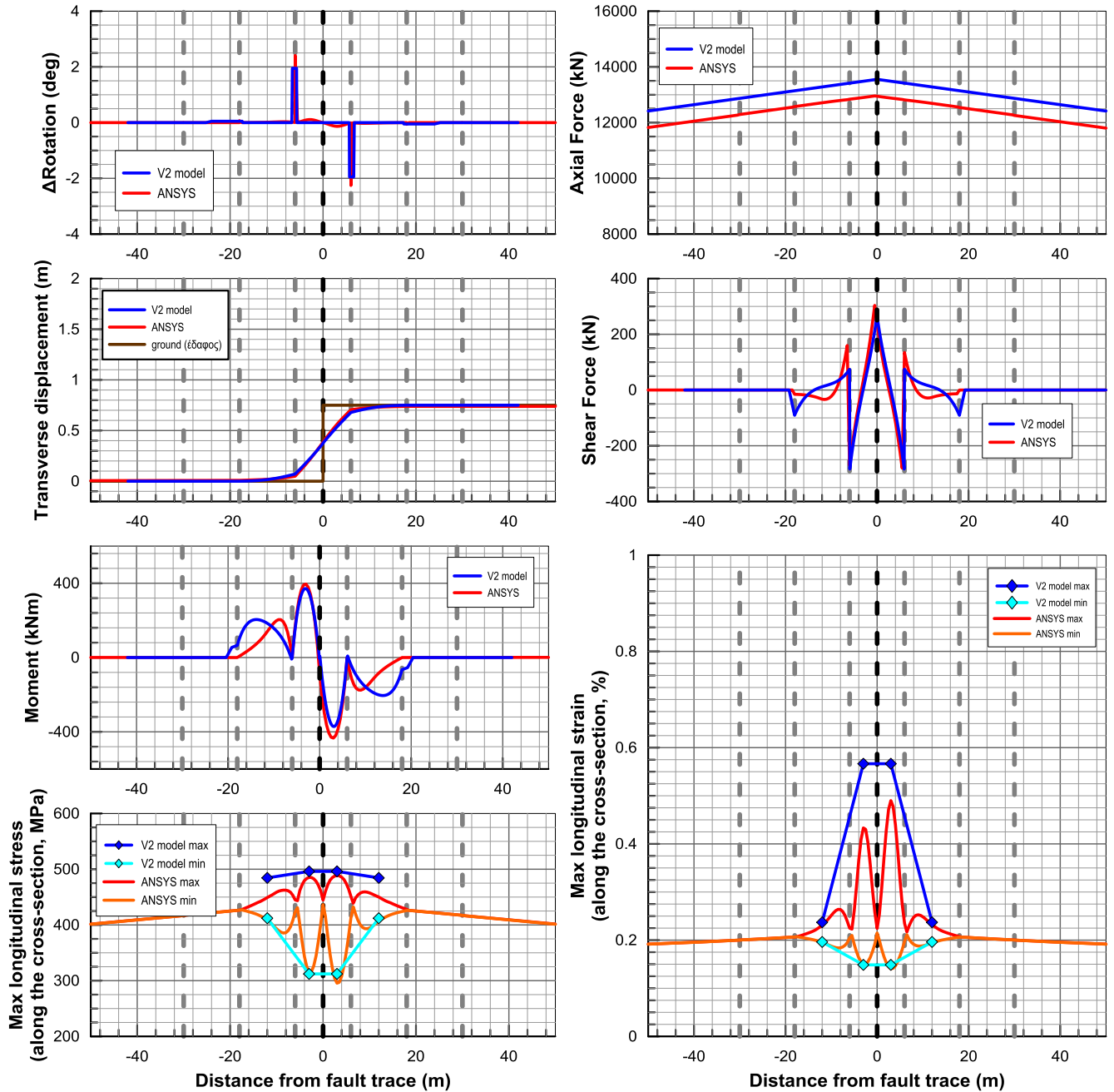
### A36) Flexible joints placed at 12m – Strike slip fault in the middle between two subsequent joints – $D_f=1,5m$ $\beta=90^\circ$



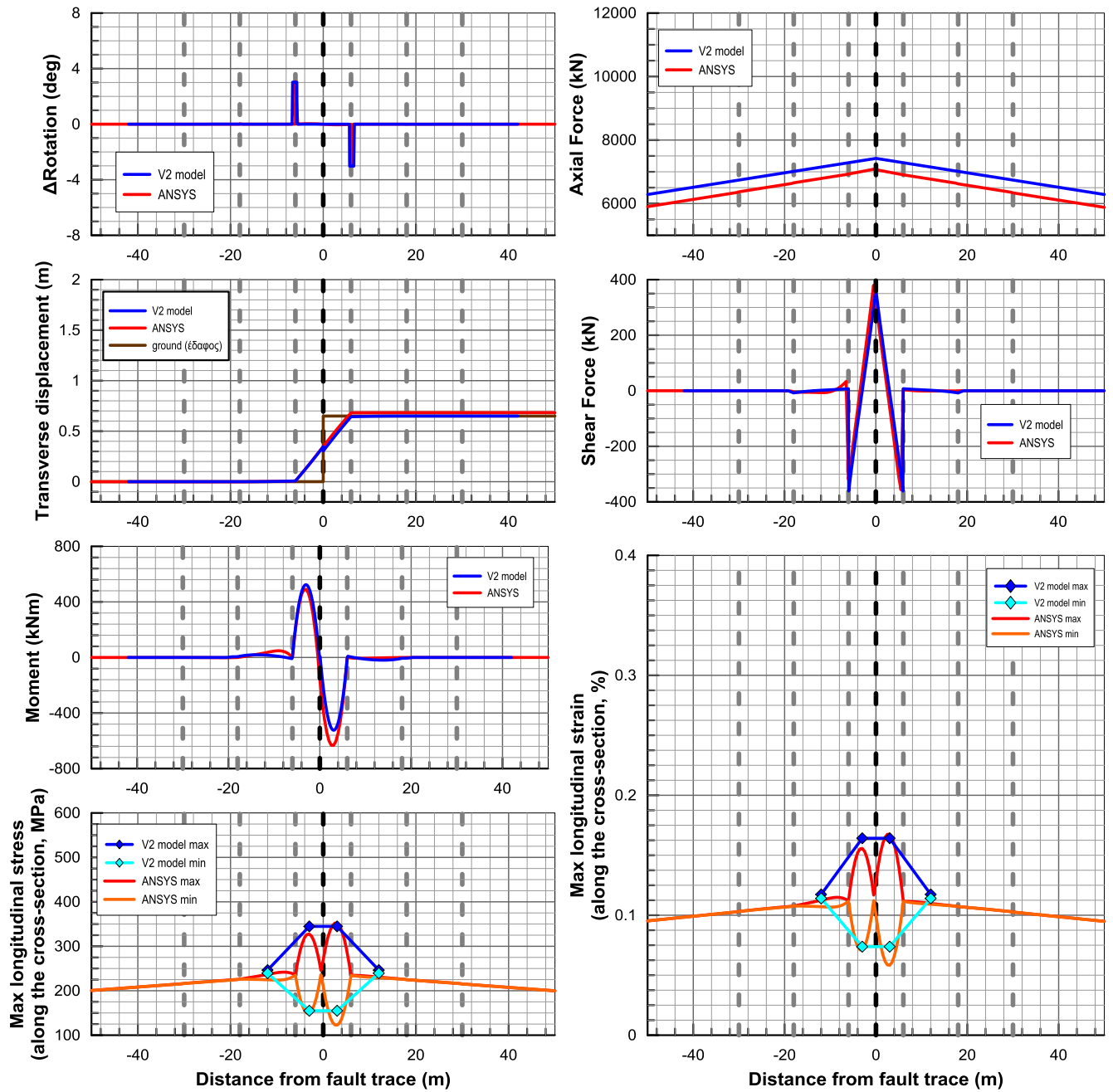
### A37) Flexible joints placed at 12m – Strike slip fault in the middle between two subsequent joints – $D_f=1,5m$ $\beta=60^\circ$



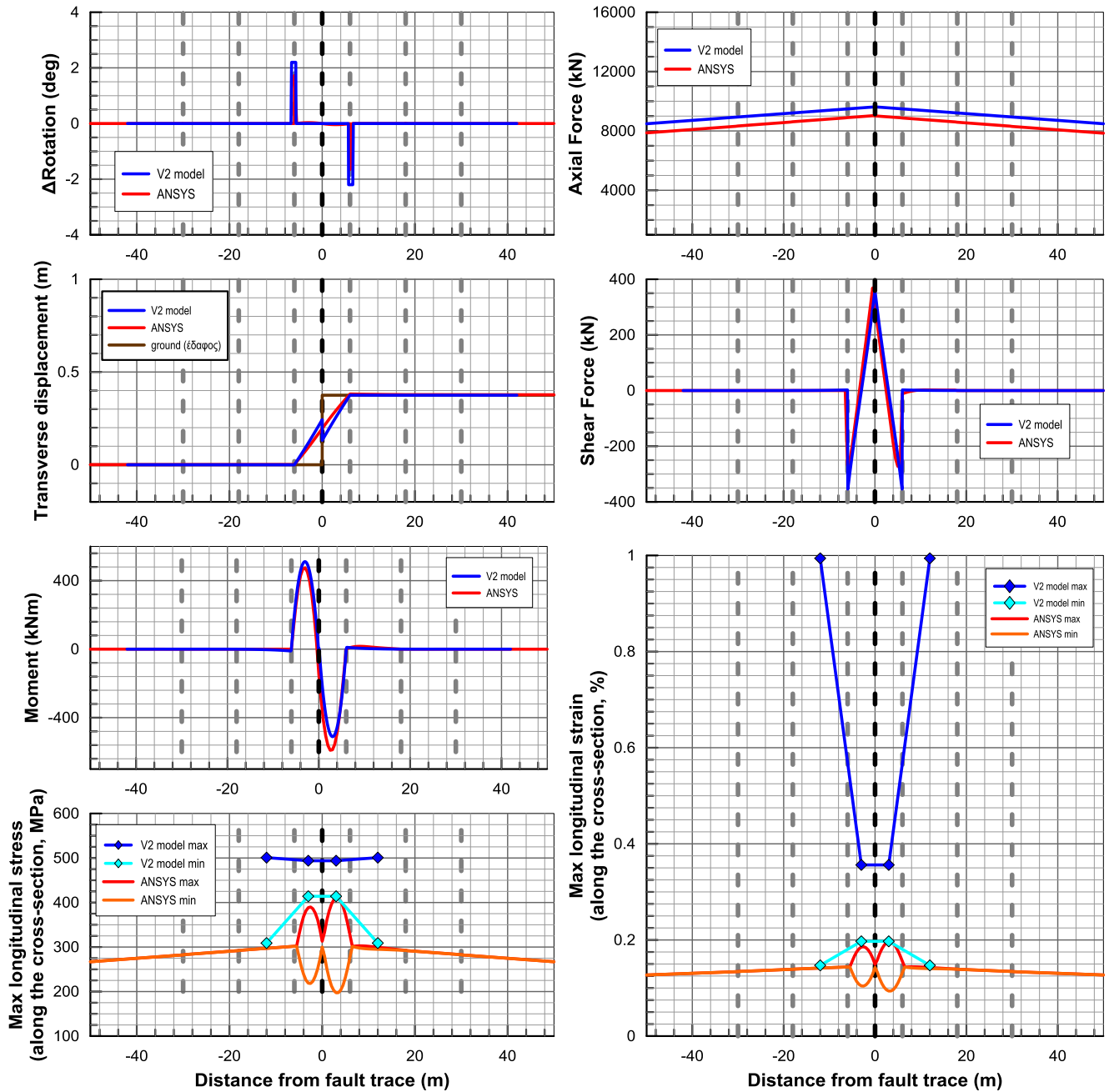
### A38) Flexible joints placed at 12m – Strike slip fault in the middle between two subsequent joints – $D_f=1,5m$ $\beta=30^\circ$



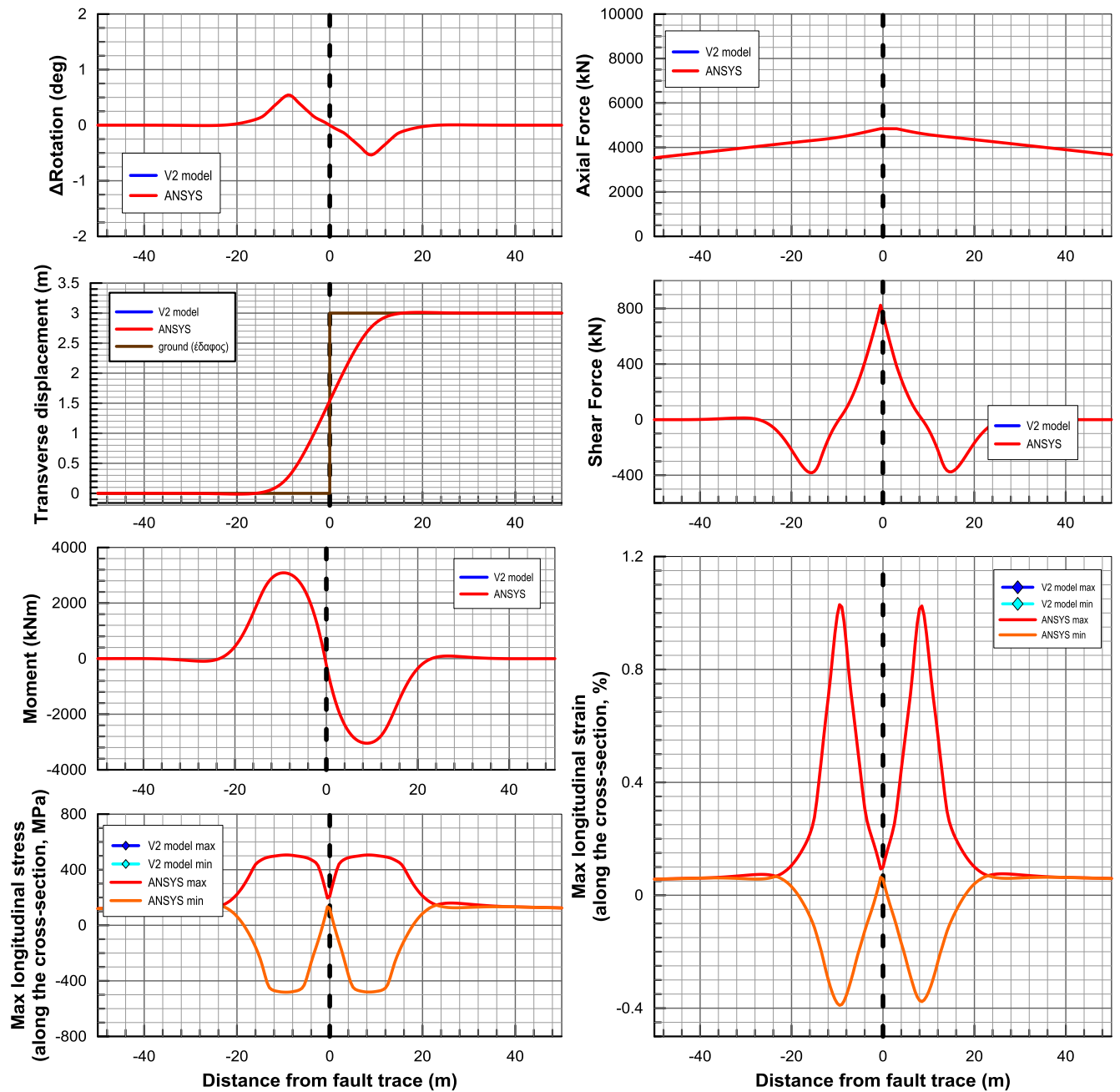
### A39) Flexible joints placed at 12m – Strike slip fault in the middle between two subsequent joints – $D_f=0.75m$ $\beta=60^\circ$



## A40) Flexible joints placed at 12m – Strike slip fault in the middle between two subsequent joints – $D_f=0.75m$ $\beta=30^\circ$

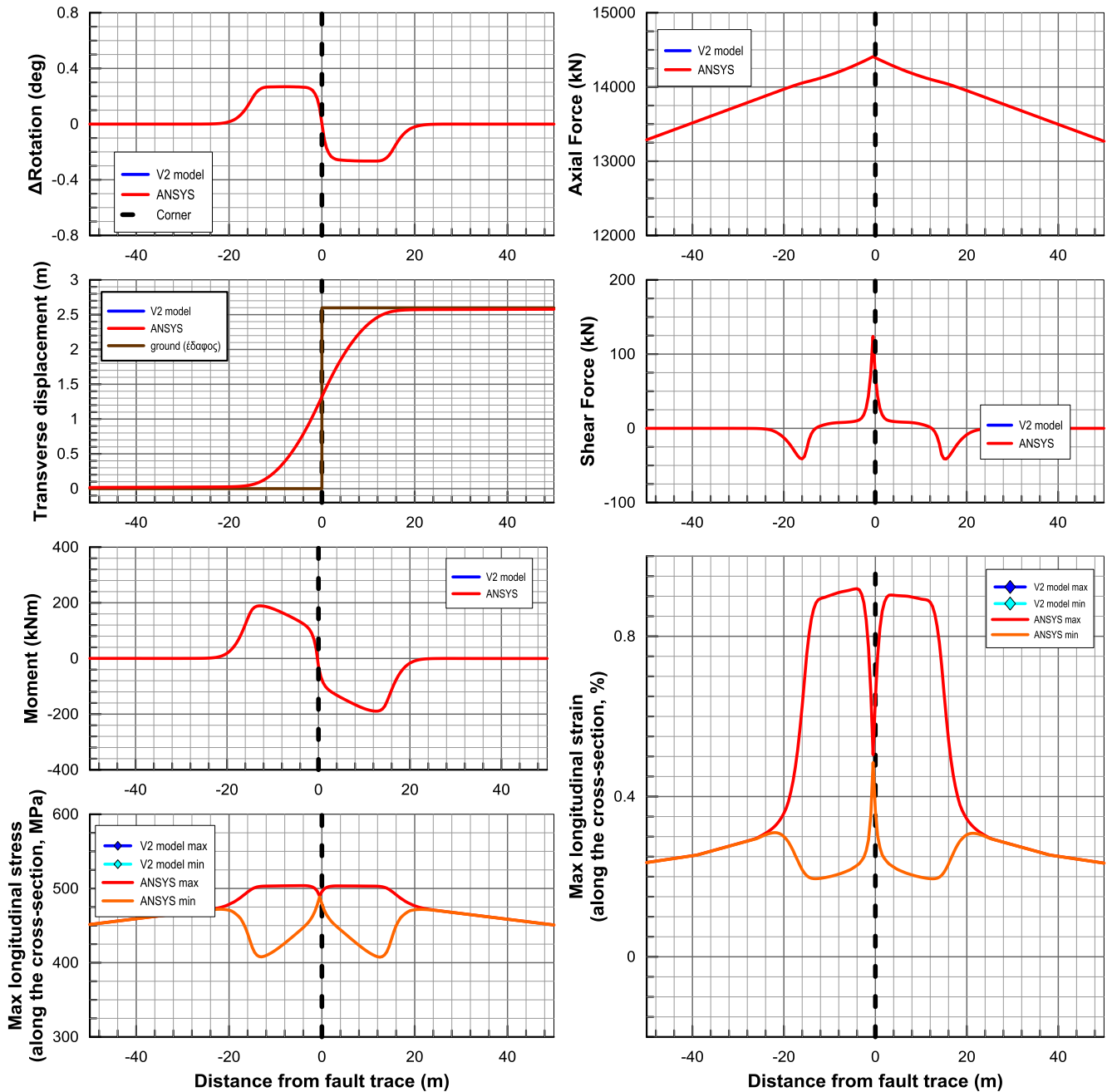


# A I) Continuous Pipeline – Strike slip fault in the middle between two subsequent joints – $D_f = 3m$ $\beta = 90^\circ$

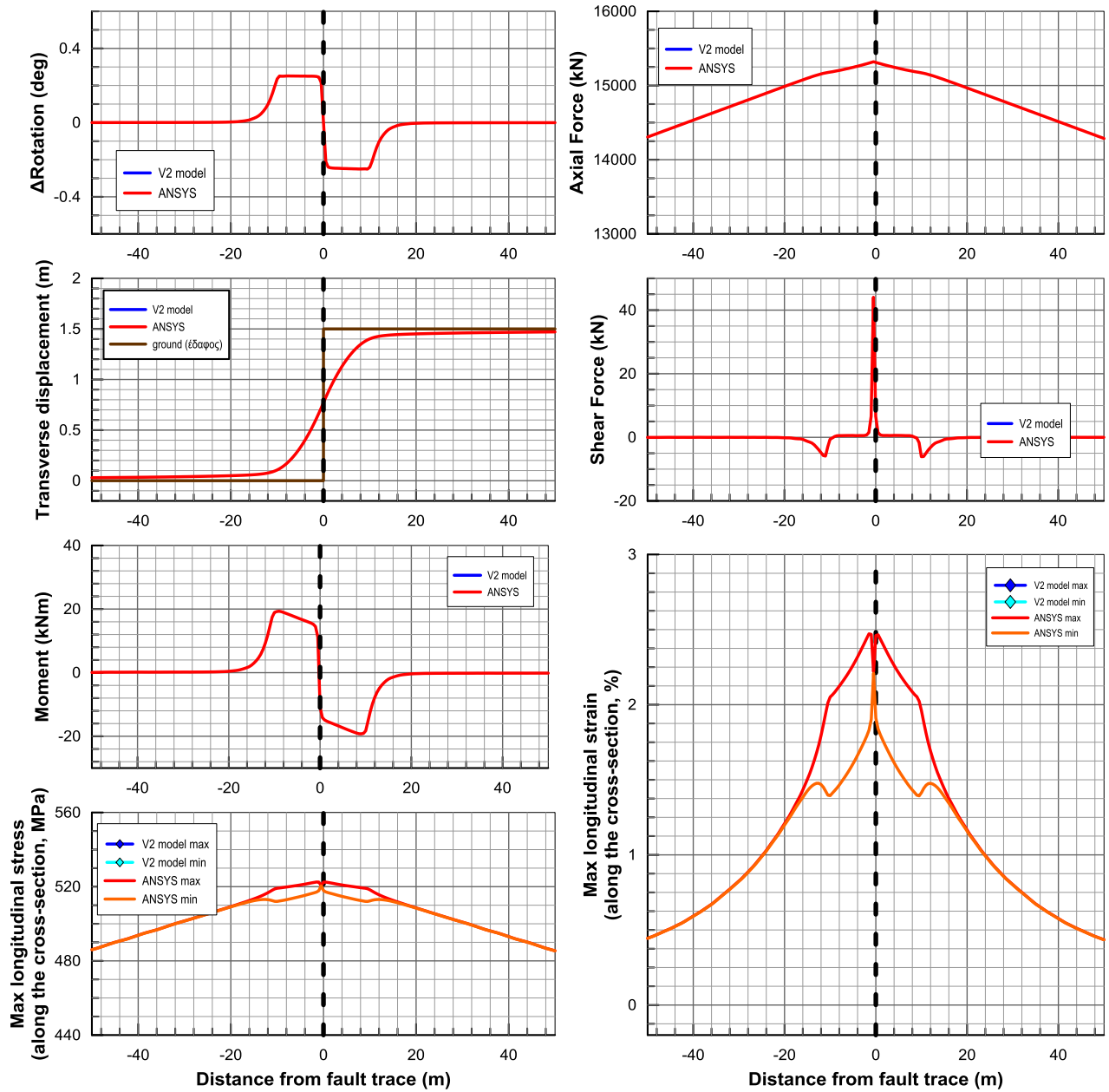




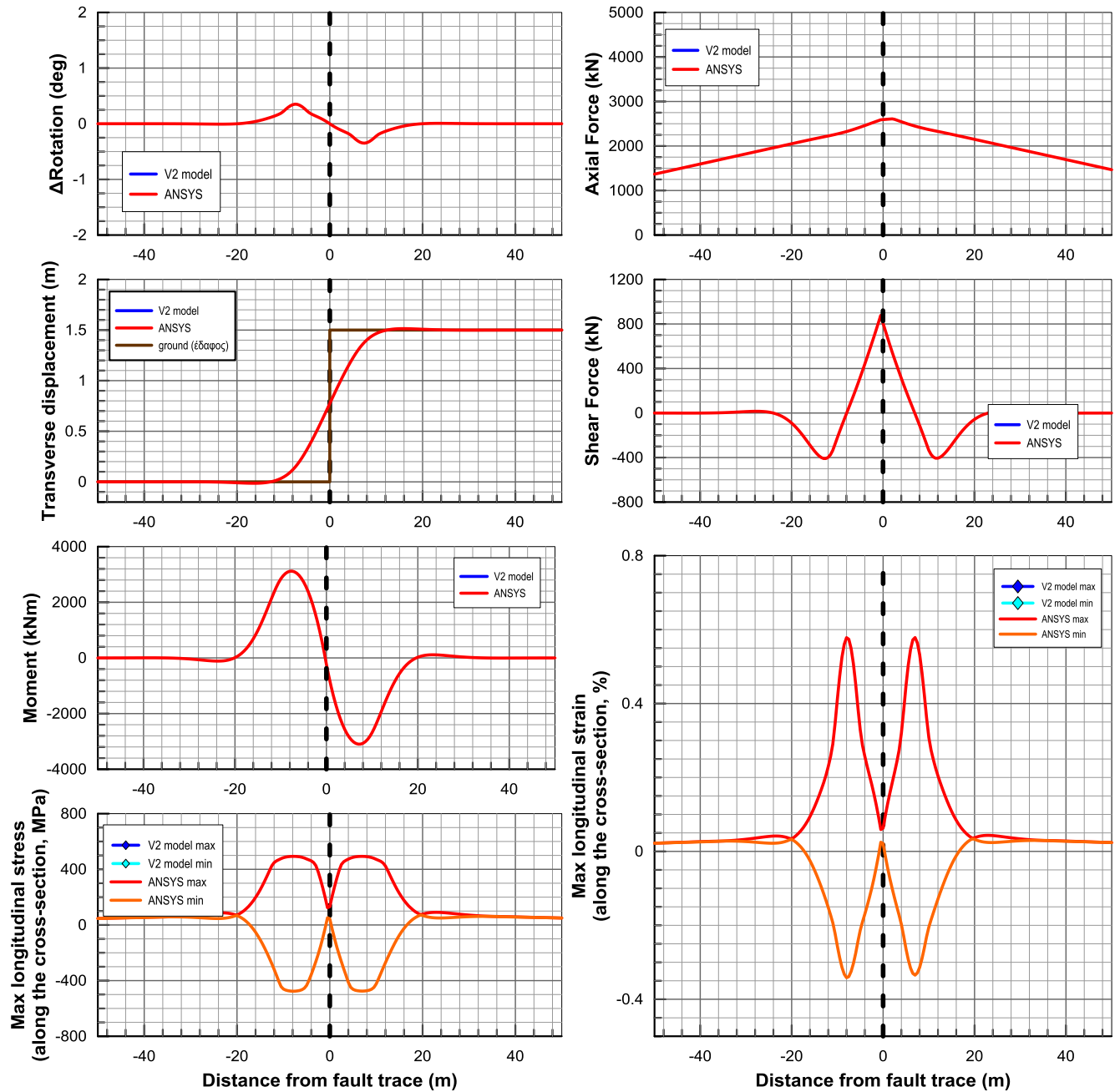
## A II) Continuous Pipeline – Strike slip fault in the middle between two subsequent joints – $D_f = 3m$ $\beta = 60^\circ$



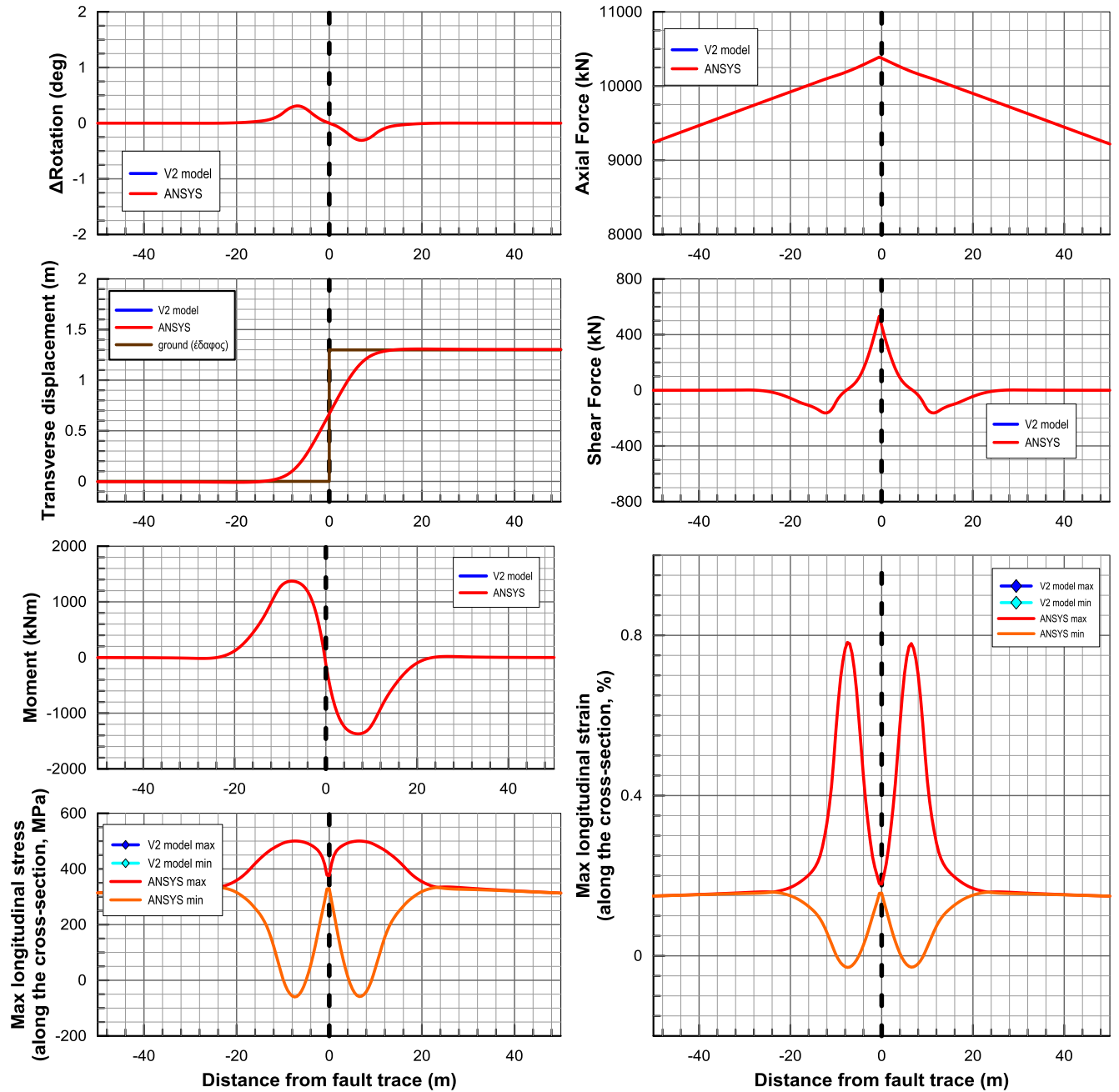
### A III) Continuous Pipeline – Strike slip fault in the middle between two subsequent joints – $D_f = 3\text{m}$ $\beta = 30^\circ$



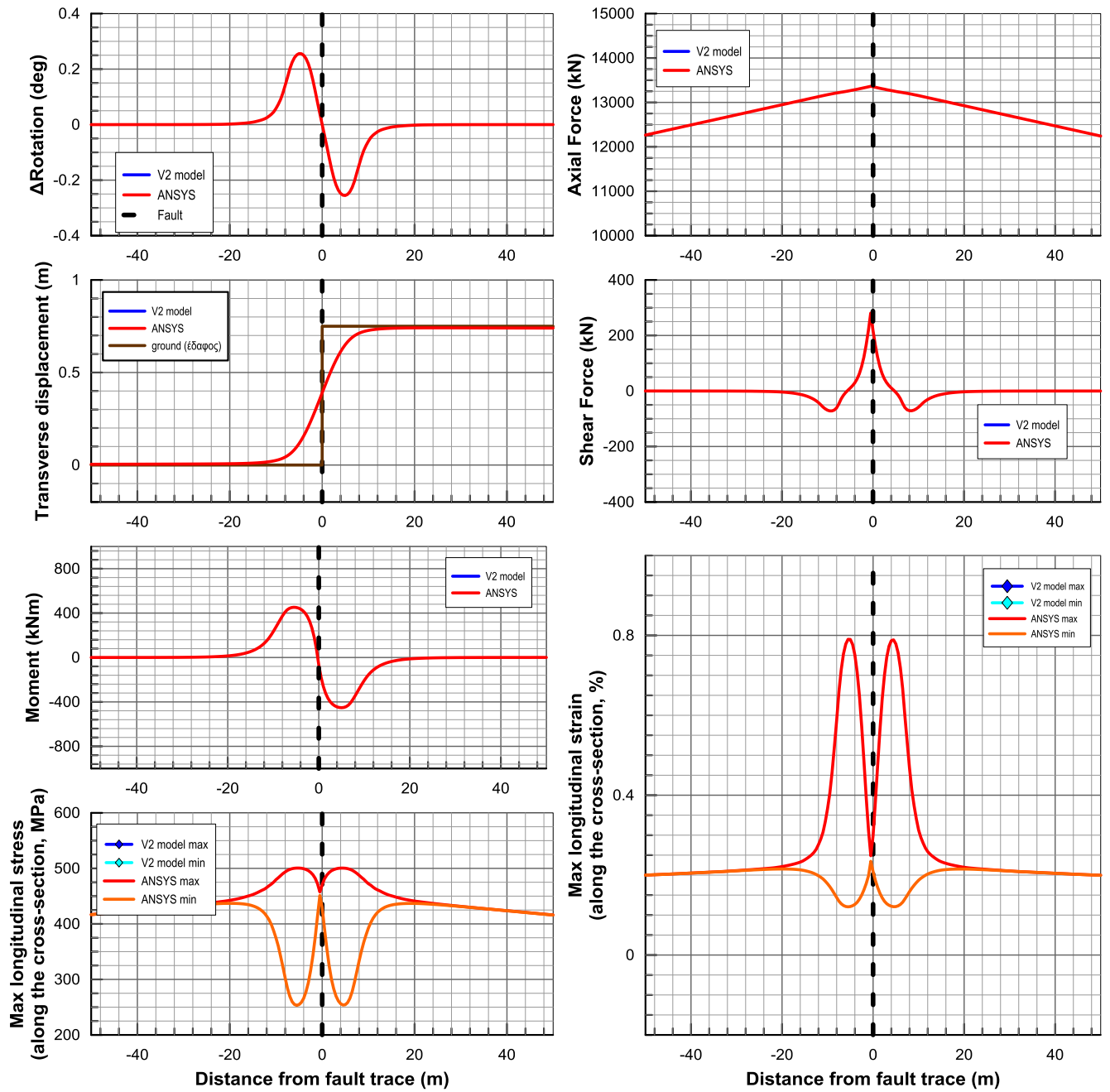
## A IV) Continuous Pipeline – Strike slip fault in the middle between two subsequent joints – $D_f = 1.5\text{m}$ $\beta = 90^\circ$



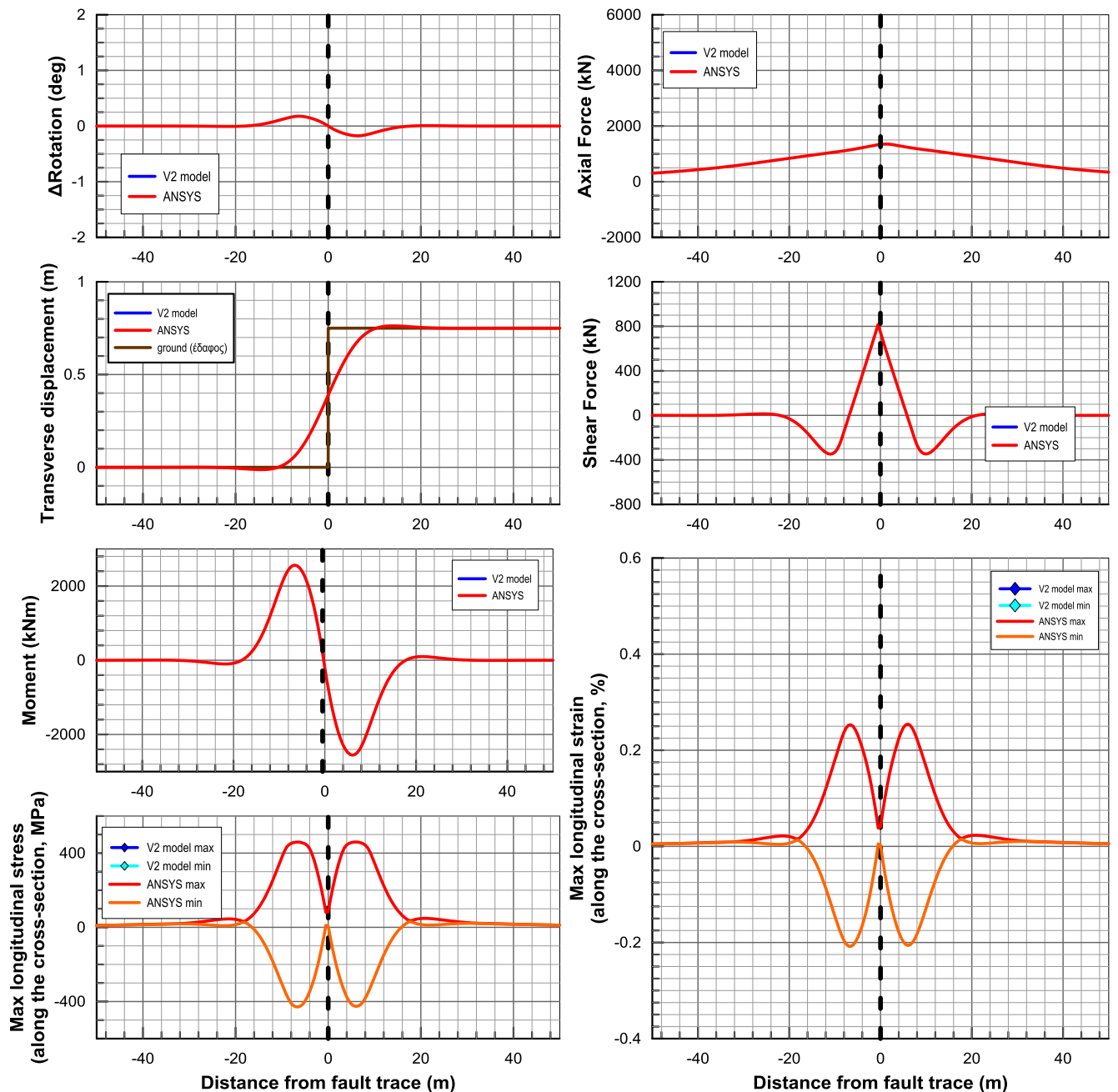
# A V) Continuous Pipeline – Strike slip fault in the middle between two subsequent joints – $D_f = 1.5m$ $\beta = 60^\circ$



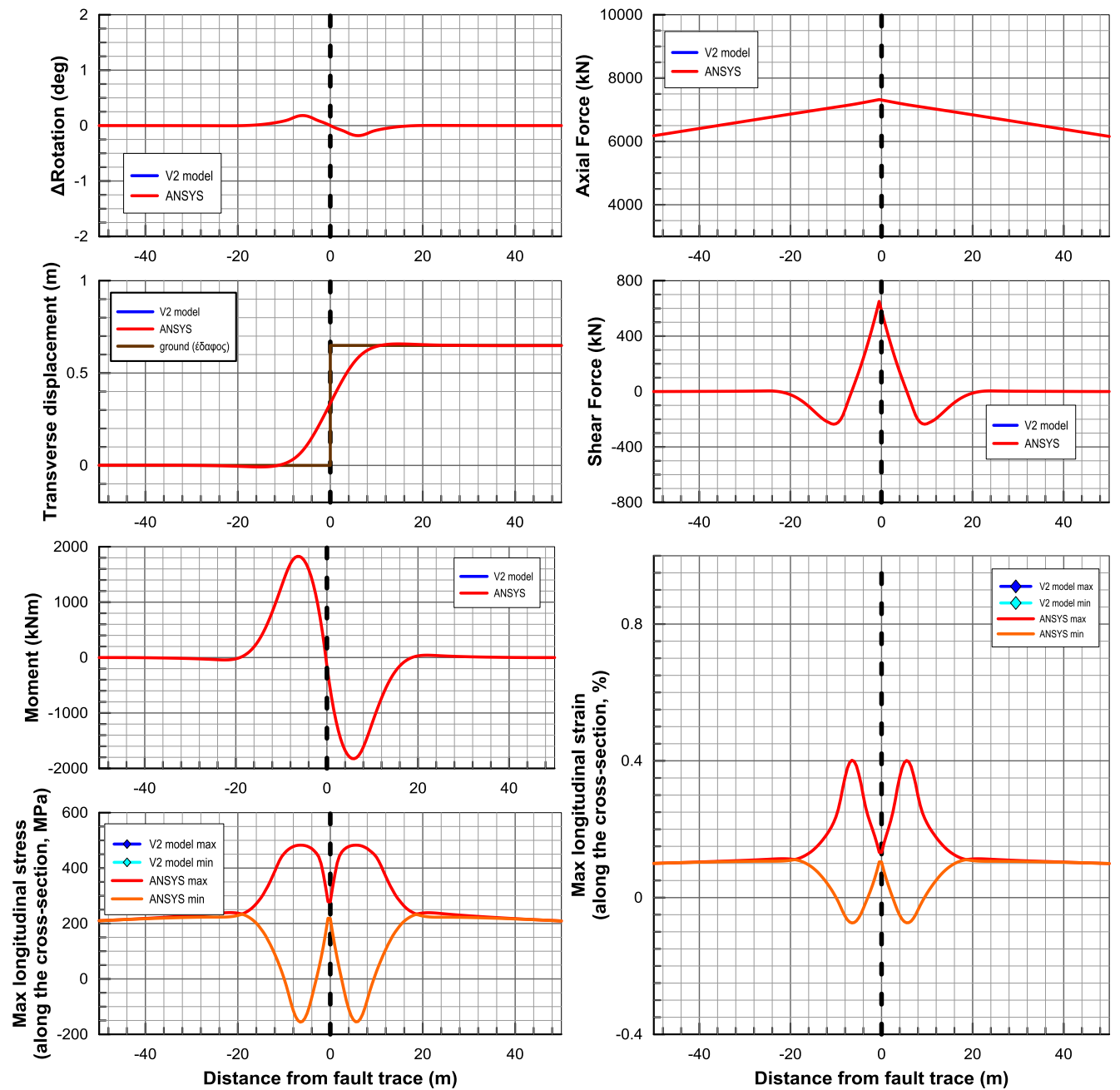
## A VI) Continuous Pipeline – Strike slip fault in the middle between two subsequent joints – $D_f = 1.5m$ $\beta = 30^\circ$



## A VII) Continuous Pipeline – Strike slip fault in the middle between two subsequent joints – $D_f = 0.75\text{m}$ $\beta = 90^\circ$



## A VIII) Continuous Pipeline – Strike slip fault in the middle between two subsequent joints – $D_f = 0.75m$ $\beta = 60^\circ$



# A IX) Continuous Pipeline – Strike slip fault in the middle between two subsequent joints – $D_f = 0.75\text{m}$ $\beta = 30^\circ$

